

**An Iterative Synthetic Route Toward Pyrenophane Chains**

by

© Kerry-Lynn M. Williams

A Thesis submitted to the

School of Graduate Studies

in partial fulfillment of the requirements for the degree of

**Master of Science**

**Department of Chemistry**

Memorial University of Newfoundland

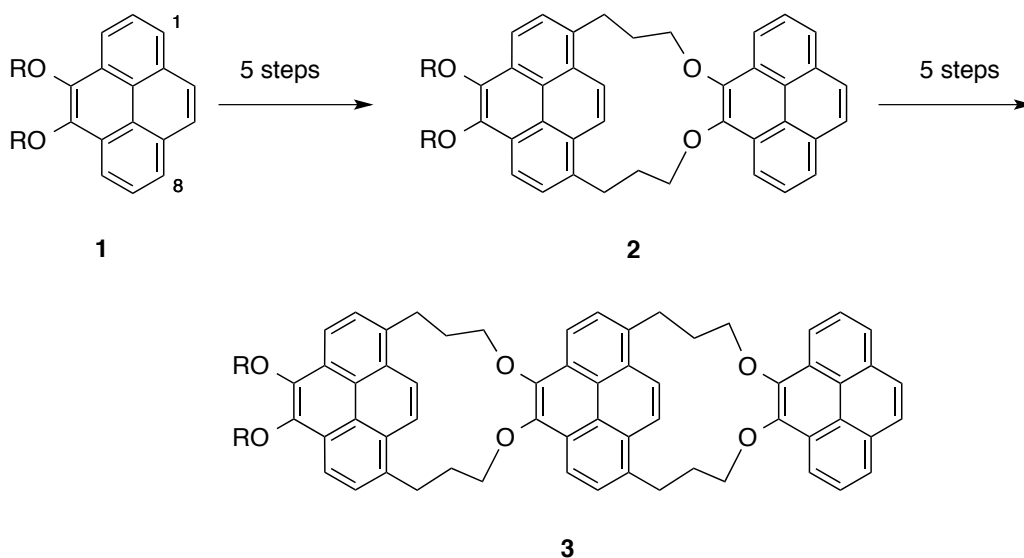
**May 2015**

St. John's

Newfoundland and Labrador

## Abstract

The use of pyrene as a building block for molecules with applications in optoelectronic devices is becoming increasingly important.<sup>1</sup> In this regard, the development of methodologies that provide convenient and highly regioselective access to functionalized pyrenes will facilitate progress in this area. For example, the Bodwell group at Memorial University recently showed that the placement of alkoxy groups at the 4 and 5 positions on pyrene (e.g. **1**) both activates the pyrene system towards electrophilic substitution and effectively hinders the 3 and 6 positions. This methodology has been used in the synthesis of (1,8-pyrenylene)-ethynylene macrocycles,<sup>2</sup> and is now at the heart of an iterative five-step strategy aimed at the synthesis of oligomeric pyrenophanes **2**, **3** and beyond. Details of the synthetic approach toward these pyrenophane chains will be presented.



## **Acknowledgements**

First and foremost, I would like to thank my supervisor, Dr. Graham Bodwell, for giving me the opportunity to work in his group over the last several years. Your expertise, understanding, and patience throughout my chemistry undergraduate and graduate education are greatly appreciated. As well, thanks for continually striving to make being a member of the Bod group an enjoyable experience. Your enthusiasm for all things (toward both chemistry and social activities) has been infectious. Thanks for organizing countless potlucks, SOCCER conferences, colloquiums, golf outings, and other Bod group activities; they have certainly made my time within the group an enjoyable one!

To the Bod group, thanks for being such a fun group of people to work with! You've made the lab environment a great one to work in, and your support, suggestions, humour and singing, have made the past couple of years fly by. To Josh, Joseph, Salah and Penchal, thanks for making our part of the lab so much fun to be in! The good music and company were a lot of fun! Thanks to Natsumi for your help on the project, your time here was a great learning experience for the both of us. Thanks to Josh for all your help with our "diketone challenge" and the monster that was the 100 g scale diketone reaction. To Kiran, Marc, Landon and Parisa, it has been a fun couple of years working with you!

As members of my supervisory committee I would like to thank Drs. Yuming Zhao and Christopher Rowley for their valuable contributions, encouragement, and advice

throughout my program. Their critical reading and suggestions during the writing of this thesis were also very helpful.

Special thanks go out to countless members of the Department of Chemistry. Although too numerous to name, I am grateful for their support. The services of C-CART are greatly acknowledged here as well. In particular, the assistance of Linda Winsor (HRMS), Dr. Céline Schneider (NMR), and Julie Collins (TGA) have been instrumental throughout my program.

Finally, I would like to thank my parents for their love and support throughout both my undergraduate and graduate programs. To put it mildly, you have made life a lot easier for me. Thanks for your continuous support, generosity, and understanding, you have helped me get to where I am today, and for that I am forever grateful.

## Table of Contents

Abstract.....	ii
Acknowledgements .....	iii
Table of Contents.....	v
List of Tables .....	vi
List of Figures.....	vii
List of Schemes .....	viii
List of Symbols, Nomenclature or Abbreviations .....	x
Chapter 1: Introduction.....	12
Chapter 2: Results and Discussion .....	29
Chapter 3: Characterization of TTFV-Pyrene-based Polymers.....	59
Chapter 4: Conclusions and Future Work .....	70
Chapter 5: Experimental.....	75
Bibliography .....	89
Appendix .....	93

## List of Tables

Table 2.1: Optimization of the loading of NMI in the oxidation of pyrene ( <b>18</b> ).....	36
Table 2.2: Optimization of the scale of the reaction to form pyrene-4,5-dione ( <b>31</b> ).....	37
Table 2.3: Optimization of the additive of the reaction to form pyrene-4,5-dione ( <b>31</b> )....	40
Table 2.4: Series of synthesized 4,5-dialkoxypyrenes. ....	44
Table 2.5: Attempted Sonogashira reactions with <b>62</b> .....	48
Table 2.6: Attempts at forming the desired pyrenophane ( <b>2</b> ).....	58
Table 3.1: Calculated $r_H$ from PGSE-diffusion NMR data.....	67

## List of Figures

Figure 1.1: General structure of a simple cyclophane.....	12
Figure 1.2: Superphane ( <b>5</b> ).....	13
Figure 1.3: Examples of cyclophanes with different functions.....	14
Figure 1.4: [2.2]Paracyclophane ( <b>9</b> ) and <i>anti</i> -[2.2]metacyclophane ( <b>10</b> ).....	15
Figure 1.5: Selected Bodwell group pyrenophanes.....	17
Figure 1.6: Preferred sites of electrophilic aromatic substitution on pyrene ( <b>18</b> ).....	20
Figure 1.7: A 1,8-pyrenylene-ethynylene macrocycle ( <b>34</b> ).....	23
Figure 1.8: Target pyrenophanes and their key design elements.....	24
Figure 1.9: <i>Anti</i> and <i>syn</i> conformers of <b>2</b> .....	25
Figure 2.1: Pure compounds isolated by Dixon <i>et al.</i> from the oxidation of pyrene ( <b>18</b> ). Several impure mixtures, including one of the lactone <b>43</b> and unknown aldehyde <b>45</b> were also obtained.....	32
Figure 2.2: Ligands used as additives in the reaction to form pyrene-4,5-dione ( <b>31</b> ).....	40
Figure 2.3: Products from attempted Sonogashira reactions with <b>62</b> .....	49
Figure 2.4: Products isolated in the Sonogashira reaction with <b>62</b> .....	50
Figure 3.1: Selected TTFV-based polymers reported by the Zhao group.....	63
Figure 3.2: Predicted structure of polymer <b>86</b> . Alkyl chains omitted for clarity.....	65
Figure 3.3: One of the CV scans of <b>86</b> .....	68

## List of Schemes

Scheme 1.1: Bodwell's general synthetic strategy toward pyrenophanes. ....	16
Scheme 1.2: Bromination reactions of pyrene ( <b>18</b> ).....	19
Scheme 1.3: a) Friedel-Crafts <i>t</i> -butylation of pyrene ( <b>18</b> ) at the 2 and 7 positions. b) Marder's borylation of pyrene ( <b>18</b> ).....	21
Scheme 1.4: a) Oxidation of the K-region of pyrene ( <b>18</b> ). b) Direct arylation at the 4- position ( <b>18</b> ).....	22
Scheme 1.5: Retrosynthesis of <b>2</b> .....	26
Scheme 1.6: Synthetic strategy toward pyrenophane chains.....	28
Scheme 2.1: Synthesis of pyrene-4,5-dione ( <b>31</b> ).....	29
Scheme 2.2: Mechanistic considerations for the RuO <sub>4</sub> oxidation of pyrene ( <b>18</b> ).....	30
Scheme 2.3: An example of an MTO-mediated epoxidation by Sharpless <i>et al.</i> .....	34
Scheme 2.4: Reduction and <i>O</i> -alkylation of a phenanthrenedione <b>54</b> , and the corresponding pyrenedione <b>31</b> .....	43
Scheme 2.5: Modification of the reductive alkylation reaction.....	44
Scheme 2.6: Synthesis of 1,8-dibromo-4,5-bis(tetradecyloxy)pyrene ( <b>62</b> ).....	46
Scheme 2.7: The dialkoxydibromopyrene ( <b>56</b> ) as a substrate for Sonogashira chemistry. .....	47
Scheme 2.8: Synthesis of diiodides <b>69</b> and <b>70</b> . ....	51
Scheme 2.9: Synthesis of the dialkyne <b>67</b> from the corresponding dibromide <b>62</b> and diiodide <b>70</b> . ....	52
Scheme 2.10: Synthesis of diol <b>71</b> from the corresponding diyne <b>67</b> . ....	53

Scheme 2.11: Conversion of diol <b>71</b> to the corresponding ditosylate <b>72</b> and dibromide <b>73</b> . .....	54
Scheme 2.12: S <sub>N</sub> 2 based macrocyclization. (Counterions not shown for clarity) .....	56
Scheme 2.13: Formation of the elimination product ( <b>78</b> ). .....	57
Scheme 2.14: E2 elimination of <b>72</b> or <b>73</b> . .....	58
Scheme 3.1: Redox transformation of TTF.....	60
Scheme 3.2: Redox-controlled conformational switching behavior of diphenyl-TTFV <b>82</b> . The molecular geometries shown in the bottom were optimized at the B3LYP/6- 311G* level of theory .....	61
Scheme 3.3: Synthesis of polymer <b>86</b> . .....	64
Scheme 4.1: Possible cyclization reaction for the formation of <b>2</b> . .....	72
Scheme 4.2: Possible cyclization reactions to form a similar pyrenophane as <b>2</b> . .....	74

## List of Symbols, Nomenclature or Abbreviations

SI units and symbols for elements do not appear in this list of abbreviations.

ASE	aromatic stabilization energy
bipy	2,2'-bipyridine
$\delta$	chemical shift (NMR)
d	doublet
DBU	1,8-diazobicyclo[5.4.0]undec-7-ene
dien	diethylenetriamine
DSC	differential scanning calorimetry
eq	equivalent(s)
ft	foot
h	hour(s)
HOMO	highest occupied molecular orbital
LC-MS	liquid chromatography mass spectrometry
LUMO	lowest unoccupied molecular orbital
m	multiplet
MTO	methyl trioxorhenium
min	minute(s)
MWNT	multi-walled carbon nanotube
NMI	<i>N</i> -methylimidazole
NMR	nuclear magnetic resonance spectroscopy
OLED	organic light-emitting diode

PA	propargyl alcohol
PGSE	pulsed gradient spin-echo
$R_f$	Retention factor
rt	room temperature
s	singlet
SWNT	single-walled carbon nanotube
t	triplet
THF	tetrahydrofuran
tlc	thin layer chromatography
TMSA	tri(methylsilyl)acetylene
TTF	tetrathiafulvalene
TTFV	tetrathiafulvalene vinylogue
UHP	urea / hydrogen peroxide
VID	valence isomerization / dehydrogenation

## Chapter 1: Introduction

Cyclophanes are a class of molecules with a history that spans over sixty years. In their simplest form, a cyclophane consists of one aromatic unit and one bridge, which connects nonadjacent positions of the aromatic system.<sup>3</sup>

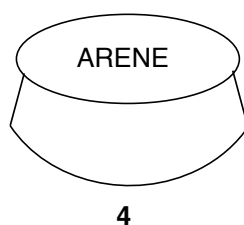


**Figure 1.1:** General structure of a simple cyclophane.

Cyclophane chemistry is a very diverse field, as variations in the aromatic unit and/or the bridge lead to a broad spectrum of molecular structures and properties. With regard to the aromatic unit, both the number and type of aromatic units can be varied from one to any larger number. The aromatic system can be polynuclear, heteroaromatic or homoaromatic, and there are even examples of cyclophanes with antiaromatic or (ironically) nonaromatic "arenes." In considering the bridge, the number of bridges and the length of the bridge can be changed. The number of potential bridging sites (nonquaternary sites) on the aromatic unit(s) limits the number of possible bridges. In most cases, a smaller bridge implies a higher amount of strain. The bridging motif (the set of bridgehead atoms) on the aromatic ring(s) can also be modified. Introducing

heteroatoms, double or triple bonds into the bridge can also lead to great variations in structure and, subsequently, properties and function. The field of cyclophane chemistry is therefore boundless, with very diverse types of compounds having already been reported. Cyclophanes are often thought of as being remarkably beautiful due simply to their structures.<sup>3</sup> A prime example is superphane (**5**), which was reported first by Boekelheide<sup>4</sup> and shortly thereafter by Hopf.<sup>5</sup>

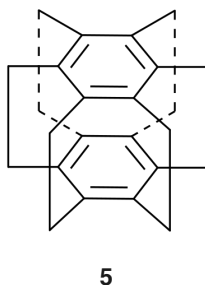


**Figure 1.2:** Superphane (**5**).

Because of the variety in structure and function, cyclophanes are of interest in anywhere from synthetic to theoretical, structural, host-guest, biological, and, materials chemistry. This is apparent in Figure 1.3, where three very different cyclophanes have three different functions.<sup>3</sup> For instance, the metallocyclophane **6** was investigated to probe the effect of completion of an arene by an organometallic fragment on the aromatic ring current.<sup>6</sup> As well, cyclophane **7** is being investigated for potential applications as a biological sensor, or receptor for biological molecules. Contrastingly, cyclophane **8** is synthesized *via* a template synthesis and, using that synthesis, a 2.5 nm cyclophane (consisting of 12 aromatic rings,  $n=2$ ) was prepared.<sup>7</sup>

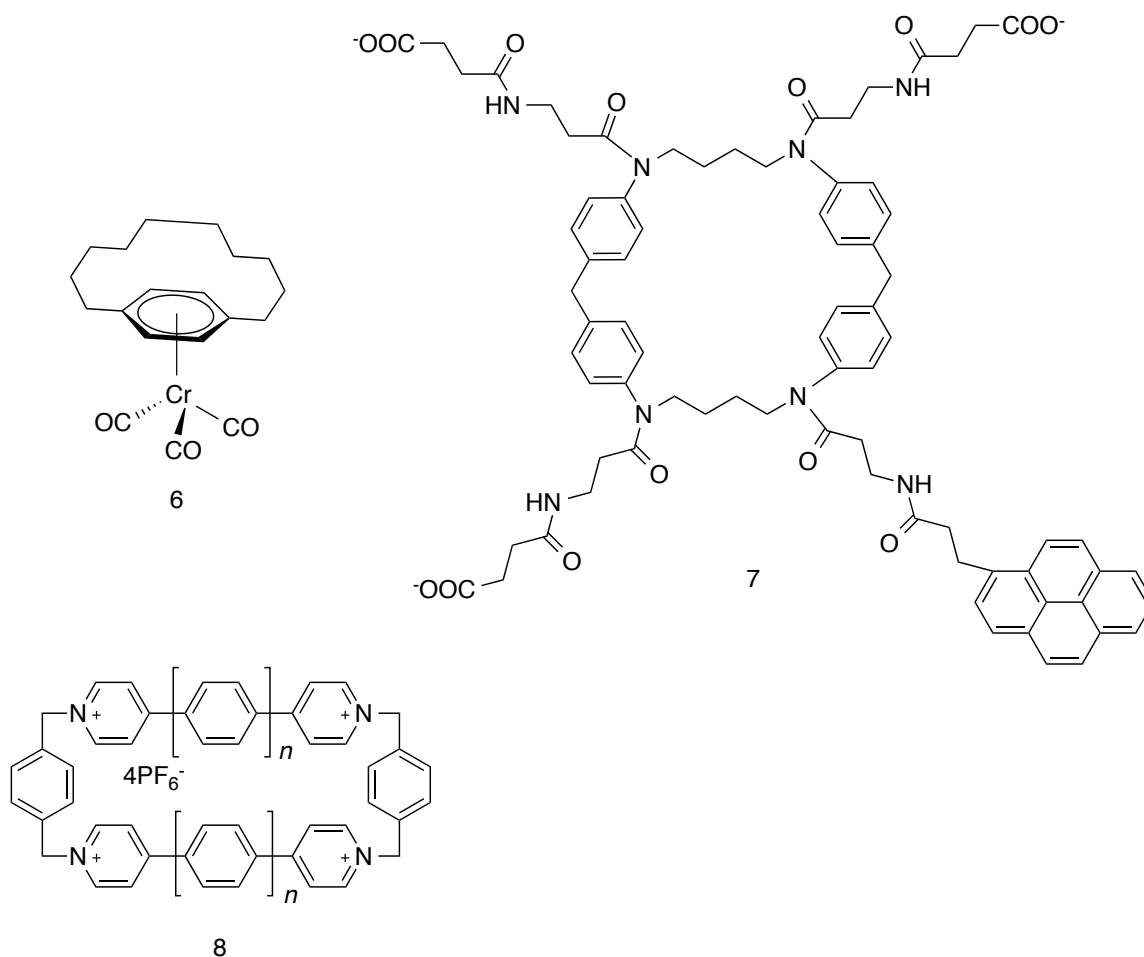


**Figure 1.3:** Examples of cyclophanes with different functions.

The word cyclophane can be broken down in several parts. *Cyclo* refers to the cyclic nature of the molecules. *Ph* corresponds to the term "phenyl", which is meant to represent the aromatic unit. In the very early days of cyclophane chemistry, this was always a benzene ring. *Ane* is representative of the nature of the tether, which in its simplest form is an aliphatic chain. The first reported example of a cyclophane, [2.2]paracyclophane, **9**, (Figure 1.2), was fortuitously discovered by Brown and Farthing

in 1949, who prepared it in trace amounts by high temperature pyrolysis of *p*-xylene. Its structure was established using X-ray crystallography.<sup>8</sup>

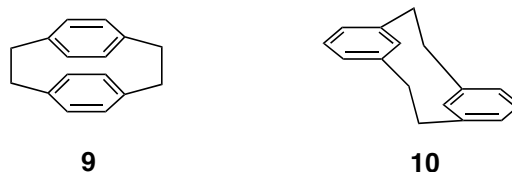
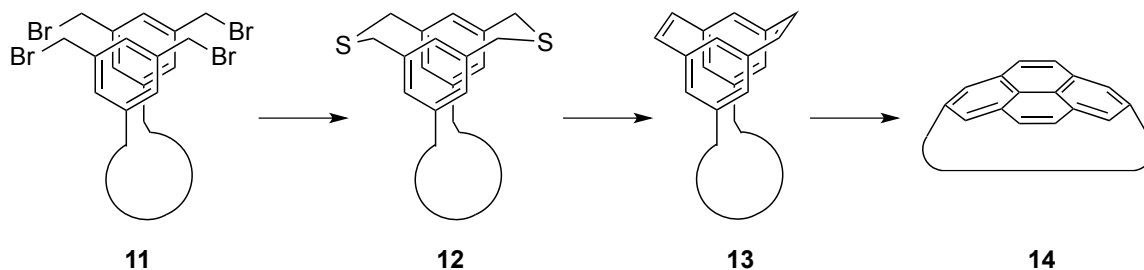


**Figure 1.4:** [2.2]Paracyclophane (**9**) and *anti*-[2.2]metacyclophane (**10**).

Although Pellegrin likely synthesized *anti*-[2.2]metacyclophane (**10**) in 1899,<sup>9</sup> [2.2]paracyclophane (**9**) was the first reported cyclophane with correctly assigned structure, and this marked the dawn of cyclophane chemistry as a distinct field. Shortly thereafter, Cram and Steinberg published a rational synthesis of the [2.2]paracyclophane (**9**).<sup>10</sup> A very striking feature of the structure of [2.2]paracyclophane (**9**) is that the benzene rings are boat-shaped. Indeed, the presence of nonplanar aromatic rings took the concept of aromaticity into the third dimension. The departure from the long and firmly held belief that aromatic molecules must be planar generated a great deal of interest in the field. Cyclophanes became desirable targets due to a number of other attractive reasons, including synthetic challenge, strain and its implications, symmetry, conformational behaviour, and unusual chemical and physical / spectroscopic properties. Today, this subject area continues to evolve and, as alluded to earlier, function is becoming a primary driver of research interest. In any case, cyclophane chemistry remains an actively investigated field of modern chemistry.<sup>3</sup>

The Bodwell group has been interested in cyclophane chemistry for the past two decades. More specifically, the focus has been on cyclophanes that have pyrene as the aromatic moiety, *i.e.* pyrenophanes. The Bodwell group is known for its synthesis and study of these molecules, and has numerous publications in the field.<sup>11-15</sup> The general synthetic strategy for the synthesis of these molecules involves the construction of a tetrabromide **11**, in which two 1,3-bis(bromomethyl)benzene units are joined by a tether of variable composition (Scheme 1.1).



**Scheme 1.1:** Bodwell's general synthetic strategy toward pyrenophanes.

Tetrabromide **11** is then converted into a cyclophanediene **13** by way of the corresponding dithiacyclophane **12**. The formation of the pyrene unit is accomplished in the final step through a valence isomerization / dehydrogenation (VID) reaction from the corresponding [2.2]metacyclophanediene.<sup>14</sup> This reaction has proved to be very powerful. It owes its success to several factors,<sup>14</sup> including the thermally allowed nature of the valence isomerization in the [2.2]metacyclophanediene system (a suprafacial  $6\pi$  electrocyclic ring closure), the formation of a new C–C bond, the formation of a new pyrene system (*ca* 75 kcal/mol of aromatic stabilization energy (ASE)) and the relative

insensitivity of the aromaticity of the pyrene system to bending out of planarity.<sup>14</sup> As such, this strategy has been successfully employed in the syntheses of a variety of pyrenophanes (Figure 1.5).

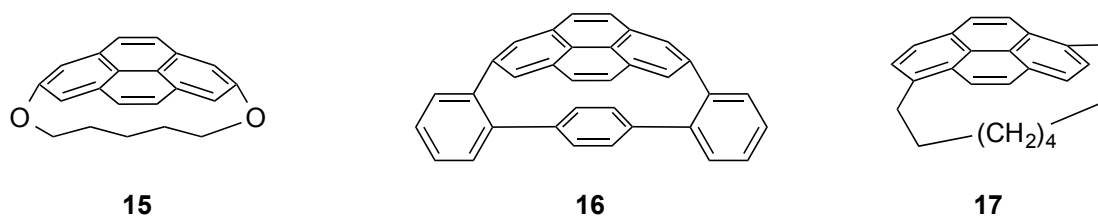


**Figure 1.5:** Selected Bodwell group pyrenophanes.

The first example is 1,8-dioxa[8](2,7)pyrenophane (**15**), which was synthesized by Mannion.<sup>11</sup> Its bridge is seven atoms in length, two of which are oxygen atoms, and it joins at the 2,7 positions on pyrene. The pyrene system is more bent than the one that can be identified in the equator of  $D_{5h}$   $C_{70}$ . The next example, **16**, which was synthesized by Zhang, is quite different.<sup>13</sup> Its bridge consists of three phenylene units, and it is an example of pyrenophane consisting of only  $sp^2$ -hybridized carbon atoms. The third example **17** is different again from the other two. Synthesized by Yang,<sup>15</sup> it is a  $C_2$ -symmetric, and therefore chiral, [10](1,6)pyrenophane.

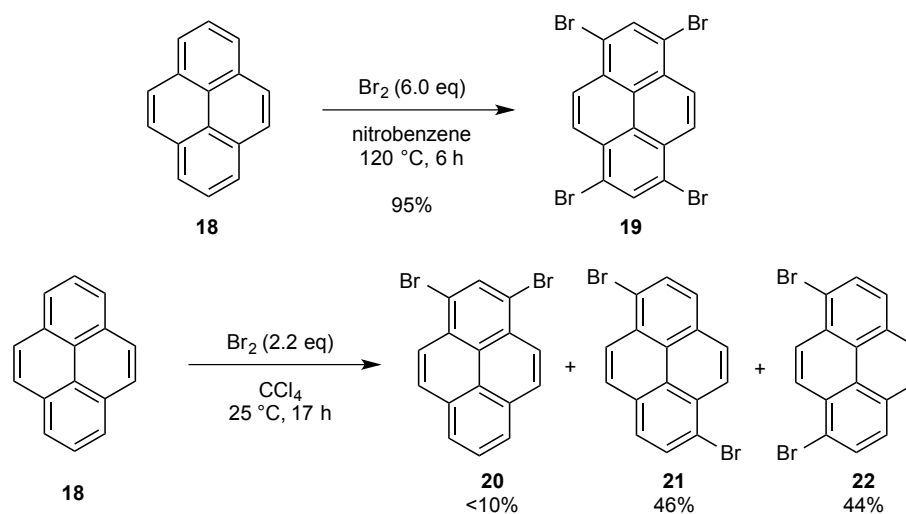
All of the syntheses leading to the pyrenophanes described above rely on the aforementioned strategy shown in Scheme 1.1. Despite pyrene being the aromatic moiety in the cyclophanes created within the Bodwell group, no pyrene derivative has ever been

used in any of the syntheses. In all cases, the nonplanar pyrene system is formed during the VID reaction.

One of the aims of the work described in this thesis is to use pyrene itself as a starting material in the synthesis of a pyrenophane. Importantly, this requires the selection of relatively unstrained pyrenophane targets. Whereas the formation of a bent (and therefore strained) pyrene can be accomplished using the very powerful VID reaction, the energy required to bend the pyrene unit in some pyrenophane precursor would be expected to pose a serious impediment to any cyclization reaction leading to the corresponding pyrenophane. Moreover, understanding the reactivity of pyrene and being able to substitute it in a controlled manner becomes important.

Pyrene was first isolated as the highest boiling extract from coal tar in 1876.<sup>16</sup> It is the smallest *peri*-fused benzenoid polycyclic aromatic hydrocarbon and is of particular interest due to its unique photophysical properties.<sup>1</sup> Not only does it have a high quantum yield (0.65 in ethanol),<sup>17</sup> but its fluorescence is also quite sensitive to its environment. Consequently, it has been used in a variety of sensing applications. In fact, it has been dubbed the “gold standard” in molecular recognition by Figuera-Duarte and Müllen.<sup>1</sup> Pyrene has a reasonably large aromatic surface and can participate in both  $\pi$ -stacking and favorable CH- $\pi$  interactions. Therefore, it has been exploited frequently in noncovalent functionalization of extended planar  $\pi$ -systems, such as carbon nanotubes and graphene.<sup>18</sup>

Pyrene readily undergoes electrophilic substitution at the 1, 3, 6 and 8 positions. These are the most electron-rich centres and are predicted to be the most reactive by calculations on Wheland intermediates.<sup>19</sup> As expected, pyrene undergoes bromination at 120 °C to yield 1,3,6,8-tetrabromopyrene (**19**) in high yield. However, what is perhaps more synthetically useful (especially for cyclophane synthesis) is a disubstituted pyrene derivative. However, this is not a straightforward exercise. For example, upon reducing the amount of bromine to 2.2 equivalents, Vollhard *et al.* obtained a mixture of constitutional isomers: the 1,3-, 1,6-, and 1,8-dibromopyrene products (**20-22**, Scheme 1.2).<sup>20</sup> Separation of these isomers is difficult and time consuming, and it is possible to obtain gram quantities of the 1,6- and 1,8-products through repeated crystallization.<sup>21</sup> What would be more useful for the synthetic community is an easier method to obtain these disubstituted pyrenes, for they are valuable building blocks for the synthesis of various types of extended  $\pi$ -systems.<sup>18</sup>



**Scheme 1.2:** Bromination reactions of pyrene (**18**).

There are limitations to the use of pyrene to obtain disubstituted pyrenes. There is a lack of well-known methodology and therefore diverse substitution patterns are difficult to obtain, especially directly from pyrene.<sup>1,18</sup> Because of these limitations, indirect methods are often used to synthesize substituted pyrene, relying on precursors like tetrahydropyrene, hexahydropyrene, metacyclophanes, naphthalene, and functionalized biphenyls.<sup>18</sup>

As previously mentioned, pyrene is activated towards electrophilic aromatic substitution

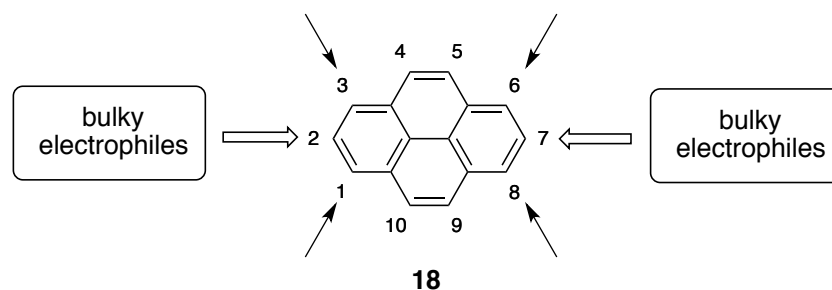
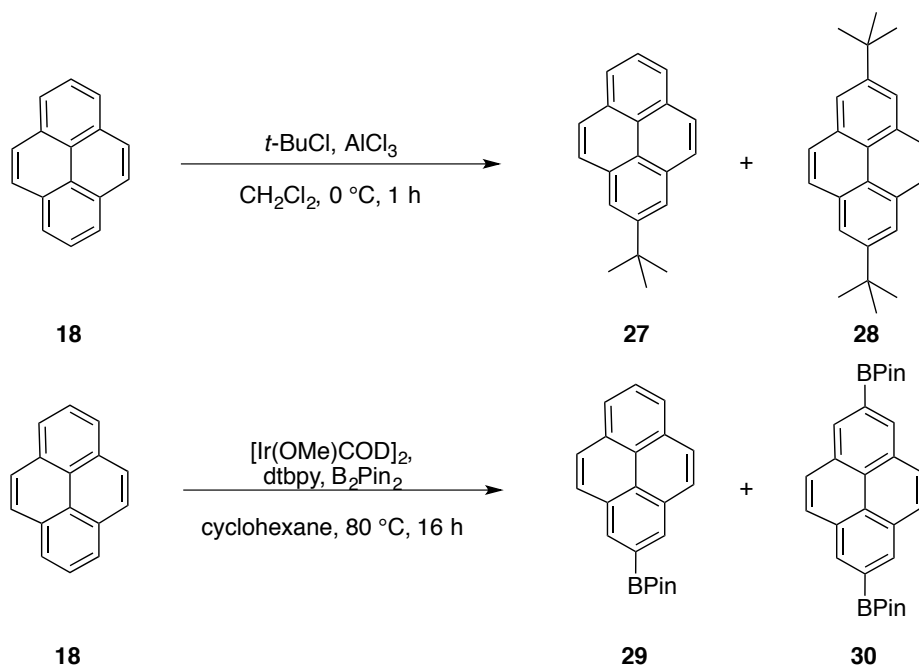


**Figure 1.6:** Preferred sites of electrophilic aromatic substitution on pyrene (**18**).

at the 1, 3, 6 and 8 positions. Originally reported by Ogino, the synthesis of simple tetrahalogenated and cyanated pyrenes has been shown, as well as monosubstitution.<sup>22</sup> However, reducing the number of molar equivalents of the electrophile to 2 or 3 leads to a hard-to-separate mixture of regioisomers. Therefore, using direct electrophilic aromatic substitution, it is hard to prepare patterns other than 1-substituted or 1,3,6,8-tetrasubstituted pyrenes. Furthermore, many of these tetrasubstituted products have very low solubility, rendering isolation, purification, characterization, and further synthetic

transformations difficult. For instance, the compounds reported by Ogino were purified by high temperature vacuum sublimation ( $> 300\text{ }^{\circ}\text{C}$ ).<sup>22</sup>

The 2 and 7 positions on pyrene can also be substituted with very high selectivity using electrophilic aromatic substitution, but only bulky electrophiles (*e.g.* *t*-butyl cation generated from *t*-butyl chloride and  $\text{FeCl}_3$ )<sup>23</sup> will react in this manner. The origin of the selectivity over the much more electronically activated 1, 3, 6 and 8 positions is that they (and the 4, 5, 9, and 10 positions) are all sterically congested *peri* positions. In combination with a bulky electrophile, there is a drastic reduction in the rate of reaction at these sites.

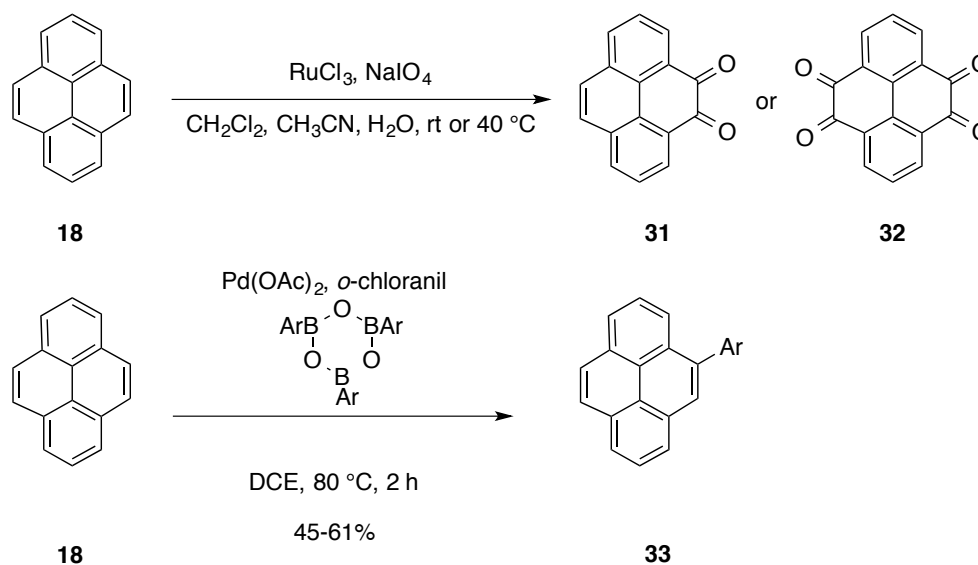


**Scheme 1.3:** a) Friedel-Crafts *t*-butylation of pyrene (**18**) at the 2 and 7 positions.

b) Marder's borylation of pyrene (**18**).

Alternatively, Marder *et al.* found that iridium-catalyzed borylation occurs exclusively at the 2 and 7 positions (Scheme 1.3).<sup>24</sup> Again, steric crowding at the 1, 3, 6 and 8 positions (as well as the 4, 5, 9, and 10 positions) is responsible for the complete selectivity at the 2 and 7 positions.

The 4, 5, 9 and 10 positions (K-regions) of pyrene can be oxidized in the presence of a ruthenium salt to give the 4,5-dione (**31**) or the 4,5,9,10-tetraone (**32**) in fair yield (45% and 36% respectively).<sup>25</sup> Itami *et al.* have also recently reported the direct arylation at the 4-position *via* a palladium catalyst (Scheme 1.4).<sup>26</sup>



**Scheme 1.4:** a) Oxidation of the K-region of pyrene (**18**). b) Direct arylation at the 4-position (**18**).

Although it is possible to directly substitute pyrene (**18**) at each of its positions, the situation becomes more complicated when even a single substituent is present. Therefore, often times, one undertakes a more labor-intensive, indirect method to obtain a particular multifunctionalized pyrene. This typically involves the construction of the pyrene system along the way.<sup>18</sup>

Recently within the Bodwell group, methodology was developed that leads exclusively to 1,8-dibromopyrene derivatives in high yield.<sup>2</sup> The positioning of alkoxy groups in the 4 and 5 positions on pyrene both activates the pyrene system towards electrophilic substitution and effectively hinders the 3 and 6 positions. This methodology was used in the synthesis of 1,8-pyrenylene-ethynylene macrocycles such as **34**.<sup>2</sup> The synthetic plan for the work described in this thesis is based on this methodology.

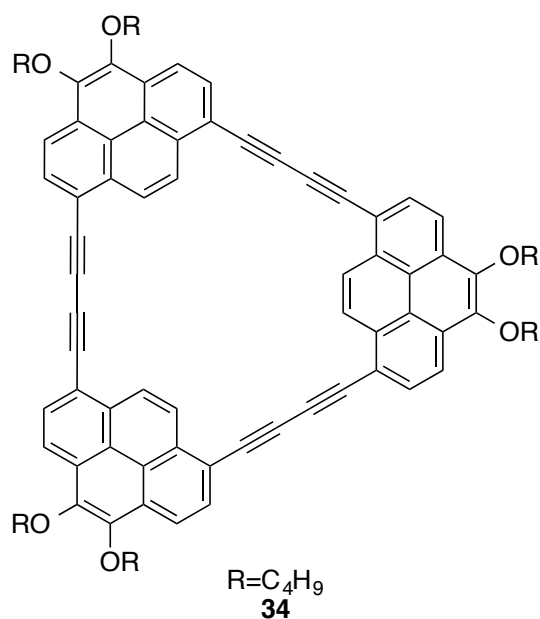


**Figure 1.7:** A 1,8-pyrenylene-ethynylene macrocycle (**34**).

The objective of this work is to develop an iterative strategy for the synthesis of a family of oligomeric (1,8)pyrenophanes (**3**) with potential application as sensors (Figure 1.8). The three key design elements are i) the repeating 1,4,5,8-tetrasubstituted pyrene system, ii) the flexible bridges that connect adjacent pyrene systems and iii) the side chains attached to one of the terminal pyrene units.

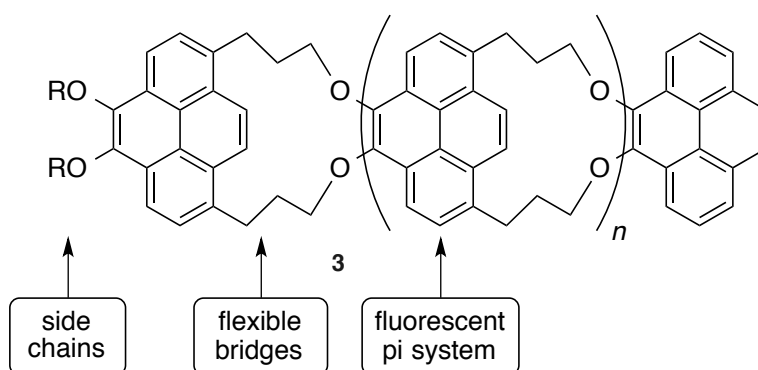


**Figure 1.8:** Target pyrenophanes and their key design elements.

As discussed earlier, pyrene is strongly fluorescent and its fluorescence behaviour is very sensitive to its environment. Whereas most sensors have a pyrene unit attached as an appendage, the intention here is to build the sensor around pyrene and rely upon excimer formation and/or the presence of guest molecules to generate an output. Four-atom bridges were chosen for initial work because they are sufficiently long as to impart very little strain into each pyrenophane system. This should not only permit the use of pyrene as a starting material, but also confer good conformational mobility to the pyrenophane

units. This mobility will presumably allow for easy access to both *syn* and *anti* conformations, as illustrated for the simplest of the targeted pyrenophanes **2** (Figure 1.9). Whereas the *anti* conformer would be expected to exhibit normal pyrene fluorescence, the *syn* conformer may exhibit excimer fluorescence. According to simple molecular models, the *syn* conformer is flexible enough to open up enough to receive a planar guest molecule such as an aromatic system, *e.g.* a nitroarene, dioxin, phenol, or caffeine. If the fluorescence of the system containing a guest differs from that of both the free *syn* and *anti* conformers, then this could form the basis of a sensor. With larger values of  $n$ , the conformational behavior becomes more complicated, as each pyrenophane unit has its own *syn* and *anti* conformations. However, the possibility of having an especially sensitive response arises. Although somewhat speculative, this may result from changes from an *all-anti* conformation to a guest-containing *all-syn* conformation, which would have all of the pyrene units (and guests) stacked in a column.

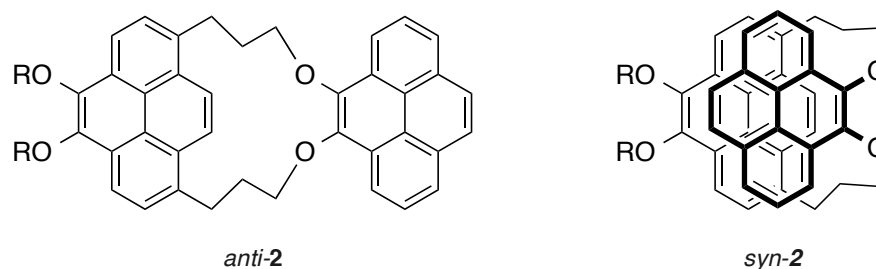
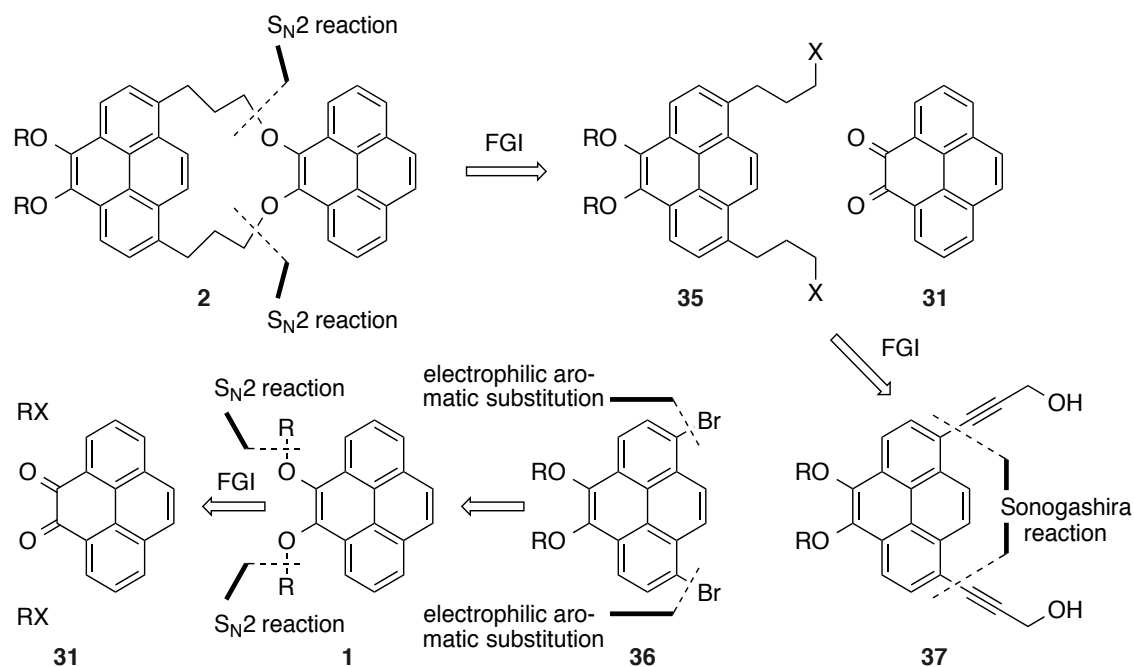


**Figure 1.9:** *Anti* and *syn* conformers of **2**.

The side chains (–OR) were initially included in the design for the purpose of maintaining solubility as the value of  $n$  becomes larger, but they may eventually prove to be more

useful. One possibility would be to change the side chains from alkoxy groups to polyether chains in order to promote water solubility. The incorporation of stimuli-responsive units as a means to control the conformation of the pyrenophane(s) should also be borne in mind once the target systems have been synthesized and shown to exhibit desirable sensing properties.

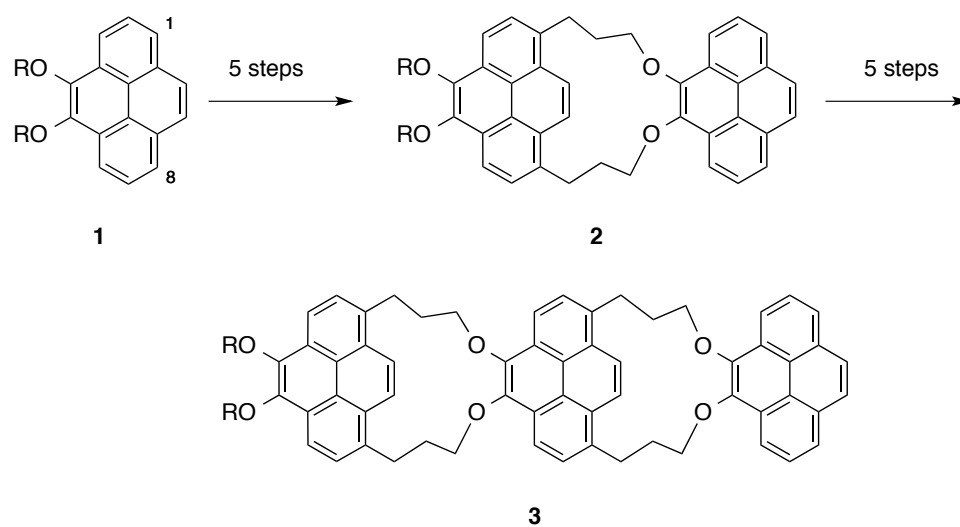
The design of the target systems **2** was heavily influenced by the pyrene chemistry described earlier. The reasons for this are i) to minimize the number of synthetic steps needed to construct a suitably unstrained and flexible pyrenophane and ii) to make the synthesis iterative in nature. The retrosynthetic analysis for pyrenophane **2** represents a single iteration (Scheme 1.5).



**Scheme 1.5:** Retrosynthesis of **2**.

An *O*-alkylation reaction ( $S_N2$  reaction) was chosen as the key cyclophane-forming step in the synthesis pyrenophane **2**. This leads back to dihalide **35** and pyrene-4,5-dione (**31**), which can be reduced to the corresponding diol directly prior to *O*-alkylation. There is ample precedent for the use of  $S_N2$  chemistry in cyclophane synthesis as a wide range of other unstrained cyclophanes, especially thiacyclophanes,<sup>3,5,14</sup> have been accessed using this type of reaction. From **35**, functional group interconversion leads back to diyne **37**, which now contains retrons for the Sonogashira cross-coupling reaction. Application of this transform brings the analysis back to dibromide **36**, which then leads back to 4,5-dialkoxypyrene **1** via completely regioselective electrophilic bromination (discussed in detail in the following Chapter). In exactly the same way that pyrenophane **2** went back to **35** and **31**, 4,5-dialkoxypyrene **1** leads back to dione **31** and a primary alkyl halide.

The iterative nature of the synthetic strategy relies upon the success of the regioselective electrophilic bromination of pyrenophane **2** at the two positions analogous to those in 4,5-dialkoxypyrene **1**. As such, the second iteration leading to pyrenophane **2** (Scheme 1.6) would consist of five steps: i) bromination, ii) Sonogashira reaction, iii) catalytic hydrogenation, iv) conversion of the alcohols to halides (or pseudohalides) and v) reduction and *O*-alkylation of dione **31** to afford pyrenophane **3**. At this point, another iteration could be initiated by electrophilic bromination, which would again be expected to occur with high selectivity at the same positions on the terminal pyrene system.

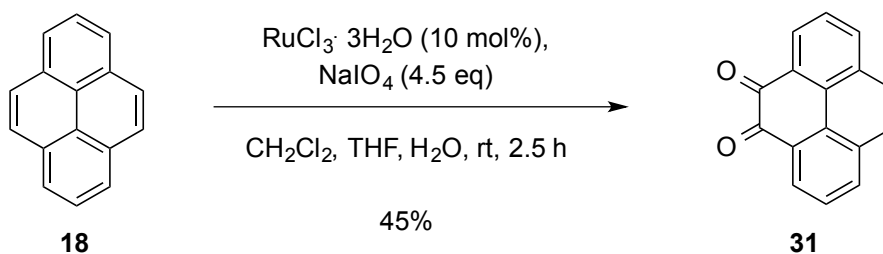


**Scheme 1.6:** Synthetic strategy toward pyrenophane chains.

At the outset of this project, the aim was to complete as many iterations as possible in the time available, to study the conformational behavior of the pyrenophanes and to investigate their sensing properties towards a selection of analytes.

## Chapter 2: Results and Discussion

To commence this project, pyrene-4,5-dione (**31**) was required. Although **31** is a commercially available compound, it is prohibitively expensive (\$105 for 25 mg<sup>\*</sup>) to serve as a starting material for multistep synthesis. It can be synthesized directly from pyrene (**18**), the most recent procedure having been reported by Harris *et al* in 2005.<sup>25</sup> A slight modification of this procedure was subsequently reported by Bodwell *et al.*,<sup>2</sup> who found that changing the solvent system from water, chloroform and acetonitrile to water, dichloromethane and tetrahydrofuran lessened the reaction time from 18 h to 2.5 h (Scheme 2.1). In either case, the reaction is rather low yielding (40–45%), but this is certainly acceptable considering the high cost of dione **31** and the direct access to a 4,5-difunctionalized pyrene. Indeed, until very recently, this was the only reaction that selectively functionalized pyrene (**18**) in the 4 and 5 positions.

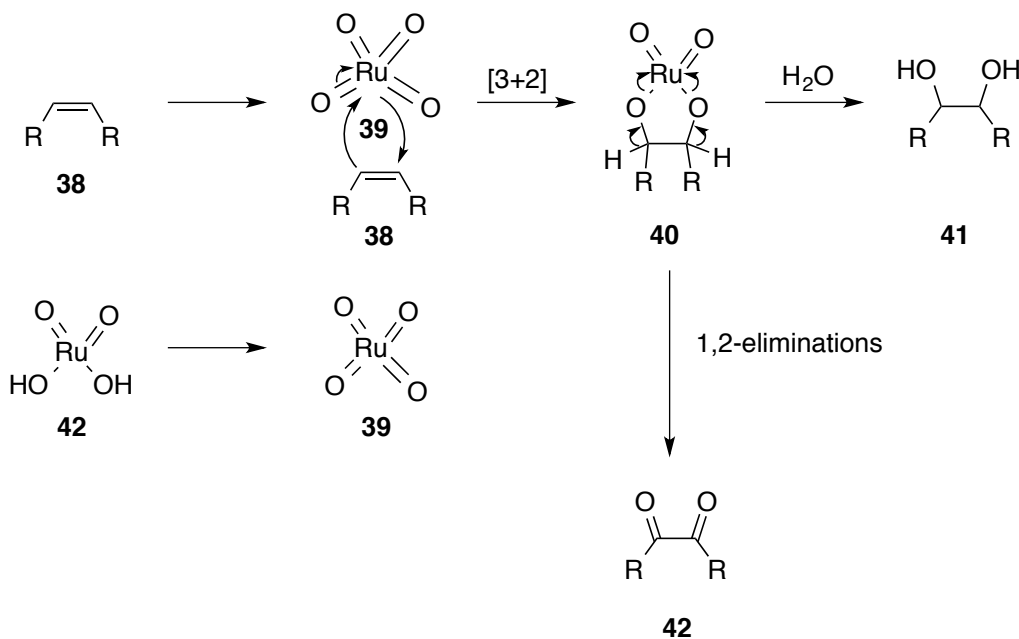


**Scheme 2.1:** Synthesis of pyrene-4,5-dione (**31**).

---

\* Sigma Aldrich, April 2014

With regard to the suggested mechanism of the reaction, ruthenium tetroxide (**39**, the active oxidant) is presumably generated *in situ* from ruthenium trichloride hydrate and sodium periodate. It has been proposed that  $\text{RuO}_4$  (**39**) reacts with pyrene in the way that osmium tetroxide reacts with alkenes, *i.e.* by a [3+2] cycloaddition at the K region of pyrene.<sup>27,28</sup> However, the osmium tetroxide mechanism usually yields 1,2-diols (*e.g.* **41**) or, as in the case of the Lemieux-Johnson oxidation, aldehydes.<sup>29-31</sup> The mechanism leading to the diketone formation has not been established, but two 1,2-eliminations from cyclic ruthenate **40** does not seem unreasonable (Scheme 2.2).



**Scheme 2.2:** Mechanistic considerations for the  $\text{RuO}_4$  oxidation of pyrene (**18**).

From a practical perspective, the isolation of the product in pure form was found to be very problematic and, as explained in detail below, this limited the scale of the reaction to roughly 2 g of pyrene (**18**). After the 2.5 h reaction, a considerable amount of an insoluble black-green residue was present and this needed to be removed by filtration. The tar-like nature of the residue made filtration difficult because the commercially available filter paper (even the most porous one available – Macherey-Nagel 616<sup>†</sup>) quickly became clogged. Through some experimentation, it was found that the use of three layers of paper towels (Merfin Vicel) was more effective.<sup>‡</sup> Nevertheless, the filtration was still slow and several washings (4-6) were usually required to extract the majority of the product from the residue. Moreover, it still did not result in the complete removal of the residue, as it often remained in the organic layer until drying and subsequent gravity filtration.

Once dry, the residue had a chalk-like consistency on top and the lower layers were more comparable to tar. The identity of this residue was not investigated. It could contain oxidized chloro impurities (from the RuCl<sub>3</sub>, which was found to be a less favorable and/or over-oxidation of pyrene. Although it has been suggested that using ruthenium dioxide in the place of ruthenium trichloride would result in less residue,<sup>28</sup> an earlier publication by

---

<sup>†</sup> MN 616 ø 150 mm, Art.-Nr: 432 015, Lot 10177.06

<sup>‡</sup> Suction filtration using filter paper was found to proceed extremely slowly. The use of Celite® was also investigated, but paper towels proved to be most effective.

Dixon *et al.*<sup>27</sup> describing this reaction reported that this modification was non-specific, with oxidation occurring at positions other than the 4 and 5 positions. It was not stated whether or not a residue formed, but several products were said to be formed, including two different dione products (*i.e.* **31** and **44**), a lactone (**43**) and an unidentified aldehyde (**45**, Figure 2.1). Harris *et al.*<sup>25</sup> also did not report the presence of any residue, but they did report the formation of several other byproducts, none of which were identified.

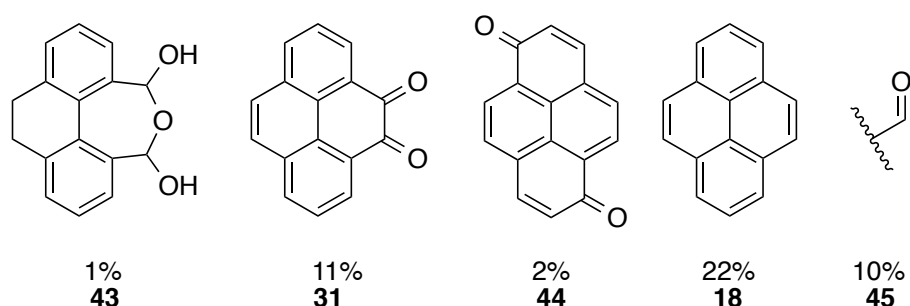


**Figure 2.1:** Pure compounds isolated by Dixon *et al.* from the oxidation of pyrene (**18**).

Several impure mixtures, including one of the lactone **43** and unknown aldehyde **45** were also obtained.

The problems with filtration were not the sole issues with the reaction leading to **31**. For a start, identifying the optimal time to stop the reaction is tricky. Waiting for the complete consumption of pyrene (**18**) is futile because the product **31** eventually starts to be consumed faster than the pyrene. It was found that the first signs (tlc analysis) of the formation of a byproduct ( $R_f = 0.34$ , dichloromethane) was the best time to stop the reaction and move onto filtration.

During the extraction that followed the filtration, the remaining residue not only pervaded both layers, but also adhered to the sides of the separatory funnel. This and the dark color of both layers made extraction a difficult task, because it was difficult to see the phase change. On top of that, the reaction was found to be quite sensitive to variations in temperature, scale, and the addition rate of NaIO<sub>4</sub>, all of which adversely affect the yield. If the reaction was heated, there was an increase in by-product formation and a corresponding reduction in yield. For contrast, when the reaction was chilled (cold tap water in a jacketed flask, or an ice bath), product formation was greatly reduced, along with the rate of the reaction. Sodium metaperiodate was found to dissolve exothermically in water. Therefore, the rate of addition of sodium metaperiodate was important: too fast, and the reaction heated up, leading to the aforementioned observed decrease in yield.

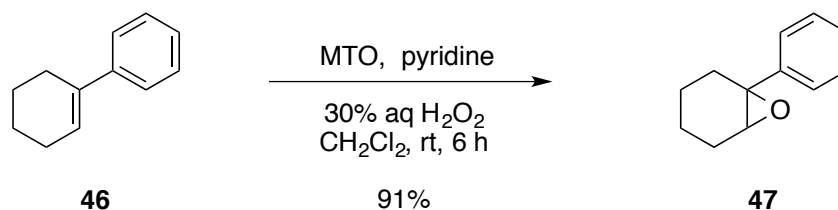
For the first year of this project, the problems associated with the oxidation of pyrene (**18**) to give pyrene-4,5-dione (**31**) were simply (but grudgingly) accepted as an inevitable limitation of this synthesis. By whatever mechanism, some of the 4.5 equivalents of sodium periodate is reduced to iodine during the reaction, as evidenced by the pink colour of the solvent in the collection flask of the rotary evaporator during the work-up and the more intense pink-purple fraction from the column.<sup>§</sup> A thiosulfate wash was incorporated into the work-up, to quench the iodine and this rendered the work-up and purification

---

<sup>§</sup> If this iodine co-mingles with the product **31** it appears as more of a brown-orange solid.

slightly easier. The time and effort required to generate synthetically useful amounts of this key starting material were obvious impediments to progress and there was a clear need for an improved procedure.

The use of *N*-heteroaromatic additives has precedent in related oxidation chemistry using rhenium, specifically methyltrioxorhenium (MTO).<sup>32,33</sup> For example, Trost and Sharpless separately found that adding pyridine to their reaction mixtures served to both “clean up” the reaction and increase turnover numbers (Scheme 2.3). Although in both cases the additive used was pyridine, there have been a number of reports of the effectiveness of aliphatic and aromatic nitrogen donor ligands, such as *N*-methylimidazole, pyridine and urea / hydrogen peroxide (UHP).<sup>34–37</sup>



**Scheme 2.3:** An example of an MTO-mediated epoxidation by Sharpless *et al.*<sup>33</sup>

In each case, the nitrogen-donor ligands were found to enhance the stability of the rhenium complexes. The adducts containing aromatic *N*-donor ligands were found to be significantly more stable than those of the aliphatic ones. This may be attributable to the fact that aromatic *N*-donor ligands are softer bases than the corresponding aliphatic ones,

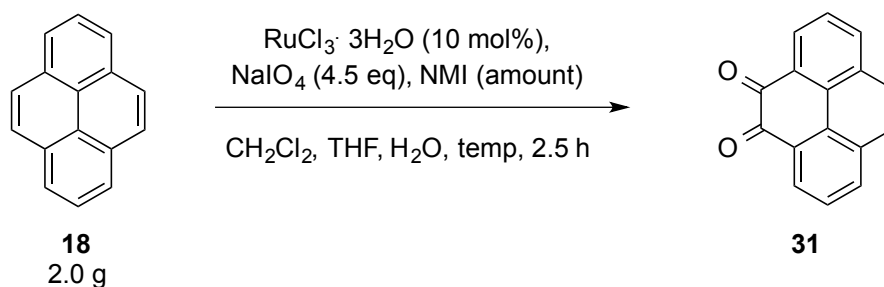
and therefore form more stable complexes with soft transition metal ions.<sup>37</sup> It was also observed that there were no significant advantages to using aromatic bidentate ligands over monodentate ligands with respect to their catalytic activity and to the stability of their peroxy species.<sup>34</sup> The coordination of the ligands to the rhenium center influences the stability, steric environment, and chemical behavior at the metal. These effects all contribute to the catalytic activity of the metal complex, but not necessarily in a cooperative or easily predictable fashion. Thus, it can be a hit-and-miss exercise to find an effective additive for a metal-mediated oxidation reaction.

Based on a suggestion by Dr. J. P. Lumb (McGill University), the use of *N*-methylimidazole (NMI)<sup>\*\*</sup> as an additive was then investigated for the conversion of **18** to **31** (Table 2.1). Three different loadings (1, 5 and 10 mol%) of NMI were investigated in the reaction. It was found that adding 5 mol% of NMI to the reaction not only reduced the amount of the precipitate formed, but also increased the yield from 45% to 52% (Entry 2). It is unclear as to whether the small increase in yield was due to the direct involvement of the NMI in the conversion of **18** to **31** or because more of the product could be extracted from the cleaner reaction mixture. Both 1 and 10 mol% loadings resulted in a decrease in the amount of the unwanted residue, but had little to no effect on yield (Entries 1 and 3). Therefore, with a more manageable work-up in hand, attempts to scale-up the reaction were undertaken, using 5 mol% of NMI.

---

<sup>\*\*</sup> This suggestion came during a poster session at a conference.

Although the increase in yield was modest, the substantial decrease in the amount of residue that formed changed the work-up and purification from being messy and time-consuming to straightforward. The drastic difference opened up the possibility of increasing the scale of the reaction and thus enabling the more-efficient production of multigram quantities of pyrene-4,5-dione (**31**).



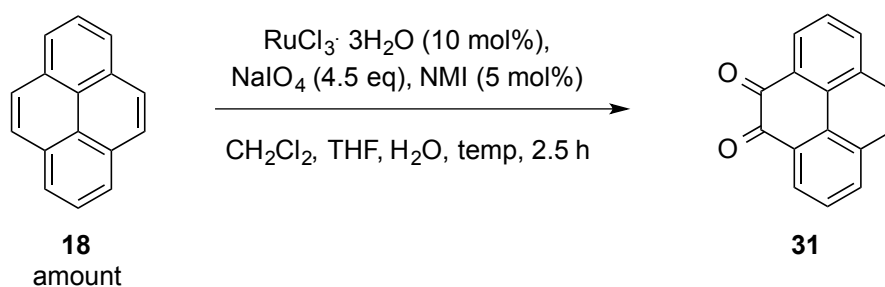
Entry	Ligand (mol%)	Yield (%)	Temperature (°C)
1	1	44	25
2	5	52	25
3	10	45	17

**Table 2.1:** Optimization of the loading of NMI in the oxidation of pyrene (**18**).

On a 2 g scale, all of the reactions with the NMI as an additive were worked up after 2.5 h. Suction filtration yielded very little of the aforementioned residue, and work up was much cleaner overall. In fact, when it came time to purify the product *via* column

chromatography, a short column (3 × 6 cm) could be used instead of the normal dimensions (3 × 20 cm). Pyrene-4,5-dione (**31**) was isolated in 52% yield (Entry 2).

The 2 g scale reaction requires a combined 130 mL of solvent. An attempt was made to reduce this amount by half before further scale-up (Entry 1, Table 2.2). However, the yield was slightly reduced (41%), and the work-up was less clean, and therefore more difficult. Therefore, it was decided to keep the original concentration for further scale-up attempts.



Entry	Pyrene, <b>13</b> (g)	$\text{RuCl}_3 \cdot 3\text{H}_2\text{O}$ (g)	$\text{NaIO}_4$ (g)	Yield (%)	Temperature (°C)
1	2.00	0.27	9.52	52	25
2	5.00	0.67	23.78	51	21
3	10.68	1.42	50.36	49	25
4	25.33	3.51	125.69	52	25
5	100.57	13.29	478.48	41	22
6	5.00	0.67	23.79	55	24

**Table 2.2:** Optimization of the scale of the reaction to form pyrene-4,5-dione (**31**).

Next, a 5 g scale reaction was attempted. As with the 2 g scale, the reaction was stopped after 2.5 h, there was a drastic reduction in the precipitate compared with the original reaction conditions, and the work-up was far cleaner. The yield remained constant at 51% (Entry 2), and it was decided to scale-up further. At the 10 g scale, there was still less precipitate than in the original 2 g reaction mixture, and the work-up remained clean. The yield of pyrene-4,5-dione (**31**) was 49% (Entry 3).

Next, a 25 g scale reaction was attempted. To facilitate stirring, a mechanical stirrer was used instead of the magnetic stirrer. The reaction was again stopped after 2.5 h, and only a small amount of precipitate was formed. Even at this scale, there was less precipitate formed than there was in the original 2 g reaction without the NMI! With a yield of 52% (Entry 4), this scale proved to be the most convenient at the lab setting. Larger scale reactions would call for the use of large glassware (round-bottomed flasks, separatory funnels, *etc.*) that was not readily available in the Bodwell laboratory.

As a proof of concept, a 100 g scale reaction was also performed. This was a rather daunting undertaking, for it required much larger equipment, much of which was improvised. The reaction was conducted in a 12 L three-neck round-bottomed flask, using a mechanical stirrer and a combined 6.5 L of solvent. Suction filtration required a large quantity of dichloromethane, and it was quite difficult to wash out the product (**31**) from the residue due to the massive scale of the reaction. In an attempt to extract the product more efficiently, an industrial-sized Soxhlet apparatus was obtained, and the

residue from the suction filtration (along with the paper towels) was loaded into it using cotton plugs instead of a thimble, and dichloromethane as the extraction solvent. The Soxhlet extraction resulted in the isolation of an additional 32 g of crude material before the column chromatographic step needed. The next obstacle with this reaction scale was to concentrate the fractions before purifying *via* column chromatography. Approximately 30 L of solvent needed to be removed under reduced pressure, which would have required an inordinate amount of time using the rotary evaporators in the Bodwell lab. Therefore, once again the Soxhlet apparatus was used, this time as a makeshift distillation apparatus; shortly before the collected solvent ran back down, it was emptied. Once the product was adsorbed onto silica gel, column chromatography was performed, using a large column and resulting in a 41% yield (Entry 5). Although this reaction can be performed on a 100 g scale, this scale is far too large and cumbersome an undertaking. The 25 g scale is about as large as can be performed comfortably in a typical lab setting.

To compare the Soxhlet extraction with the traditional extraction in this reaction on a more manageable scale, a 5 g reaction was conducted. Soxhlet extraction accounted for a 5% increase in the yield to give a total yield of 55% (Entry 6).

A series of experiments was then performed (Table 2.3) to try to deduce the role of the NMI in the reaction. The ligand was varied, to see if the same result could be attained with a different additive.

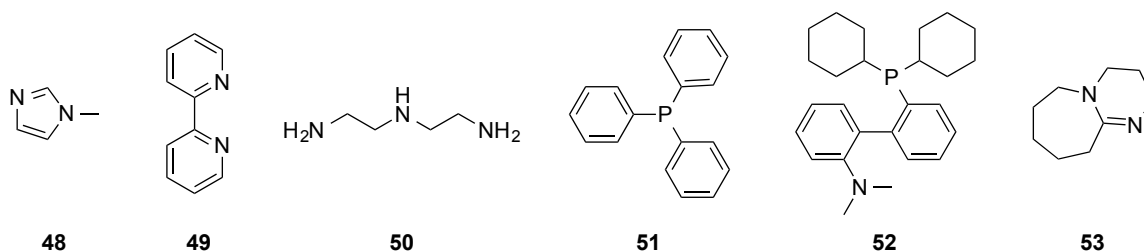
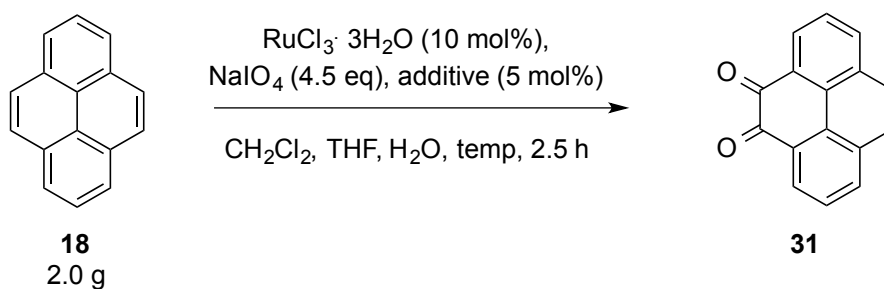


**Figure 2.2:** Ligands used as additives in the reaction to form pyrene-4,5-dione (**31**).

Two other nitrogen-donor ligands with varying denticities were also tried. 2,2'-Bipyridine (bipy, **49**), and diethylenetriamine (dien, **50**) were both used at the optimal loading for NMI (5 mol%), and while they both brought about a decrease in the amount of the residue that formed, they had no beneficial effect on yield (Entries 1 and 2).



Entry	Ligand	Yield (%)	Temperature (°C)
1	bipy ( <b>49</b> )	43	26
2	dien ( <b>50</b> )	43	21
3	PPh <sub>3</sub> ( <b>51</b> )	36	23
4	DavePhos ( <b>52</b> )	45	21
5	DBU ( <b>53</b> )	45	23

**Table 2.3:** Optimization of the additive of the reaction to form pyrene-4,5-dione (**31**).

The use of a phosphorus-based ligand, triphenylphosphine (**51**), did not lead to a reduction in the amount of residue formed, and the yield dropped to 36% (Entry 3). It is possible that triphenylphosphine oxide<sup>38</sup> was formed *in situ*, which essentially removed the ligand from the reaction and made it resemble a ligand-free reaction. A more hindered phosphine ligand, DavePhos (**52**) was also tried. Unlike triphenylphosphine, DavePhos was found to substantially reduce the amount of the residue that formed, rendering suction filtration trivially easy. In fact, the use of DavePhos resulted in the greatest reduction of residue, and therefore the easiest work-up. Unfortunately, the yield remained at 45% (Entry 4). Despite the success with DavePhos, NMI remained an excellent and much more cost-efficient option.

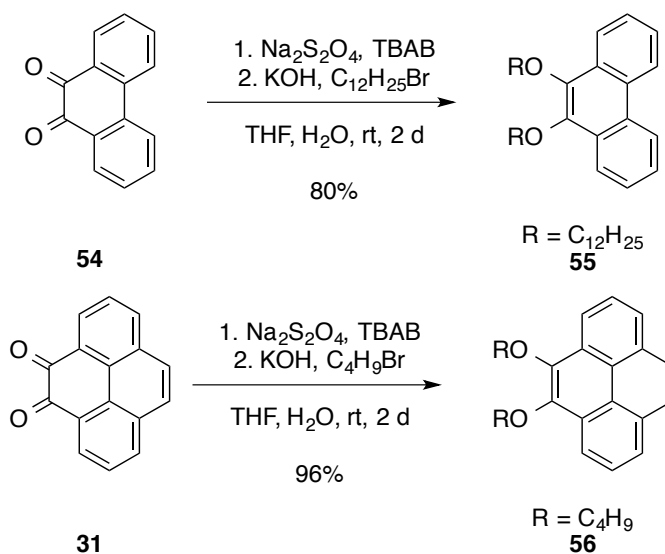
In some of the reported MTO experiments, the addition of Lewis base additives in the oxidation reactions not only enhanced the selectivity of the reactions but also accelerated the olefin oxidation.<sup>34,36,37</sup> As well, it was found that with a higher  $pK_a$  value of the conjugate acid of the additive, the stronger and more stable is the Re-ligand interaction.<sup>34</sup> Therefore, to see if basicity played a role in the conversion of **18** to **31**, the addition of DBU (**53**) was attempted. Although cleaner than the original 2 g scale reaction, there was more residue formed than with the NMI. The yield, however, remained at 45% (Entry 5).

Between all of these trials, the rate of the reaction did not appear to be significantly affected as judged by TLC analysis of the reaction progress. Therefore, unlike in the article by Sharpless *et al.*,<sup>33</sup> it is difficult to say whether the addition of NMI, or any of the other

ligands for that matter, served to accelerate the rate of oxidation. At the very least, no dramatic changes in rate were observed. Additionally, the denticity of the ligands also did not appear to affect the yield or quantity of residue.

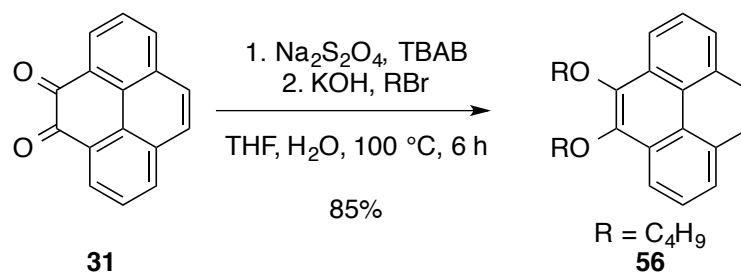
Instead of serving as a ligand on the active oxidant, it is possible that the additive is serving to de-coordinate the ruthenium from the product *ortho*-quinone **40**, thereby reducing the amount of residue observed. It is, however, difficult to say why just 5 mol% resulted in such a drastic reduction in the amount of residue formed. Furthermore, it is possible that the *ortho*-quinone-ruthenium complex **40** is unstable under the oxidizing conditions, and may lead to a mixture of over-oxidized products, which may be some of what is observed in the residue. Without further investigation, it is hard to say exactly what the role of the NMI is. However, now that the reaction is scalable and less time-consuming to perform, the modifications to the pyrene oxidation reaction made pyrene-4,5-dione (**31**) much more readily available, thus providing an excellent situation to make meaningful progress with the intended synthetic plan.

The next reaction in the planned synthetic sequence was the reduction and *O*-alkylation of pyrene-4,5-dione (**31**) to form a 4,5-dialkoxypyrene (**1**). This procedure was adapted from a similar reduction and *O*-alkylation of phenanthrenedione **54** (Scheme 2.4).<sup>39</sup>



**Scheme 2.4:** Reduction and *O*-alkylation of a phenanthrenedione **54**,<sup>39</sup> and the corresponding pyrenedione **31**.<sup>2</sup>

Although the reductive alkylation gave the 4,5-dialkoxypyrene (**56**) in 96% yield, it required a 48 h reaction time. Therefore the procedure was modified in an attempt to reduce the reaction time (Scheme 2.5). It was found that using a temperature of 100 °C instead of 25 °C reduced the reaction time from 2 d to 6 h, however, there was also an accompanying reduction in yield (from 96% to 85%). A series of 4,5-dialkoxypyrenes was synthesized, with alkyl chains ranging from 10 carbons to 20 (Table 2.4). Yields were consistently very good (85%) and the reaction could be scaled up to at least 10 g of dione **31**. There is no reason to expect that further scale-up could not be achieved comfortably.



**Scheme 2.5:** Modification of the reductive alkylation reaction.

Entry	Alkyl Chain	Yield (%)
1	$\text{C}_{10}\text{H}_{21}$ ( <b>57</b> )	85
2	$\text{C}_{12}\text{H}_{25}$ ( <b>58</b> )	85
3	$\text{C}_{14}\text{H}_{29}$ ( <b>59</b> )	85
4	$\text{C}_{16}\text{H}_{33}$ ( <b>60</b> )	84
5	$\text{C}_{20}\text{H}_{41}$ ( <b>61</b> )	85

**Table 2.4:** Series of synthesized 4,5-dialkoxypyrenes.

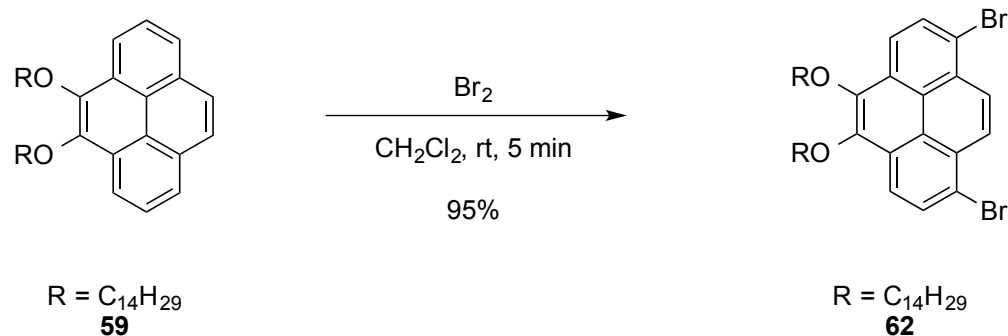
A minor challenge with the initial purifications of the 4,5-dialkoxypyrenes was the separation of the desired product from the excess alkyl halide (a total of 4 equivalents are used) by column chromatography. When eluting with 10% dichloromethane/hexanes, the product and alkyl halide could not be separated completely.<sup>††</sup> This problem was solved

<sup>††</sup> The products, usually solid, return to liquid form when excess alkyl halide is present.

by first eluting the column with hexanes (250—300 mL) before changing to the more polar elution solvent. This proved to be easy for smaller scale reactions (2 or 4 g), but it became laborious for larger scale reactions. This could potentially be avoided by using less of an excess of the alkyl halide in the reaction, but the smaller scales were sufficient for the purposes of this project. Although this aspect of the alkylation reaction was not investigated, it would be a worthwhile pursuit in the future.

The 4,5-dialkoxypyrenes were quite easy to handle. Readily soluble in most organic solvents, they were neither light- nor air-sensitive and no special handling precautions were required. They were, for the most part, all waxy white-yellow solids at room temperature. Interestingly, the 4,5-dialkoxypyrene **59** (14-carbon alkyl chains) behaved somewhat differently from the other 4,5-dialkoxypyrenes. When the reaction mixture was left to cool to room temperature, a sponge-like solid would form in the flask, covering the top of the reaction mixture. Occasionally, this layer was hard enough to resist being punctured by a spatula. During work-up, a similar sponge-like solid would form in the organic layer(s) during extraction if left to sit at room temperature for more than a few minutes. Unfortunately, this did not prove to be a suitable method for isolation of the product in pure form (and thus avoiding column chromatography). Upon removal of the solvent following column chromatography, the product solidified much more easily than all of the other 4,5-dialkoxypyrenes. For this reason, the C<sub>14</sub> alkyl chain was used.

The presence of the alkoxy groups at the 4 and 5 positions on pyrene serves two purposes: i) to activate the pyrene system towards electrophilic aromatic substitution, and ii) to sterically hinder the 3 and 6 positions. Consequently, the addition of molecular bromine (2.2 equivalents dissolved in dichloromethane)<sup>‡‡</sup> to the 4,5-dialkoxy pyrene (**59**) yielded the corresponding 1,8-dibromopyrene product (**62**) exclusively within 5 min at room temperature in 95% yield (Scheme 2.6).



**Scheme 2.6:** Synthesis of 1,8-dibromo-4,5-bis(tetradecyloxy)pyrene (**62**).

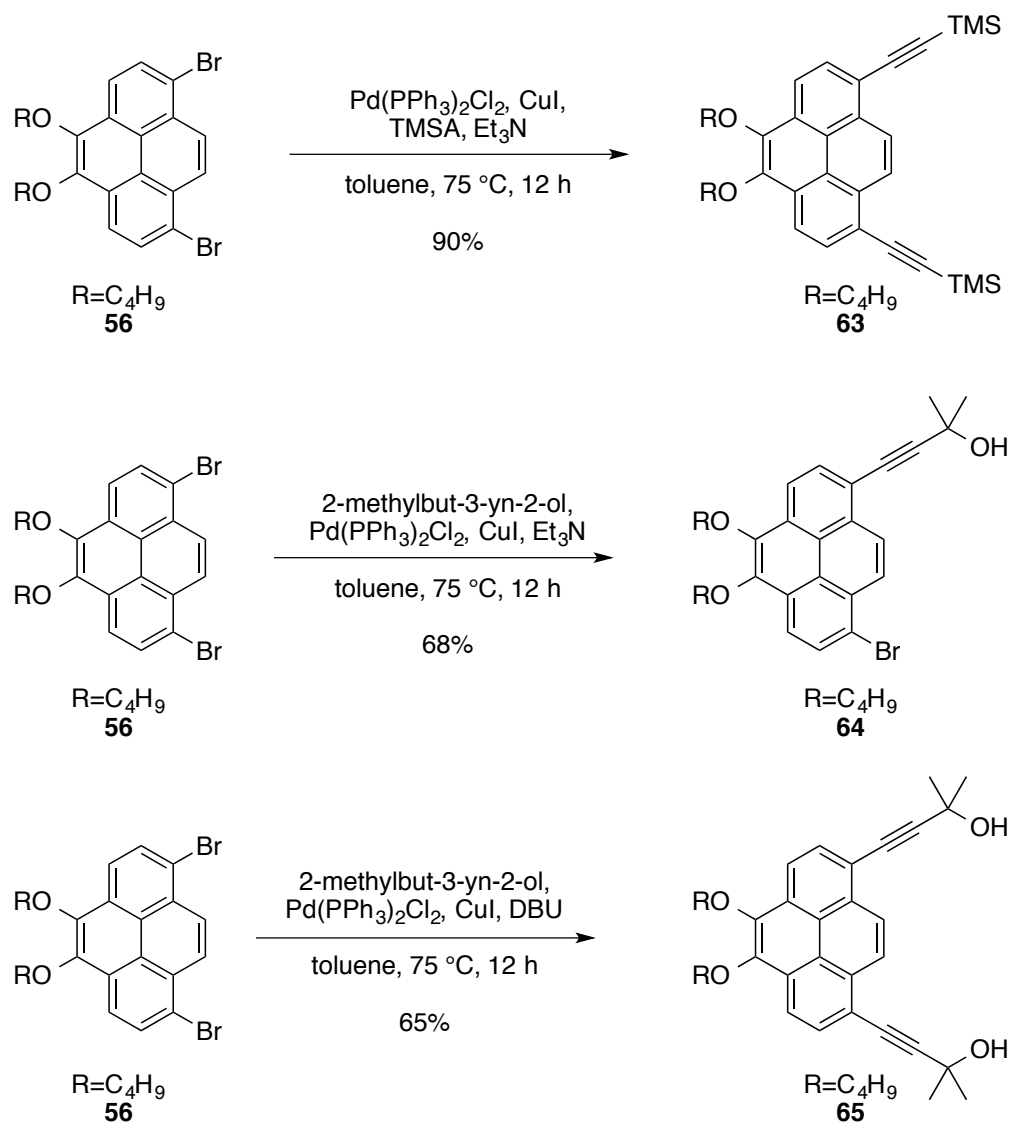
The introduction of functionality at the 4 and 5 positions has made a formerly painstaking and nontrivial synthesis (of 1,8-dibromopyrene(s)) much easier, and consequently provided the opportunity for their use as building blocks for a variety of 1,8-substituted pyrene molecules.<sup>2</sup>

With ready access to multigram quantities of 1,8-dibromo-4,5-bis(tetradecyloxy)pyrene,

---

<sup>‡‡</sup> Addition of neat bromine does not work.

attention was turned to installing the carbon chains that were slated to become the bridges in the target pyrenophanes. Previous work within the group led to the successful conversion of dibromide **56** into alkynes **63-65** using Sonogashira cross-coupling with (trimethylsilyl)acetylene and 2-methylbut-3-yn-2-ol respectively (Scheme 2.7).<sup>2</sup>



**Scheme 2.7:** The dialkoxydibromopyrene (**56**) as a substrate for Sonogashira chemistry.<sup>2</sup>

For the purposes of this project, a three-carbon chain with functionality at the end was required, so the alkyne that was chosen to be used in the Sonogashira reaction was propargyl alcohol (PA, 2-propyn-1-ol). Since the synthetic plan involves subsequent  $S_N2$  chemistry at the site of the OH functionality, it was critically important to omit the two methyl groups that are present in 2-methylbut-3-yn-2-ol (*vide supra*). This leaves a primary carbon instead of a tertiary carbon for use in the planned  $S_N2$  reactions. Despite the structural similarity between 2-methylbut-3-yn-2-ol and propargyl alcohol, the Sonogashira reaction between dibromide **62** and propargyl alcohol did not proceed nearly as well as with 2-methylbut-3-yn-2-ol (Table 2.5).

Entry	Base	Alkyne (eq)	$PdCl_2(PPh_3)_3$ (mol%)	CuI (mol%)	Result
1	Et <sub>3</sub> N	PA (2.0)	5	10	Complex mixture
2	Et <sub>3</sub> N	PA (2.4)	4	10	Mono-coupling
3	Et <sub>3</sub> N	PA (4.0)	4	8	Dialkyne (minor)
4	Et <sub>3</sub> N	TMSA (4.0)	4	8	Dialkyne
5	DBU	TMSA (4.0)	4	8	Dialkyne
6	DBU	PA (4.0)	4	8	Dialkyne
7	DBU	PA (4.0)	10	20	Dialkyne

**Table 2.5:** Attempted Sonogashira reactions with **62**.

Using the same conditions developed previously in the Bodwell group (Scheme 2.7), the reaction of propargyl alcohol with dibromide **62** resulted in the complete consumption of **62** and the formation of a dark, complex mixture of products (Entry 1). When the number of equivalents of the alkyne was increased to 2.4, the mono-coupled product **66** was obtained in 32% yield (Entry 2). A fair amount of the dibromide **62** (54%) was recovered. Further increasing the amount of alkyne to 4.0 equivalents yielded the desired dialkyne **67** but in just 16% yield (Entry 3). A substantial amount (73%) of the mono-coupled product **66** was recovered (Entry 4). These rather erratic results were puzzling, especially since the same batch of carefully purified and stored catalyst was used<sup>§§</sup> and all glassware was consistently acid washed and oven dried.

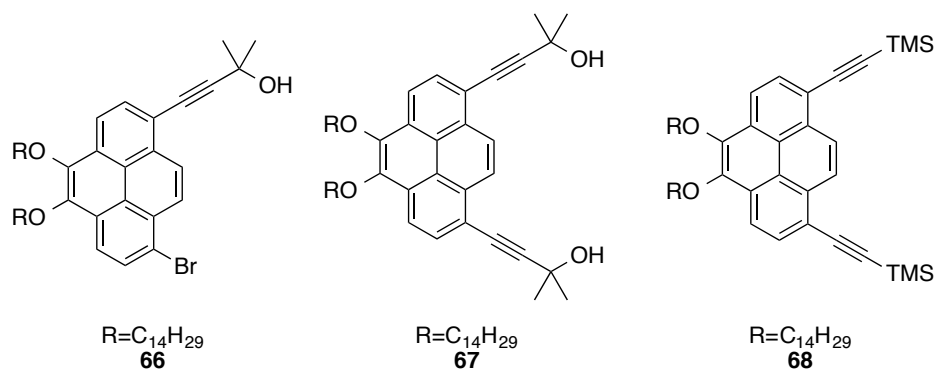


**Figure 2.3:** Products from attempted Sonogashira reactions with **62**.

---

<sup>§§</sup> The same catalyst was used successfully in other Sonogashira reactions within the Bodwell group.

To determine whether the problem rested with the alkyne, propargyl alcohol was replaced by TMSA. This time, the desired dialkyne **68** was obtained in 71% yield. (Entry 4). 1,8-Diazabicyclo[5.4.0]undec-7-ene (DBU) was then used instead of triethylamine as the base, to see if it would enhance product formation.<sup>40</sup> The desired alkyne **68** was obtained in 86% yield (Entry 5). Using these conditions with propargyl alcohol yielded the dialkyne **67** in only 14% yield. Since the disubstituted product was still formed in low yield, and there was no evidence of dehalohydrogenation (mass spectrometry and <sup>1</sup>H-NMR analysis), the catalyst loading was increased to 10 mol% (Entry 7).<sup>41</sup> The yield of the disubstituted product remained low (26%). Since variation of the base, catalyst, alkyne had not significantly improved the outcome of the reaction, it was decided to change the aryl halide from the dibromide **62** to the corresponding diiodide.

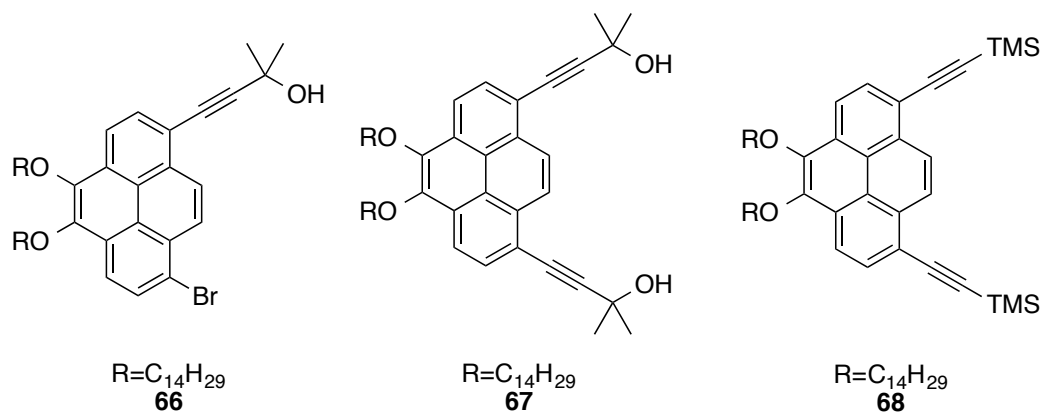
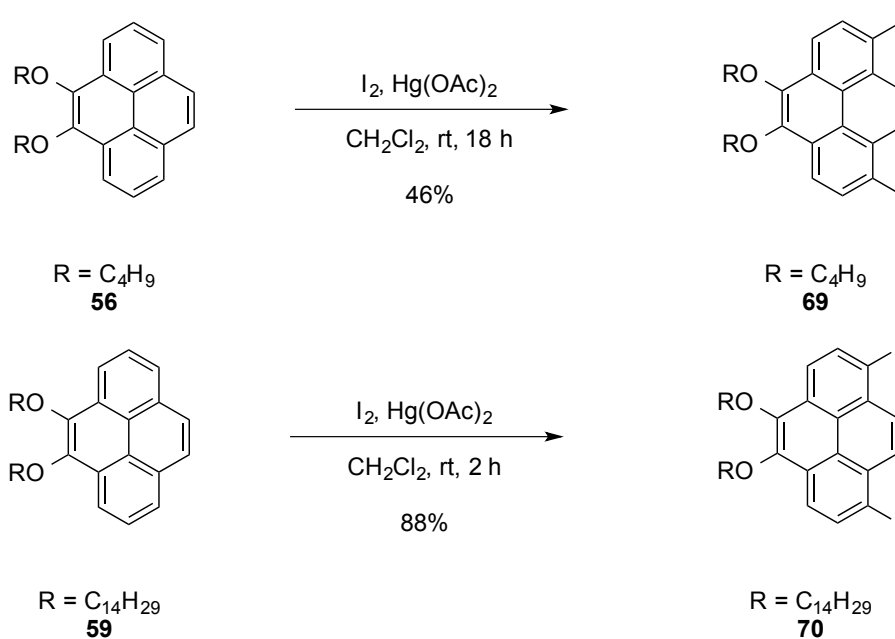


**Figure 2.4:** Products isolated in the Sonogashira reaction with **62**.

Previous work in the group led to the formation of a 1,8-diiodo-4,5-dialkoxypyrene (**69**) in 46% yield from the corresponding dialkoxide using mercuric acetate and molecular iodine.<sup>42</sup> Upon repeating this reaction exactly, a similar result was obtained. It was then found that the yield of this reaction could be increased from 46% to 88% just by carefully monitoring the reaction progress by tlc. Originally, the reaction was left for 18 h at room temperature, but the reaction was found to go to completion after only 2 h (Scheme 2.8).

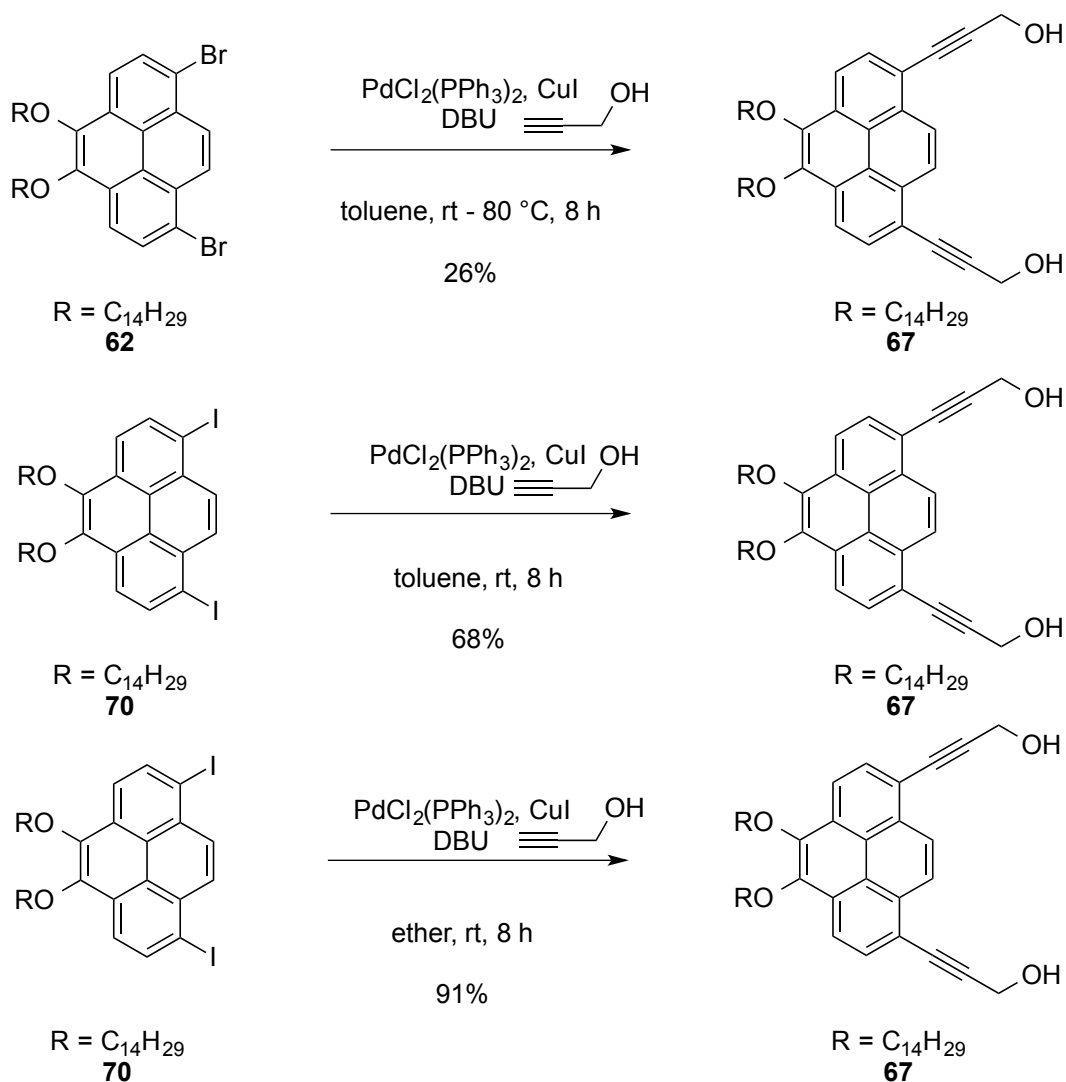


**Scheme 2.8:** Synthesis of diiodides **69** and **70**.

Evidently, the yield quickly reaches a maximum and then decreases with time. This emphatically underscores the great importance of carefully monitoring one's reactions.

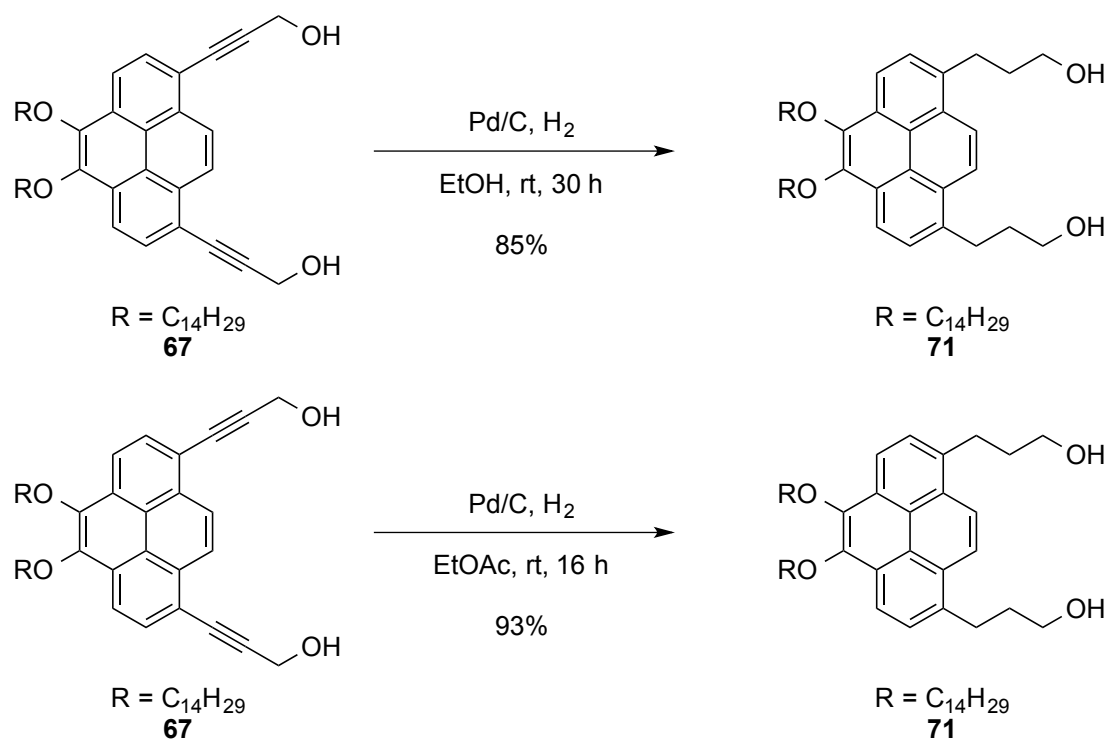
With diiodide **70** in hand, the Sonogashira coupling was reinvestigated. Using the “optimized” coupling procedure for dibromide **59**, the dialkyne **67** was obtained in 68%

yield from the diiodide **70**. Changing the solvent used from toluene to diethyl ether (to facilitate solvent removal during work-up) further increased the yield to 91% (Scheme 2.9).



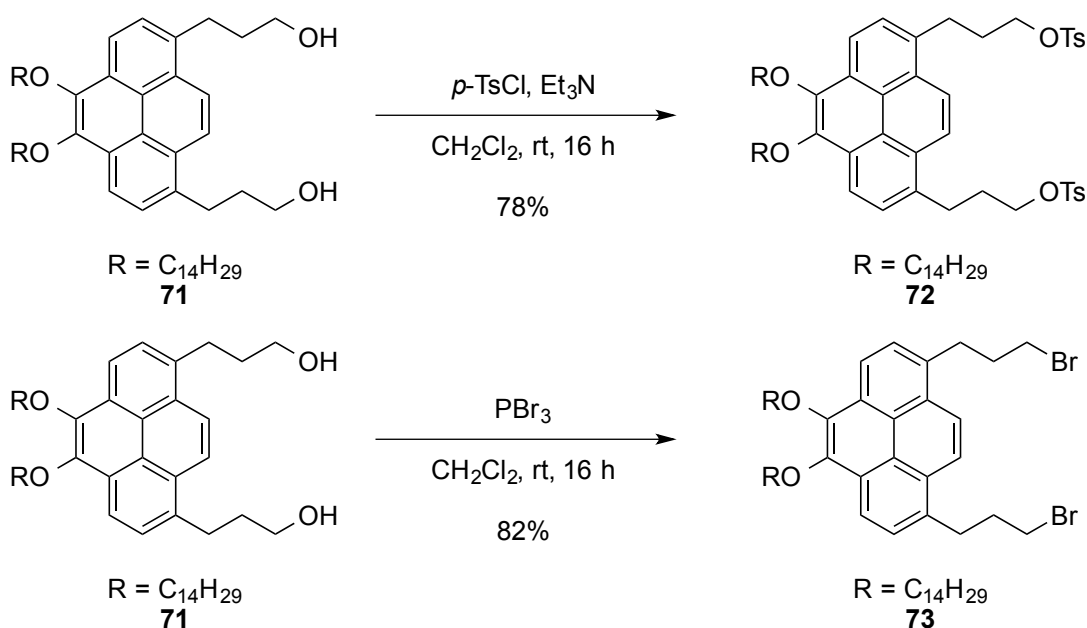
**Scheme 2.9:** Synthesis of the dialkyne **67** from the corresponding dibromide **62** and diiodide **70**.

The alkyne units of **67** were then hydrogenated using conditions previously reported by the Bodwell group for a structurally different aryl alkyl alkyne.<sup>15</sup> This was done to increase the flexibility in the newly-introduced side chains and thus provide access to a reasonable transition state geometry for the planned  $S_N2$  reaction leading to cyclophane formation. Using palladium on carbon as the catalyst and ethanol as the solvent, the corresponding diol was obtained in 85% yield. Switching the solvent used to ethyl acetate yielded diol **71** in 93% yield (Scheme 2.10).



**Scheme 2.10:** Synthesis of diol **71** from the corresponding diyne **67**.

The key step of this synthetic strategy, the reduction and *O*-alkylation to close the pyrenophane, requires an alkyl halide. Therefore the diol **71** was converted into the corresponding ditosylate (**72**, 76%) and dibromide (**73**, 82%) using standard conditions (Scheme 2.11). As expected, both compounds were obtained as stable solids. No attempts were made to find optimal conditions for these products.



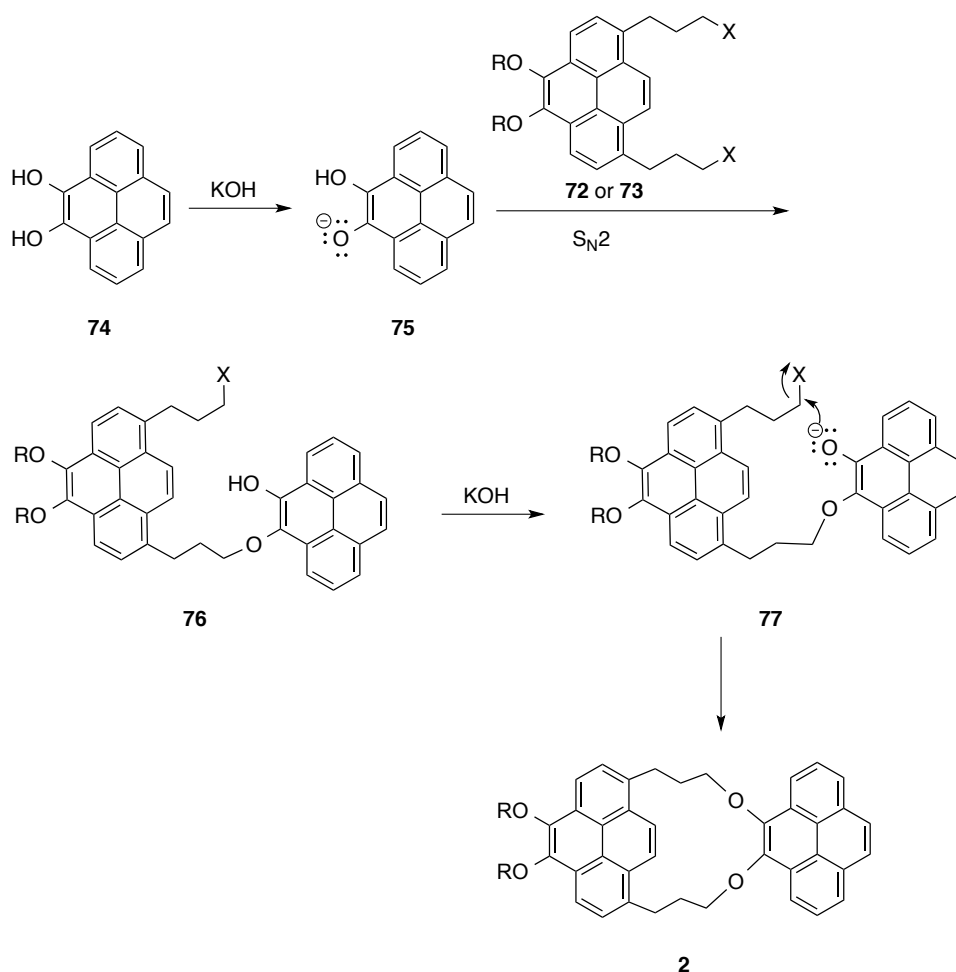
**Scheme 2.11:** Conversion of diol **71** to the corresponding ditosylate **72** and dibromide **73**.

Pyrenophane formation was to be carried out using the reaction described earlier for the synthesis of 4,5-dialkoxypyrenes **57-61**, *i.e.* by reduction of dione **31** followed by *O*-alkylation using either ditosylate **72** or dibromide **73** (Table 2.6). Mechanistically, this was expected to occur via two successive  $S_N2$  reactions (Scheme 2.12). Deprotonation of diol **74** would generate **75**, which would react in an  $S_N2$  fashion with **72** or **73** to afford

intermediate **76** Deprotonation of the remaining OH group would give anion **77**, which sets the stage for the key step of the overall sequence: an "intramolecular S<sub>N</sub>2-like" macrocyclization.<sup>\*\*\*</sup> The foremost consideration here is whether anion **77** is able to easily adopt a conformation in which the nucleophile (the negatively charged oxygen atom) is oriented at the back side of the C—Br bond. Examination of simple molecular models suggests that this key requirement should be achievable without the build-up of significant strain. Calculations may have provided more insight, but none were performed.

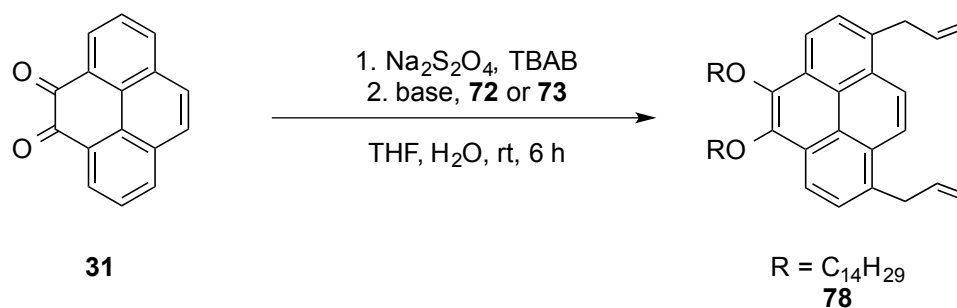
---

<sup>\*\*\*</sup> Of course, an intramolecular S<sub>N</sub>2 reaction cannot be bimolecular (the "2" in S<sub>N</sub>2), but the nucleophilic displacement event is mechanistically identical to that of the intermolecular version.



**Scheme 2.12:**  $\text{S}_{\text{N}}2$ -like macrocyclization. (Counterions not shown for clarity)

An important change from the conditions used for the synthesis of 4,5-dialkoxypyrenes **57-61** was the reduction in the number of molar equivalents of the base (KOH) from 4.0 to 2.1. This was done with the intention of minimizing competition from E2 elimination, which would prevent cyclophane formation at either stage of the reaction. Disappointingly, the first attempt to form pyrenophane **2** (20 mg scale) using dibromide **73** yielded the double elimination product **78** with no signs (mass spectrometry and  $^1\text{H-NMR}$  analysis) of the desired pyrenophane **2** (Entry 1, Table 2.6).

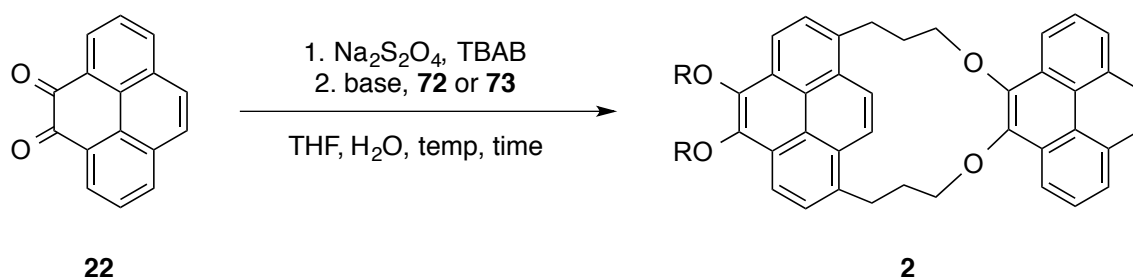


**Scheme 2.13:** Formation of the elimination product (**78**).

Since elimination is favoured over substitution at higher temperatures, the reaction temperature was reduced to room temperature, but to no avail as diallylpyrene **78** was the only product isolated (Entry 2). Changing the alkyl halide to the corresponding ditosylate (**72**) and performing the reaction at room temperature once again yielded the double elimination product **78** (Entry 3).

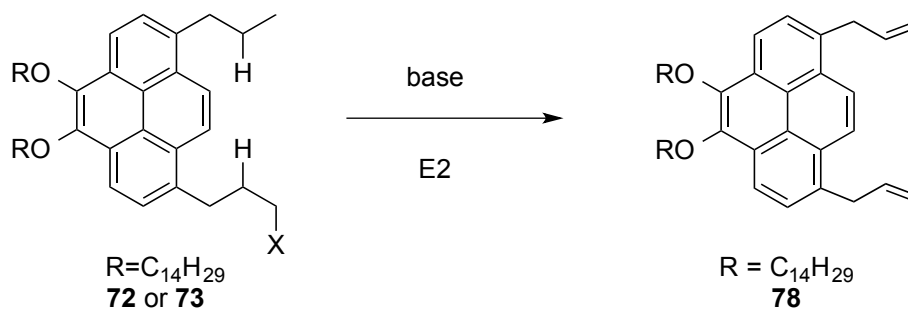
Since the  $pK_a$  of the second OH group in catechol is 13,<sup>43</sup> KOH should be strong enough to doubly deprotonate 4,5-dihydroxypyrene **74** prior to the first alkylation. This means that there should be 0.1 equivalents of KOH available to participate in E2 reactions. It is therefore quite surprising that the double elimination product is formed. Since substitution can be favoured over elimination by reducing the basicity of the base, KOH was replaced by  $\text{K}_2\text{CO}_3$ . Even more surprisingly, the double elimination product was still the only product observed (Entry 4). Changing the counter ion in the base from  $\text{K}^+$  to  $\text{Na}^+$  was also attempted, but the desired pyrenophane was not obtained (Entries 5 and 6). It appears that elimination is quite facile under these conditions. Despite high dilution

conditions (to favour intramolecular macrocyclization), it appears as though the alkyl halide (**72** or **73**) undergoes E2 elimination upon addition to the reaction mixture, so it is possible that the anion generated from the deprotonation of **74** is acting as the base. It is unclear why it would behave as a base in this case and as a nucleophile in the previously described alkylations.



Entry	Alkyl Halide	Base	Temperature (°C)	Result
1	dibromide <b>73</b>	KOH	100	elimination
2	dibromide <b>73</b>	KOH	24	elimination
3	ditosylate <b>72</b>	KOH	23	elimination
4	ditosylate <b>72</b>	K <sub>2</sub> CO <sub>3</sub>	24	elimination
5	dibromide <b>73</b>	NaOH	22	elimination

**Table 2.6:** Attempts at forming the desired pyrenophane (**2**).



**Scheme 2.14:** E2 elimination of **72** or **73**.

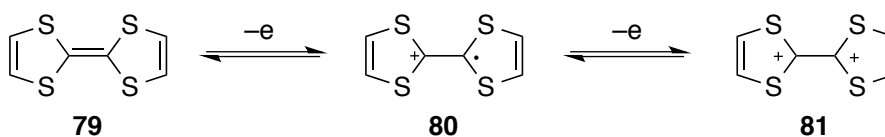
### Chapter 3: Characterization of TTFV-Pyrene-based Polymers

Organic electronic materials are molecular, oligomeric or polymeric  $\pi$ -systems that are typically constructed from some combination of aromatic systems, vinylene and ethynylene units. The function of these materials is mainly dependent on the nature of their  $\pi$ -systems, their shape, and their noncovalent interactions. When considering organic electronic materials, the behavior depends largely on the absolute and relative energies of the highest occupied molecular orbital (HOMO) and lowest unoccupied molecular orbital (LUMO) levels, as well as orbital interactions. When designing molecule-based organic electronic materials, the tuning of both the HOMO / LUMO gap and HOMO / LUMO levels are important factors to consider. Performance can be controlled by tuning the HOMO / LUMO levels as well as solid-state properties (*e.g.* aggregation, crystal packing). Molecules with a low-lying LUMO can easily accept an electron, whereas those with a high-lying HOMO can easily donate an electron. Molecules with narrow HOMO / LUMO gaps are of particular interest due to their ability to undergo promotion of an electron from the HOMO to the LUMO. These are the fundamental processes that are exploited in all organic electronic devices.

Three basic strategies are typically used to provide both a narrow HOMO / LUMO gap in organic materials and relatively independently tunable HOMO and LUMO levels: i) variation of the nature of the aromatic system(s), ii) extending  $\pi$ -conjugation in the molecule, and iii) functionalization with strategically placed electron donor and electron

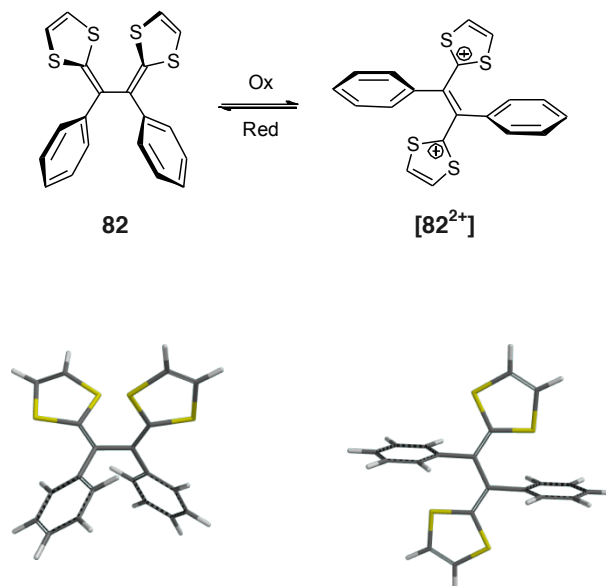
acceptor groups (electronic push-pull effect).<sup>44,45</sup> Each of these principles has been successfully employed in the design of  $\pi$ -conjugated systems. In recent studies,<sup>46,47</sup> there has been a growing interest in providing new electron donor / electron acceptor materials, driven by the need for molecules that improve efficiency and performance in applications such as solar cells and OLEDs.

Tetrathiafulvalenes (TTF) and derivatives are often used as donor moieties in donor-acceptor (D-A) materials due to their good stability and redox properties. The sulfur heterocycle can be sequentially oxidized into a radical cation and dication (Scheme 5.1). Indeed, since its discovery in 1970, TTFs have been among one of the most heavily studied classes of heterocyclic systems.<sup>48</sup> Functionalized TTF derivatives have been reported in applications ranging from electrochemical switches, sensors, surface modification agents, and so on.<sup>48</sup> There has also been a sustained effort to make  $\pi$ -extended TTFs to better control their electronic and solid-state packing properties.<sup>48</sup>



**Scheme 3.1:** Redox transformation of TTF.

Tetrathiafulvalene vinylogues (TTFVs) are a type of  $\pi$ -extended TTFs, which contain an additional two (or some higher even number)  $sp^2$ -hybridized carbon atoms between the dithiole rings. TTFVs have conformational switching properties under redox conditions due to Coulombic interaction and steric strain (Scheme 3.2).<sup>48</sup>



**Scheme 3.2:** Redox-controlled conformational switching behavior of diphenyl-TTFV **82**.

The molecular geometries shown in the bottom were optimized at the B3LYP/6-311G\* level of theory.<sup>†††</sup>

In its oxidized form, TTFV (**[82<sup>2+</sup>]**) prefers a *trans* conformation due to the Coulombic repulsion between the two positively charged dithiolium rings. Reduction relieves this

<sup>†††</sup> Calculations performed by Prof. Y. Zhao, Memorial University.

repulsion, and the TTFV molecule adopts a more stable *cisoid* conformation. In the past few years, TTFVs have been used as building blocks for functional systems such as molecular tweezers, redox-active polymers, and a stimuli-responsive polymers which was found to effectively disperse single-walled carbon nanotubes (SWNTs) in various organic solvents.<sup>49-51</sup>

SWNTs have remarkable properties, but their application in organic electronic devices is very limited due to poor solubility and structural heterogeneity (chirality and size) and varying levels of impurities such as metals, amorphous carbon and multiwalled carbon nanotubes (MWNT). SWNTs are often functionalized to enable their homogeneous dispersion in various solvents and bulk materials. One of the more popular approaches to SWNT solubilization is to use supramolecular interactions, which enable functionalization and dispersion without deteriorating the  $sp^2$  hybridization at any point on the nanotube structure and thus maintaining their electronic characteristics.<sup>52,53</sup> Conjugated polymers, which often include aromatic units, have been used as supramolecular dispersion agents because they participate in favorable  $\pi$ -stacking interactions with SWNTs. They also tend to have good solubility and specially designed polymers can even exhibit selectivity when interacting with SWNTs. For example, TTFV-based polymers have been shown to selectively and reversibly functionalize SWNTs.<sup>50,51</sup> TTFV-fluorene (**83**) and TTFV-phenylacetylene (**84**) polymers were reported by the Zhao group (Figure 3.1).<sup>51,54</sup>

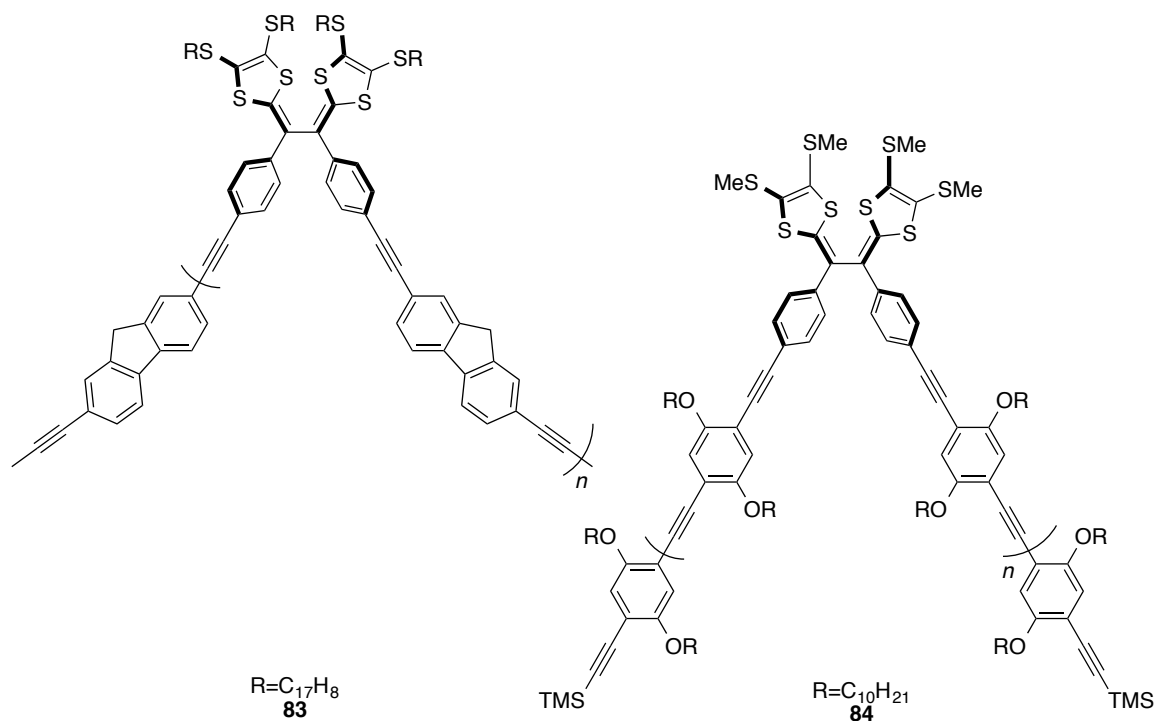
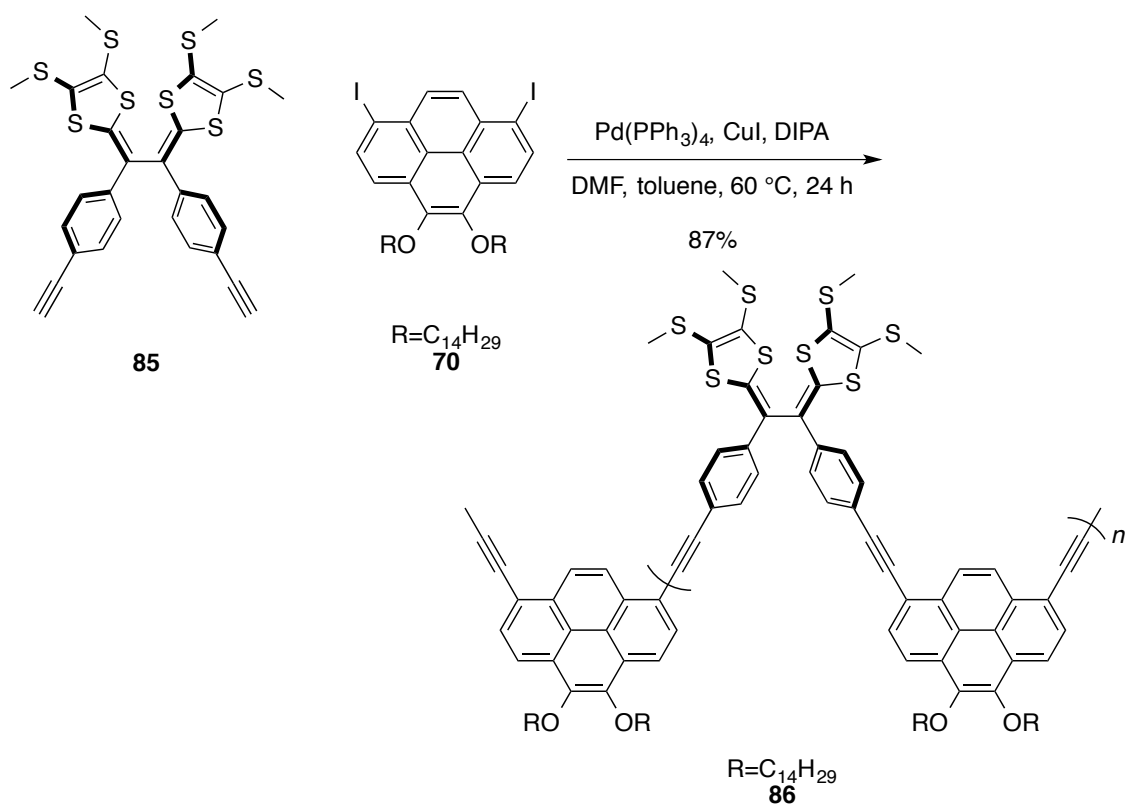


**Figure 3.1:** Selected TTFV-based polymers reported by the Zhao group.

Incorporating a larger polycyclic aromatic hydrocarbon system in this type of designed polymer may lead to the development a polymer with superior properties. A larger aromatic surface could enhance the interaction between the polymer and the SWNTs. As presented in Chapter 1, pyrene has a relatively large surface and is known to interact strongly with the basal plane of graphite via  $\pi$ -stacking. It also interacts strongly with SWNTs in the same manner.<sup>52,55–62</sup>

In collaboration with the Zhao group, the objective of this project was to synthesize a TTFV-pyrene-based polymer, study its electronic and physical properties, and determine whether if it is capable of dispersing SWNTs. TTFV derivative **85** bearing two terminal

alkynes has been used by the Zhao group in the synthesis of various polymers such as **83** and **84**. Having been able to synthesize multigram quantities of diiodide **70**, the opportunity to combine these two systems in a polymer presented itself. Subjection of the two bifunctional species **85** and **70** to Sonogashira conditions led to the formation of polymer **86** in 87% yield (Scheme 3.3).<sup>‡‡‡</sup> This reaction was found to be easily reproducible.



**Scheme 3.3:** Synthesis of polymer **86**.

<sup>‡‡‡</sup> The synthesis of **85** and **86** were carried out by Eyad Younes (Zhao group, Memorial University).

A series of experiments were then performed to learn more about the behavior and characteristics of the polymer. To determine thermal stability and obtain information about phase changes, differential scanning calorimetry (DSC) experiments were performed. A slight transition (neither significant nor representative of a phase change) at about 85 °C was observed, which corresponded to a heat flux of 0.2 mW. The weak nature of this transition may indicate that it corresponds to a liquid crystalline (LC) glass transition or perhaps desolvation or instrumental error. A large increase in heat flux occurred at about 300 °C, which is indicative of decomposition. As far as stability is concerned, DSC revealed that the polymer was thermally stable to at least 150 °C, and thus could likely be used in devices up to temperatures of about 100 °C.

Spartan molecular mechanics calculations using the MMFF force field<sup>§§§</sup> predict that polymer **86** could adopt a folded structure with stacking observed between pyrene units (Figure 3.2). The observed stacking of pyrene is similar to the columnar stacking observed in some discotic liquid crystal materials.

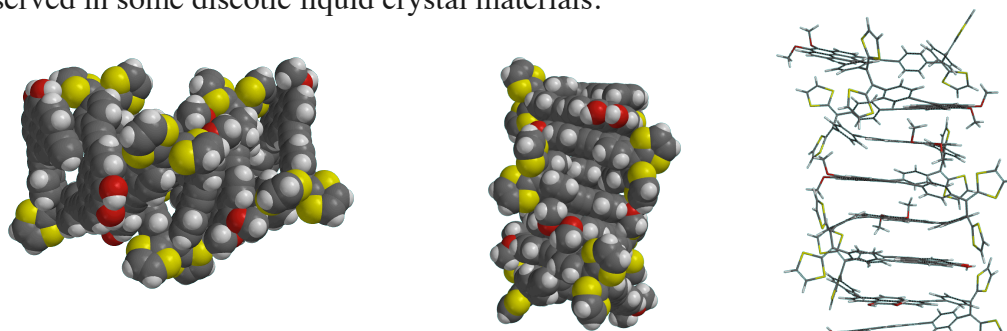


**Figure 3.2:** Predicted structure of polymer **86**. Alkyl chains omitted for clarity.

---

<sup>§§§</sup> Calculations performed by Prof. Y. Zhao, Memorial University.

Variable temperature  $^1\text{H-NMR}$  experiments were therefore performed over a range from room temperature to  $100\text{ }^\circ\text{C}$ . The polymer **86** did not show any temperature-dependent behaviour, which suggests that the event observed at  $85\text{ }^\circ\text{C}$  in the DSC may not be LC in nature. Melting point analysis shows that melting starts around  $200\text{ }^\circ\text{C}$ , but that decomposition occurs. This is supported by the DSC data, for there is a slight endothermic change followed by a larger exothermic process at around  $260\text{ }^\circ\text{C}$ .

Next, pulsed gradient spin-echo (PGSE) diffusion NMR experiments were run in order to learn more about the size and behavior of the species in solution. PGSE-diffusion NMR experiments provide accurate, noninvasive molecular diffusion measurements on complex chemical mixtures and multicomponent solutions. The data extracted from these experiments enable the determination of a diffusion coefficient, from which a hydrodynamic radius can be calculated using the Stokes–Einstein equation:

$$D = \frac{k_B T}{6\pi\eta r_H} \quad (1)$$

where  $D$  is the diffusion coefficient,  $k_B$  is the Boltzmann constant,  $T$  is temperature,  $\eta$  is viscosity, and  $r_H$  is the hydrodynamic radius.

The Stokes–Einstein equation assumes a molecule is spherical in shape. By taking into account the frictional drag associated with different shapes of molecules, it can be adjusted to solve for other shapes:

$$D = \frac{k_B T}{4\pi\eta r_H} \quad (2)$$

The above equation assumes the molecule is prolate (or oblong) instead of spherical. If the molecule is more linear, the following equation (3) can be used:

$$D = \frac{k_B T}{2\pi\eta r_H} \quad (3)$$

Using the average diffusion coefficient ( $5.468 \times 10^{-9} \text{ m}^2/\text{s}$ ) obtained from the PGSE diffusion NMR experiments, the hydrodynamic radii were calculated for each shape (Table 3.1).

Entry	Shape	Hydrodynamic Radius (nm)
1	Spherical	2.35
2	Prolate	3.52
3	Linear	7.04

**Table 3.1:** Calculated  $r_H$  from PGSE-diffusion NMR data.

Comparing this to the previously calculated structures (Figure 3.2), there some agreement with the  $r_H$  corresponding to the spherical shape. The calculated simplified structure is expected to have a molecular radius of about 1.3 nm. Alkyl chains, if present, will theoretically account for an additional approximately 1 nm. Although close, it is important to consider that the experimental data does not allow for the calculation of

molecular radius, simply the hydrodynamic radius. More calculations (specifically for the expected hydrodynamic radius) would be helpful.

Cyclic voltammetry experiments were performed\*\*\*\* using Ag / AgCl as the reference electrode, and a thin film of polymer **86** deposited on a glassy carbon working electrode. The scans show that the oxidation / reduction of the TTFV polymer is highly reversible. As shown in Figure 3.3, a redox wave pair is clearly observed in the cyclic voltammogram, with an anodic peak at +0.69 V and a cathodic peak at +0.52 V. The voltammetric behaviour resembles that of the TTFV monomer, indicating that the oxidation and reduction occurs at the TTFV moieties in a simultaneous manner.

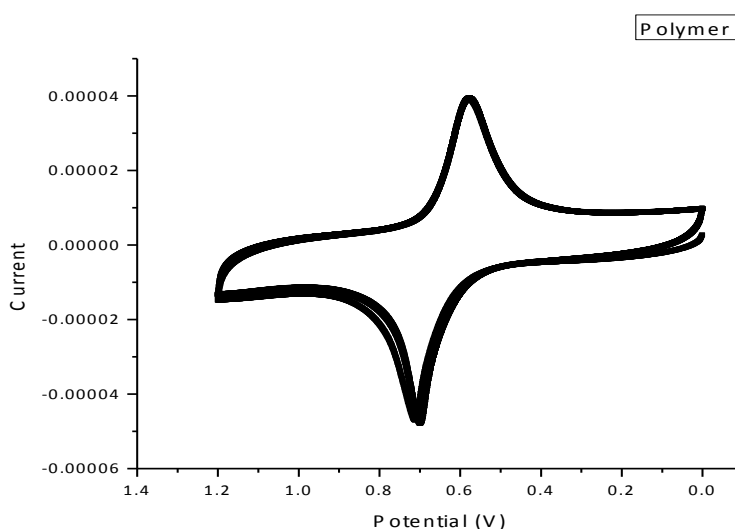


**Figure 3.3:** One of the CV scans of **86**.

---

\*\*\*\* CV experiments were performed by E. Younes (Zhao group, Memorial University).

In conclusion, a series of experiments were conducted to learn more about the shape and properties of polymer **86**. The polymer was found to be thermally stable, and could conceivably be used in devices up to about 100 °C. Through PGSE-diffusion NMR experiments the hydrodynamic radius was predicted, which is in agreement with the calculated value. The molecule therefore likely adopts a globular structure in solution. Only the TTFV moiety was found to undergo reversible redox chemistry, with the pyrene moiety remaining intact. This is an ongoing collaborative effort between the Bodwell and Zhao groups.

## Chapter 4: Conclusions and Future Work

Although the pyrenophane **2** was not successfully synthesized, progress was made through the first iteration of the planned synthetic route up to the penultimate step. The final [1+1] coupling step failed due to competition from elimination. Along the way, considerable attention was paid to the improvement of the first step in the synthesis, the oxidation of the starting material, pyrene (**18**) to pyrene-4,5-dione (**31**). It was found that the addition of 5 mol% of *N*-methylimidazole transformed the work-up and purification steps of the reaction from being very difficult and time-consuming to becoming much more straightforward. This enabled the reaction to be scaled up far beyond the previous 2 g limit using the original procedure. The reaction can now be performed comfortably with slightly improved yields on a 25 g scale of pyrene (**18**), using routinely available laboratory glassware. One reaction was conducted on a 100 g scale, but the reaction was difficult to handle using regular lab glassware and equipment. Although the role of the additive remains unclear, its use was found to be a valuable modification of a useful reaction.

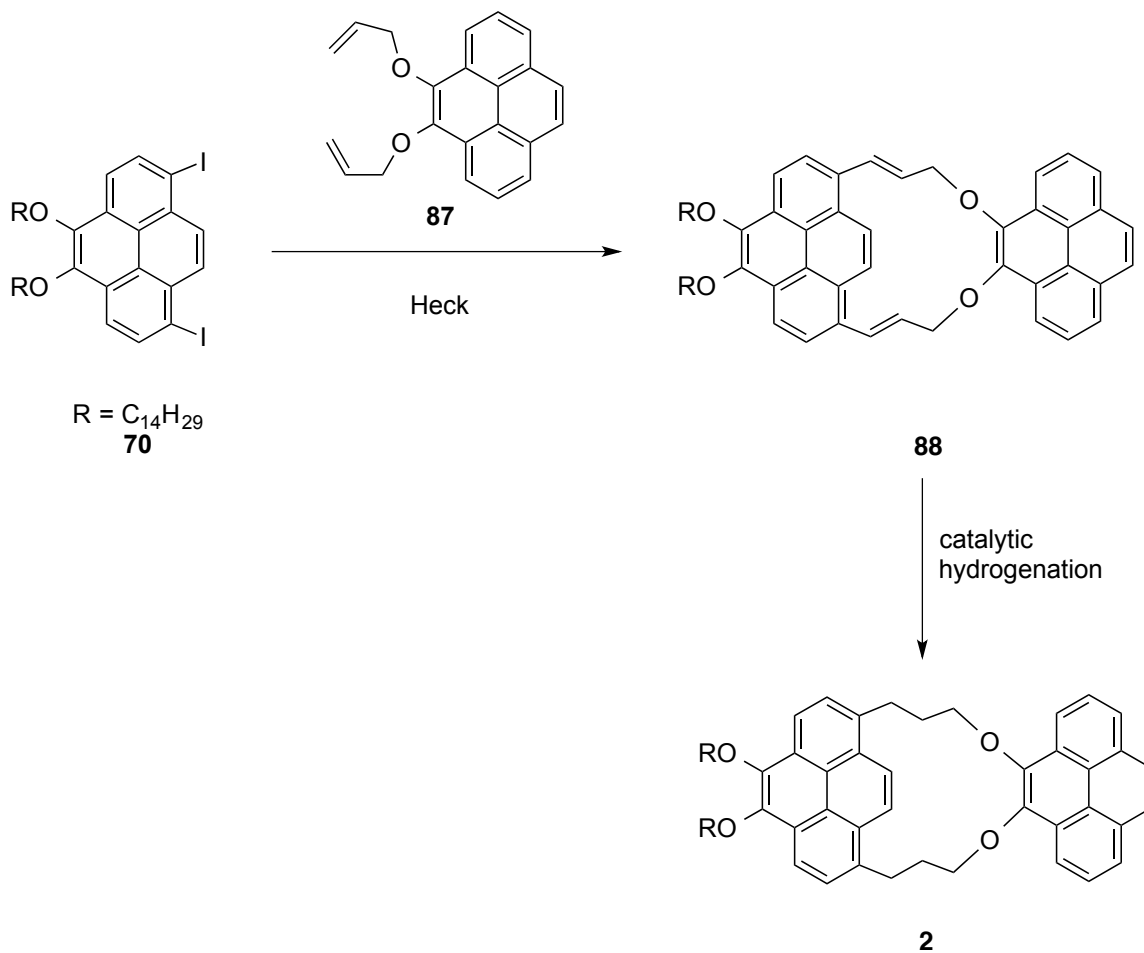
The yield of the iodination of pyrene (**18**) to give diiodide **70** was improved from 46% to 88%. The greater availability of this compound was beneficial to the synthetic route because its Sonogashira reaction with propargyl alcohol proceeded in much higher yield (91%) than that with the corresponding dibromide **62** (26%). Not only did diiodide **70** contribute to the improvement of the planned synthetic route, but it is also a potentially

useful synthetic building block for other types of designed  $\pi$ -systems using different cross-coupling reactions.

Using a TTFV derivative **85** and the diiodide **70**, polymer **86** was synthesized by E. Younes and a series of experiments were conducted to learn more about its shape and properties. The polymer was found to be thermally stable, and could conceivably be used in devices up to about 100 °C. Through PGSE-diffusion NMR experiments the hydrodynamic radius was calculated, which is in agreement with the calculated value. The molecule therefore likely adopts a globular structure in solution. Only the TTFV moiety was found to undergo reversible redox chemistry, with the pyrene moiety remaining intact. This is an ongoing collaborative effort between the Bodwell and Zhao groups.

Although the [1+1] cyclization reaction to afford pyrenophane **2** was unsuccessful, this does not mean that the general strategy is fatally flawed. Beyond simply extending the length of the bridges (*e.g.* using homopropargyl alcohol in the Sonogashira reaction), a variety of other types of cyclophane-forming reactions could be investigated. One possibility is to exploit the Heck reaction between 4,5-bis(allyloxy)pyrene (**87**) and diiodide **70** (Scheme 4.1). The resulting pyrenophane **88** with *E*-configured double bonds does not appear to be significantly strained according to examination of simple molecular models. In contrast, the corresponding pyrenophane with triple bonds, which would result from the use of 4,5-bis(propargyloxy)pyrene, would clearly be very strained.

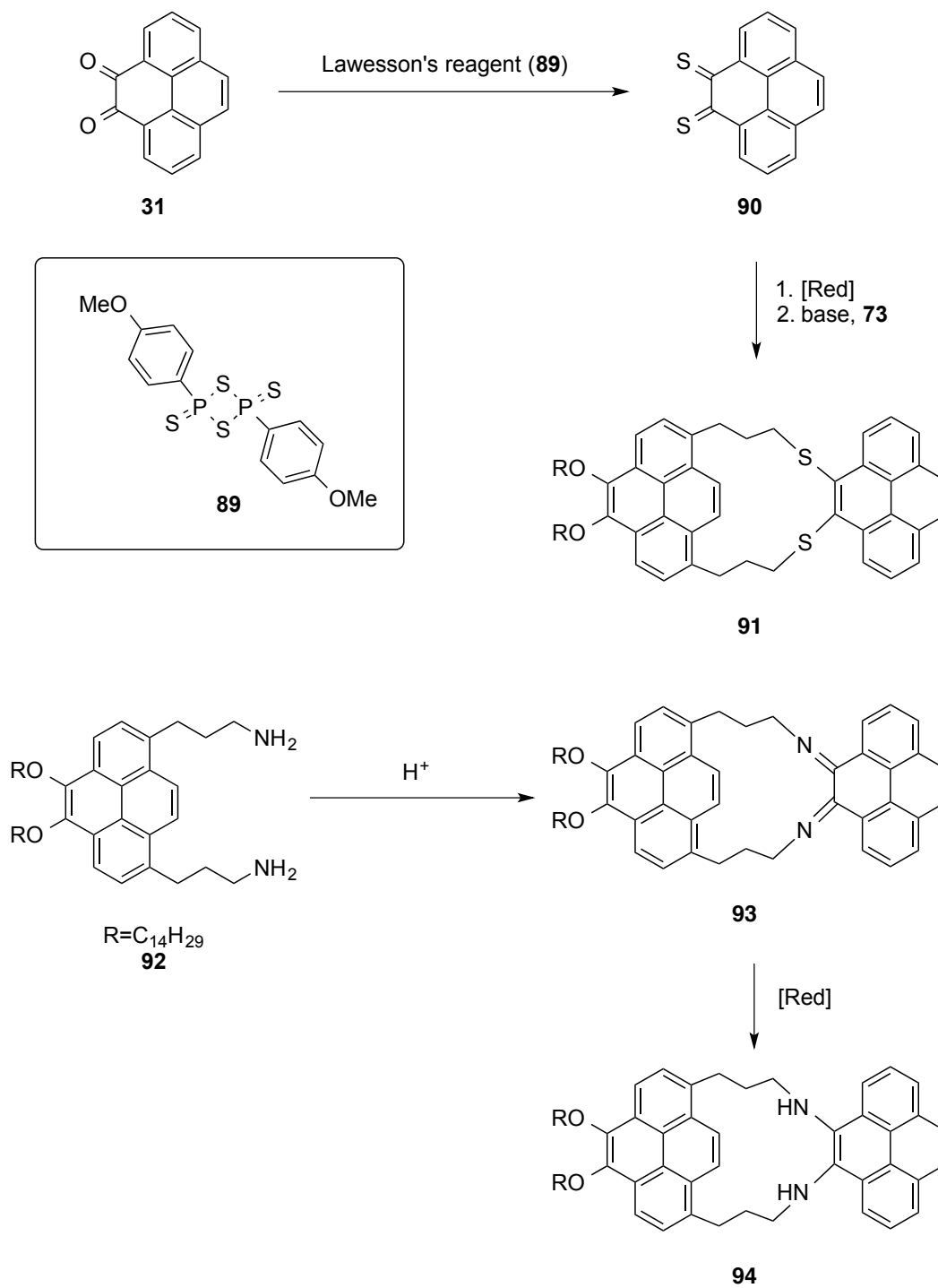
Catalytic hydrogenation of **88** would afford pyrenophane **2** and the second iteration could then be initiated.



**Scheme 4.1:** Possible cyclization reaction for the formation of **2**.

Another intriguing possibility is to convert dione **31** into the corresponding bis(thioketone) **90**, perhaps with Lawesson's reagent (**89**, Scheme 4.2). The reductive alkylation of this compound with dibromide **73** would be expected to afford

dithiapyrenophane **90**. The much greater nucleophilicity and much lower basicity of the thiolate than alkoxide $\leq$  would be expected to greatly favour the desired substitution reactions over the undesired elimination reactions. Alternatively, the condensation of diamine **92** (*e.g.* from **72** or **73** *via* FGI) with dione **31** would be expected to afford diimine **93**, reduction of which would afford diamine **94**. A complication here may be the need to protect the nitrogen atoms before commencing the second iteration.



**Scheme 4.2:** Possible cyclization reactions to form a similar pyrenophane as **2**.

## Chapter 5: Experimental

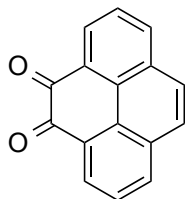
All reaction solvents were ACS grade and were used as received. NMR solvents were dried over activated molecular sieves (4 Å) before use. All reagents and starting materials were used as received. Flash silica gel was used for all column chromatography.

**NMR.** CDCl<sub>3</sub> solutions were used for recording <sup>1</sup>H NMR and <sup>13</sup>C NMR spectra unless otherwise noted. All <sup>1</sup>H NMR spectra were acquired using either a Bruker AVANCE 500 spectrometer operating at 500 MHz or a Bruker AVANCE III 300 spectrometer operating at 300 MHz (as noted). All <sup>13</sup>C NMR spectra were acquired using a Bruker AVANCE III 300 spectrometer operating at 75 MHz. Data was processed and analyzed using MestRenova software (Mnova NMR).

**Mass Spectrometry.** Mass spectra were recorded on an Agilent 1100 series LC/MSD (Quad) chromatographic system by flow injection analysis. Samples were dissolved in CH<sub>2</sub>Cl<sub>2</sub> unless otherwise noted, and ionized by atmospheric pressure chemical ionization (APCI, positive mode). Mass spectra for the higher molecular weight analytes were recorded using a High Resolution MSD Waters Micromass GCT Premier mass spectrometer. High resolution spectra were obtained by Linda Winsor (Memorial University).

**Melting Points.** Melting points were recorded using a Stanford Research Systems Optimelt Automated Melting Point System with Digital Image Processing Technology.

**Pyrene-4,5-dione (31):**



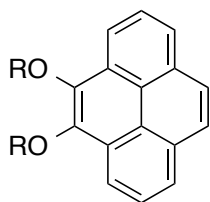
To a solution of pyrene (2.000 g, 9.888 mmol) in  $\text{CH}_2\text{Cl}_2$  (40 mL) and THF (40 mL) were added  $\text{RuCl}_3 \cdot 3\text{H}_2\text{O}$  (0.266 g, 0.995 mmol) and  $\text{H}_2\text{O}$  (50 mL). To the resulting dark green solution was added *N*-methylimidazole (0.03 mL, 0.4 mmol) and then  $\text{NaIO}_4$  (9.517 g, 44.49 mmol), slowly over 10–15 min. The resulting solution was stirred at room temperature for 2.5 h. The reaction mixture was suction filtered using three layers of paper towels (Merfin Vicel) as filter paper.<sup>††††</sup> The residue was washed with  $\text{CH}_2\text{Cl}_2$  until the washings ran colourless. To the resulting dark red-orange filtrate was added  $\text{H}_2\text{O}$  (500 mL) and the organic phase was separated. The aqueous phase was extracted with  $\text{CH}_2\text{Cl}_2$  (3 × 50 mL) and the combined organic layers were washed with  $\text{H}_2\text{O}$  (2 × 50 mL),  $\text{Na}_2\text{S}_2\text{O}_3$  (2 × 50 mL),  $\text{H}_2\text{O}$  (50 mL) and brine (50 mL) to afford a clear red-orange solution, which was then dried over anhydrous  $\text{MgSO}_4$ . The solvent was removed under reduced pressure and the residue was subjected to column chromatography (4 × 26 cm) ( $\text{CH}_2\text{Cl}_2$ ). The first compound eluted (a black solid,  $R_f = 0.35$ ) could not be identified.

---

<sup>††††</sup> When regular filter paper was used, the filtration proceeded extremely slowly.

The only other product to be eluted was pyrene-4,5-dione (**31**), which was obtained as an orange solid (1.202 g, 53%):  $R_f$  (40% ethyl acetate/hexanes) = 0.46; mp = 301–304 °C (dec), (Lit.<sup>25</sup> mp = 302–304 °C);  $^1\text{H}$  NMR (500 MHz,  $\text{CDCl}_3$ )  $\delta$  = 8.47 (dd,  $J$  = 7.6, 1.2 Hz, 2H), 8.16 (dd,  $J$  = 8.0, 1.3 Hz, 2H), 7.83 (s, 2H), 7.74 (t,  $J$  = 7.7 Hz, 2H);  $^{13}\text{C}$  NMR (75 MHz,  $\text{CDCl}_3$ )  $\delta$  = 180.50, 135.77, 132.08, 130.21, 130.15, 128.47, 128.01, 127.28; MS (APCI-(+),  $\text{CH}_2\text{Cl}_2$ ):  $m/z$  (%) 233 ( $[\text{M}+1]^+$ , 100); HRMS (EI-(+),  $\text{CH}_2\text{Cl}_2$ ): calcd for  $\text{C}_{16}\text{H}_8\text{O}_2$  232.0524, found 232.0523.

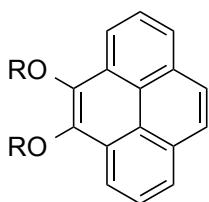
#### General Procedure for the Synthesis of 4,5-Dialkoxypyrenes:



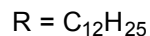
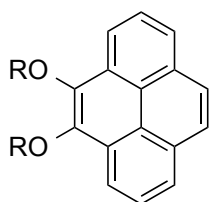
To a solution of pyrene-4,5-dione (**31**) in THF (100 mL) and  $\text{H}_2\text{O}$  (100 mL) were added TBAB (0.3 equiv.) and  $\text{Na}_2\text{SO}_3$  (3 equiv.). The resulting clear orange solution was stirred at room temperature for 5 min. To the solution was added a solution of KOH (4 equiv.) in  $\text{H}_2\text{O}$  (100 mL). The resulting solution was deep red, and the flask was immediately capped. To this solution was added the alkyl halide (4 equiv.). The flask was equipped with a capped condenser and was stirred at 100 °C for 6 h. The reaction mixture was cooled to room temperature and the layers were separated. The aqueous layer was extracted with ethyl acetate (3 × 15 mL) and the THF layer was washed with  $\text{H}_2\text{O}$  (15 mL) before being combined with the other organic extracts. The combined organic extracts were washed with  $\text{H}_2\text{O}$  (3 × 15 mL) to afford a clear yellow solution, which was

then dried over anhydrous  $\text{MgSO}_4$ . The solvent was removed under reduced pressure and the residue was subjected to column chromatography ( $3 \times 20$  cm) using hexanes (350 mL) and then 10%  $\text{CH}_2\text{Cl}_2$ /hexanes.

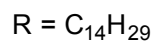
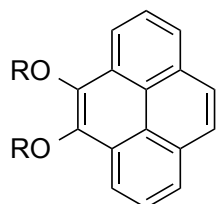
**4,5-Bis(decyloxy)pyrene (57):**



According to the general procedure, pyrene-4,5-dione (**31**) (2.001 g, 8.623 mmol), THF (100 mL),  $\text{H}_2\text{O}$  (100 mL), TBAB (0.850 g, 2.637 mmol) and  $\text{Na}_2\text{SO}_3$  (4.507 g, 25.88 mmol), followed by a solution of KOH (3.908 g, 69.65 mmol) in  $\text{H}_2\text{O}$  (100 mL) and 1-bromodecane (9.532 g, 29.56 mmol) were employed to yield 4,5-bis(decyloxy)pyrene (**57**) (3.772 g, 85%):  $R_f$  (20%  $\text{CH}_2\text{Cl}_2$ /hexanes) = 0.43; mp 36-39 °C; IR (solid)  $\nu = 1214, 1168 \text{ cm}^{-1}$ ;  $^1\text{H}$  NMR (500 MHz,  $\text{CDCl}_3$ )  $\delta = 8.49$  (d,  $J = 7.8$  Hz, 2H), 8.14 (d,  $J = 7.5$  Hz, 2H), 8.06 (s, 2H), 8.02 (t,  $J = 7.7$  Hz, 2H), 4.34 (t,  $J = 6.7$  Hz, 4H), 1.95–2.01 (m, 4H), 1.55–1.65 (m, 4H), 1.25–1.45 (m, 24H), 0.87–0.90 (m, 6H);  $^{13}\text{C}$  NMR (75 MHz,  $\text{CDCl}_3$ )  $\delta = 144.10, 131.07, 128.92, 127.30, 125.93, 124.27, 122.86, 119.43, 73.80, 31.93, 30.63, 29.70, 29.63, 29.61, 29.37, 26.34, 22.71, 14.13$ ; MS (APCI(+), MeOH):  $m/z$  (%) 515.4 ( $[\text{M}+1]^+$ ). HRMS (EI(+),  $\text{CH}_2\text{Cl}_2$ ): calcd for  $\text{C}_{36}\text{H}_{50}\text{O}_2$  514.7810, found 514.7812.

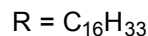
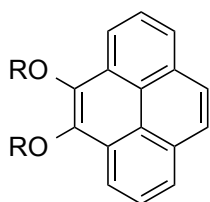
**4,5-Bis(dodecyloxy)pyrene (58):**

According to the general procedure, pyrene-4,5-dione (**31**) (2.02 g, 9.98 mmol), THF (100 mL), H<sub>2</sub>O (100 mL), TBAB (0.42 g, 1.3 mmol) and Na<sub>2</sub>SO<sub>3</sub> (4.55 g, 26.1 mmol) followed by a solution of KOH (2.03 g, 3.62 mmol) in H<sub>2</sub>O (100 mL) and 1-bromododecane (9.976 g, 40.03 mmol) were employed to afford 4,5-bis(dodecyloxy)pyrene (**58**) (2.08 g, 85%): *R<sub>f</sub>* (20% CH<sub>2</sub>Cl<sub>2</sub>/hexanes) = 0.43; mp 53-54 °C; <sup>1</sup>H NMR (300 MHz, CDCl<sub>3</sub>) δ = 8.49 (dd, *J* = 1.1, 7.8 Hz, 2H), 8.13 (dd, *J* = 1.2, 7.6 Hz, 2H), 8.04 (s, 2H), 8.02 (t, *J* = 7.7 Hz, 2H), 4.33 (t, *J* = 6.7 Hz, 4H), 1.93–2.02 (m, 4H), 1.56–1.66 (m, 4H), 1.27–1.54 (m, 32H), 0.86–0.90 (m, 6H); <sup>13</sup>C NMR (75 MHz, CDCl<sub>3</sub>) δ = 144.13, 131.09, 128.94, 127.32, 125.95, 124.29, 122.88, 119.45, 73.83, 31.98, 30.67, 29.75, 29.72, 29.64, 29.42, 26.37, 22.74, 14.16.

**4,5-Bis(tetradecyloxy)pyrene (59):**

According to the general procedure, pyrene-4,5-dione (**31**) (3.027 g, 13.04 mmol), THF (100 mL), H<sub>2</sub>O (100 mL), TBAB (1.266 g, 3.927 mmol) and Na<sub>2</sub>SO<sub>3</sub> (6.793 g, 39.02 mmol) followed by a solution of KOH (5.911 g, 105.3 mmol) in H<sub>2</sub>O (100 mL) and 1-bromotetradecane (14.430 g, 52.04 mmol) were employed to afford 4,5-bis(tetradecyloxy)pyrene (**59**) (13.796 g, 85%): *R<sub>f</sub>* (20% CH<sub>2</sub>Cl<sub>2</sub>/hexanes) = 0.43; mp 57–58 °C; <sup>1</sup>H NMR (500 MHz, CDCl<sub>3</sub>) δ = 8.49 (d, *J* = 7.8 Hz, 2H), 8.13 (d, *J* = 7.6 Hz, 2H), 8.05 (s, 2H), 8.01 (t, *J* = 7.7 Hz, 2H), 4.34 (t, *J* = 6.7 Hz, 4H), 1.93–2.02 (m, 4H), 1.57–1.65 (m, 4H), 1.27–1.45 (m, 40H), 0.86–0.90 (m, 6H); <sup>13</sup>C NMR (75 MHz, CDCl<sub>3</sub>) δ = 144.12, 131.08, 128.93, 127.31, 125.94, 124.28, 122.87, 119.44, 73.82, 31.97, 30.66, 29.75, 29.71, 29.63, 29.41, 26.36, 22.73, 14.15; MS (APCI-(+), CH<sub>2</sub>Cl<sub>2</sub>): *m/z* (%) 627.6 ([M+1]<sup>+</sup>); HRMS (ESI-(+), CH<sub>2</sub>Cl<sub>2</sub>): calcd for C<sub>44</sub>H<sub>66</sub>O<sub>2</sub> 626.5063, found 626.5045.

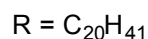
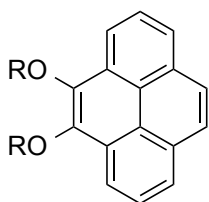
#### 4,5-Bis(hexadecyloxy)pyrene (**60**):



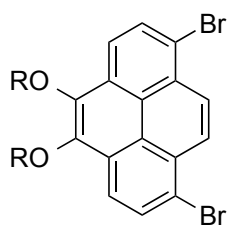
According to the general procedure, pyrene-4,5-dione (**31**) (2.00 g, 8.62 mmol), THF (100 mL), H<sub>2</sub>O (100 mL), TBAB (0.83 g, 2.57 mmol) and Na<sub>2</sub>SO<sub>3</sub> (4.49 g, 25.79 mmol) followed by a solution of KOH (3.86 g, 68.79 mmol) in H<sub>2</sub>O (100 mL) and 1-bromohexadecane (13.18 g, 43.16 mmol) were employed to afford 4,5-bis(hexadecyloxy)pyrene (**60**) (5.01 g, 85%): *R<sub>f</sub>* (20% CH<sub>2</sub>Cl<sub>2</sub>/hexanes) = 0.43; mp 62–65

°C;  $^1\text{H}$  NMR (300 MHz,  $\text{CDCl}_3$ )  $\delta$  = 8.49 (dd,  $J$  = 1.2, 7.8 Hz, 2H), 8.14 (dd,  $J$  = 1.1, 7.6 Hz, 2H), 8.05 (s, 2H), 8.02 (t,  $J$  = 7.7 Hz, 2H), 4.34 (t,  $J$  = 6.7 Hz, 4H), 1.93–2.03 (m, 4H), 1.57–1.66 (m, 4H), 1.26–1.45 (m, 46H), 0.85–0.90 (m, 6H);  $^{13}\text{C}$  NMR (75 MHz,  $\text{CDCl}_3$ )  $\delta$  = 144.11, 131.08, 128.93, 127.31, 125.94, 124.28, 122.87, 119.44, 76.60, 73.82, 31.96, 30.65, 29.75, 29.73, 29.63, 29.40, 26.36, 22.73, 14.15.

#### 4,5-Bis(icosyloxy)pyrene (61):



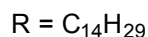
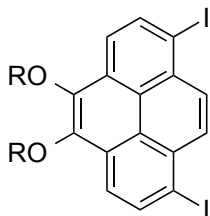
According to the general procedure, pyrene-4,5-dione (**31**) (2.002 g, 8.705 mmol), THF (100 mL),  $\text{H}_2\text{O}$  (100 mL), TBAB (0.834 g, 2.587 mmol) and  $\text{Na}_2\text{SO}_3$  (4.513 g, 25.92 mmol) followed by a solution of KOH (3.918 g, 69.83 mmol) in  $\text{H}_2\text{O}$  (100 mL) and 1-bromoicosane (15.738 g, 43.54 mmol) were employed to afford 4,5-bis(icosyloxy)pyrene (**61**) (5.885 g, 85%):  $R_f$  (20%  $\text{CH}_2\text{Cl}_2$ /hexanes) = 0.43; mp 76–80 °C;  $^1\text{H}$  NMR (300 MHz,  $\text{CDCl}_3$ )  $\delta$  = 8.49 (d,  $J$  = 1.1, 7.8 Hz, 2H), 8.14 (dd,  $J$  = 1.2, 7.7 Hz, 2H), 8.05 (s, 2H), 8.02 (t,  $J$  = 7.7 Hz, 2H), 4.34 (t,  $J$  = 6.7 Hz, 4H), 1.93–2.03 (m, 4H), 1.57–1.66 (m, 4H), 1.26–1.45 (m, 64H), 0.85–0.90 (m, 6H);  $^{13}\text{C}$  NMR (75 MHz,  $\text{CDCl}_3$ )  $\delta$  = 144.11, 131.08, 128.93, 127.31, 125.94, 124.28, 122.87, 119.44, 73.82, 31.96, 30.65, 29.75, 29.70, 29.63, 29.40, 26.36, 22.72, 14.15.

**1,8-Dibromo-4,5-bis(tetradecyloxy)pyrene (62):**

In a 16 mL sample vial, 4,5-bis(tetradecyloxy)pyrene (**59**) (2.51 g, 1.94 mmol) was dissolved in  $CH_2Cl_2$  (20 mL). In another vial,  $Br_2$  (1.43 g, 8.95 mmol) was dissolved in  $CH_2Cl_2$  (1 mL). To the 4,5-bis(tetradecyloxy)pyrene solution was added the bromine solution dropwise over several minutes. After the addition of each drop of the bromine solution, the red-orange colour immediately dissipated until the addition was complete. The mixture was washed with a 5% solution of NaOH (10 mL) and then  $H_2O$  (10 mL) to afford a clear red-orange solution, which was then dried over anhydrous  $MgSO_4$ . The solvent was removed under reduced pressure and the residue was subjected to column chromatography (3 × 20 cm) (10%  $CH_2Cl_2$ /hexanes). The only compound to be eluted was 1,8-dibromo-4,5-bis(tetradecyloxy)pyrene (**62**) (1.42 g, 93%):  $R_f$  (20%  $CH_2Cl_2$ /hexanes) = 0.56; mp = 80-83 °C;  $^1H$  NMR (300 MHz,  $CDCl_3$ )  $\delta$  = 8.53 (s, 2H), 8.37 (d,  $J$  = 8.4 Hz, 2H), 8.27 (d,  $J$  = 8.5 Hz, 2H), 4.31 (t,  $J$  = 6.7 Hz, 4H), 1.95–2.01 (m, 4H), 1.55–1.64 (m, 4H), 1.26–1.43 (m, 40H), 0.86–0.93 (m, 6H);  $^{13}C$  NMR (75 MHz,  $CDCl_3$ )  $\delta$  = 143.80, 130.74, 129.45, 128.72, 127.49, 120.87, 73.92, 31.96, 30.54, 29.74, 29.70, 29.68, 29.56, 29.40, 26.29, 22.72, 14.15; MS (APCI-(+),  $CH_2Cl_2$ ):  $m/z$  (%) 785.4

( $M^+ \text{ } ^{81}\text{Br}^{79}\text{Br}$ ), 783.4 ( $M^+ \text{ } ^{79}\text{Br}$ , 100;  $^{-81}\text{Br}$ ). HRMS (ESI-(+),  $\text{CH}_2\text{Cl}_2$ ): calcd for  $\text{C}_{44}\text{H}_{64}\text{O}_2\text{Br}_2$ , 782.3273, found 782.3274.

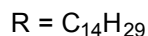
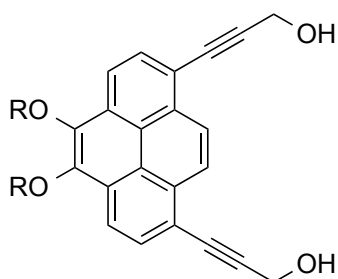
**1,8-Diiodo-4,5-bis(tetradecyloxy)pyrene (70):**



To a stirred solution of 4,5-bis(tetradecyloxy)pyrene (**59**) (1.501 g, 2.394 mmol) in  $\text{CH}_2\text{Cl}_2$  (30 mL) was added mercuric acetate (1.678 g, 5.266 mmol). The reaction mixture was left to stir for 5 min. Iodine (1.339 g, 5.272 mmol) was then added and the resulting mixture was left to stir for 2.5 h at room temperature. The reaction mixture was filtered through a plug of Celite<sup>®</sup> and extracted with  $\text{CH}_2\text{Cl}_2$  (3 × 20 mL). The combined organic extractions were then with a solution of sodium bisulfite (50 mL), 5%  $\text{NaHCO}_3$  solution (50 mL), water (2 × 50 mL) and brine (50 mL). The resulting clear yellow solution was then dried over  $\text{MgSO}_4$  and excess solvent was removed under reduced pressure. The residue was adsorbed onto silica gel and subjected to column chromatography (10%  $\text{CH}_2\text{Cl}_2$ /hexanes) to afford 1,8-diiodo-4,5-bis(tetradecyloxy)pyrene (**70**) (1.871 g, 89%) as a white solid:  $R_f$  (10% d  $\text{CH}_2\text{Cl}_2$ /hexanes) = 0.48; mp = 89.0-90.0 °C;  $^1\text{H}$  NMR (300 MHz,  $\text{CDCl}_3$ )  $\delta$  = 8.54 (d, 8.4 Hz, 2H), 8.37 (s, 2H), 8.22 (d,  $J$  = 8.4 Hz, 2H), 4.31 (t,  $J$  = 6.7 Hz, 4H), 1.95 (quint,  $J$  = 7.1 Hz, 4H), 1.59–1.61 (m, 6H), 1.26–

1.45 (m, 38H), 0.88 (t,  $J = 6.2$  Hz, 6H);  $^{13}\text{C}$  NMR (75 MHz,  $\text{CDCl}_3$ )  $\delta = 181.27, 143.91, 137.47, 132.94, 132.39, 129.37, 123.12, 121.31, 96.18, 73.91, 34.08, 31.96, 30.54, 29.74, 29.71, 29.69, 29.56, 29.47, 29.41, 28.21, 26.29, 22.73, 14.15$ ; MS (APCI-(+),  $\text{CH}_2\text{Cl}_2$ ):  $m/z$  (%) 879.8; HRMS (ESI-(+),  $\text{CH}_2\text{Cl}_2$ ): calcd for  $\text{C}_{44}\text{H}_{64}\text{O}_2\text{I}_2$ , 878.7867, found 878.7868.

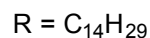
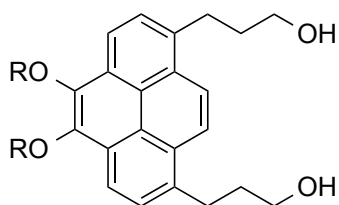
**1,8-Bis(3-hydroxy-1-propynyl)-4,5-bis(tetradecyloxy)pyrene (67):**



In an acid-washed and oven-dried 100 mL Schlenk flask, 1,8-dibromo-4,5-bis(tetradecyloxy)pyrene (322 mg, 0.367 mmol) was dissolved in diethyl ether (30 mL). The resulting clear pale yellow solution was degassed via 3 freeze-pump-thaw cycles.  $\text{PdCl}_2(\text{PPh}_3)_2$  (27 mg, 0.039 mmol) and  $\text{CuI}$  (15 mg, 0.0790 mmol) were then added and the resulting clear yellow solution was left to stir for 5 min. DBU (0.6 mL, 4.0 mmol) was then added and the resulting orange solution was cooled on an ice bath for 10 min. Propargyl alcohol (0.6 mL, 10.4 mmol) was then added and the ice bath was removed. The resulting orange-brown solution was left to gradually warm to room temperature and stir for 12 h. The solvent was removed under reduced pressure. The yellow solid residue was dissolved in  $\text{CH}_2\text{Cl}_2$  (50 mL) and washed with saturated  $\text{NH}_4\text{Cl}$  solution ( $2 \times 100$

mL), H<sub>2</sub>O (2 × 100 mL) and brine (100 mL). The combined organic layers were dried over Na<sub>2</sub>SO<sub>4</sub> and the decanted supernatant was concentrated under reduced pressure. The residue was adsorbed on silica gel and subjected to column chromatography (20% ethyl acetate/hexanes, then ethyl acetate) to afford 1,8-bis(1-propyn-3-ol)-4,5-bis(tetradecyloxy)pyrene (**67**) (0.245 g, 91%) as a yellow solid: *R<sub>f</sub>* (40% ethyl acetate/hexanes) = 0.34; mp = 115–118 °C (dec); <sup>1</sup>H NMR (500 MHz, CDCl<sub>3</sub>) δ = 8.49 (d, *J* = 7.8 Hz, 2H), 8.14 (d, *J* = 7.5 Hz, 2H), 8.06 (s, 2H), 8.02 (t, *J* = 7.7 Hz, 2H), 4.34 (t, *J* = 6.7 Hz, 4H), 1.95–2.01 (m, 4H), 1.55–1.65 (m, 4H), 1.25–1.45 (m, 24H), 0.87–0.90 (m, 6H); <sup>13</sup>C NMR (75 MHz, CDCl<sub>3</sub>) δ = 144.10, 131.07, 128.92, 127.30, 125.93, 124.27, 122.86, 119.43, 73.80, 31.93, 30.63, 29.70, 29.63, 29.61, 29.37, 26.34, 22.71, 14.13; MS (APCI(+), CH<sub>2</sub>Cl<sub>2</sub>): *m/z* (%); 743.6; HRMS (ESI(+), CH<sub>2</sub>Cl<sub>2</sub>): calcd for C<sub>50</sub>H<sub>70</sub>O<sub>4</sub>, 742.5900, found 742.5896.

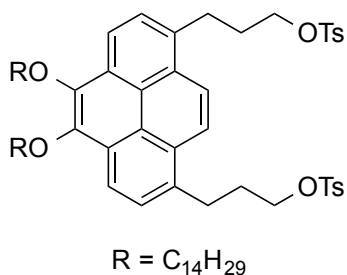
**1,8-Bis(3-hydroxypropyl)-4,5-bis(tetradecyloxy)pyrene (71):**



To a stirred solution of 1,8-bis(3-hydroxy-1-propynyl)-4,5-bis(tetradecyloxy)pyrene (**56**) (0.212 g, 0.289 mmol) in ethyl acetate (25 mL) was added 10% Pd/C (0.102 g). The reaction mixture was stirred at room temperature under an atmosphere of hydrogen (balloon), and the progress of the reaction was monitored by <sup>1</sup>H NMR. After 18 h the

mixture was filtered through a plug of Celite<sup>®</sup> and the clear yellow filtrate was concentrated under reduced pressure. The residue was filtered through a plug of silica (using a sintered glass crucible with suction) using ethyl acetate as the eluent to afford 1,8-bis(3-hydroxypropyl)-4,5-bis(tetradecyloxy)pyrene (**71**) (0.200 g, 93%) as a yellow powdery solid:  $R_f$  (40% ethyl acetate/hexanes) = 34; mp = 63.0-65 °C; <sup>1</sup>H NMR (500 MHz, CDCl<sub>3</sub>)  $\delta$  = 8.41 (d,  $J$  = 8 Hz, 2H), 8.32 (s, 2H), 7.89 (d,  $J$  = 8 Hz 2H), 4.30 (t,  $J$  = 6.7 Hz, 4H), 3.79 (t,  $J$  = 6.2 Hz, 4H), 3.45 (t,  $J$  = 7.7, 4H), 2.08-2.18 (m, 4H), 1.92-2.01 (m, 4H), 1.55–1.63 (m, 4H), 1.27–1.45 (m, 49H), 0.86–0.90 (m, 6H); <sup>13</sup>C NMR (75 MHz, CDCl<sub>3</sub>)  $\delta$  = 143.30, 135.07, 128.40, 127.69, 127.29, 123.14, 119.19, 73.73, 62.44, 34.60, 31.94, 30.63, 29.73, 29.69, 29.62, 29.55, 29.39, 26.35, 22.70, 14.13; MS (APCI, positive mode, CH<sub>2</sub>Cl<sub>2</sub>):  $m/z$  (%) 743 ([M+1]<sup>+</sup>, 100), ; HRMS (ESI-(+), CH<sub>2</sub>Cl<sub>2</sub>): calcd for C<sub>60</sub>H<sub>85</sub>O<sub>6</sub> 742.5900, found 742.5908.

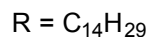
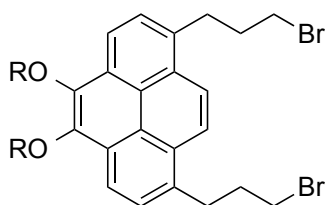
**1,8-Bis(3-tosylpropyl)-4,5-bis(tetradecyloxy)pyrene (72):**



To a stirring solution of **71** (0.057 g, 0.0769 mmol) in CH<sub>2</sub>Cl<sub>2</sub> (2.5 mL) was added Et<sub>3</sub>N (0.6 mL, 4.3 mmol). Purified *p*-TsCl (0.038 g, 0.199 mmol) was added and the reaction was left to stir at room temperature. After 18 h, the reaction was quenched with the addition of H<sub>2</sub>O (5 mL). The reaction mixture was extracted with CH<sub>2</sub>Cl<sub>2</sub> (3 × 5 mL), and

the combined organic extracts were washed with  $\text{NH}_4\text{Cl}$  (5 mL),  $\text{H}_2\text{O}$  ( $2 \times 5$  mL), and brine (5 mL), and dried over anhydrous  $\text{MgSO}_4$ . Excess solvent was removed under reduced pressure. The residue was adsorbed onto silica gel then subjected to column chromatography (20% ethyl acetate/hexanes) to afford 1,8-bis(3-tosylpropyl)-4,5-bis(tetradecyloxy)pyrene (**72**) (0.63 g, 78%) as a yellow solid:  $R_f$  (40% ethyl acetate/hexanes) = 0.54; mp = 115–118 °C (dec);  $^1\text{H}$  NMR (300 MHz,  $\text{CDCl}_3$ )  $\delta$  = 8.34 (d,  $J$  = 8 Hz, 2H), 8.17 (s, 2H), 7.81 (d,  $J$  = 8.3 Hz, 2H), 7.70 (m, 8H), 7.30 (m, 4H), 4.30 (t,  $J$  = 6.6 Hz, 4H), 4.13 (d,  $J$  = 6 Hz, 4H), 3.38 (t,  $J$  = 6.7 Hz, 4H), 3.22 (m, 4H), 2.40 (s, 10H), 2.19–2.30 (m, 4H), 1.94–2.04 (m, 4H), 1.58–1.63 (m, 4H), 1.27–1.45 (m, 30H), 0.86–0.90 (m, 6H);  $^{13}\text{C}$  NMR (75 MHz,  $\text{CDCl}_3$ )  $\delta$  = ; MS (APCI, positive mode,  $\text{CH}_2\text{Cl}_2$ ):  $m/z$  (%) 1052.6 ( $[\text{M}+1]^+$ , 100), ; HRMS (ESI-(+),  $\text{CH}_2\text{Cl}_2$ ): calcd for  $\text{C}_{64}\text{H}_{90}\text{O}_8\text{S}_2$  1051.5266, found 1051.5251.

**1,8-Bis(3-bromopropyl)-4,5-bis(tetradecyloxy)pyrene (73):**



To a stirred solution of **71** (0.047 g, 0.063 mmol) in  $\text{CH}_2\text{Cl}_2$  (5 mL) was added  $\text{PBr}_3$  (0.1 mL, 1.1 mmol). The reaction mixture was capped and left to stir at room temperature. After 16 h, the reaction was quenched by the addition of  $\text{H}_2\text{O}$  (5 mL). It was extracted with  $\text{CH}_2\text{Cl}_2$  ( $2 \times 2$  mL), washed with 5%  $\text{NaHCO}_3$  (5 mL),  $\text{H}_2\text{O}$  ( $2 \times 2$  mL) and brine (2

mL). The combined organic layers were dried over  $\text{MgSO}_4$  and the excess solvent was removed under reduced pressure. The residue was adsorbed onto silica gel and subjected to column chromatography (20% ethyl acetate / hexanes) to afford **73** as a yellow solid (0.045 g, 82%):  $R_f$  (40% ethyl acetate/hexanes) = 0.52; mp = 114–118 °C (dec);  $^1\text{H}$  NMR (300 MHz,  $\text{CDCl}_3$ )  $\delta$  = 8.61 (2, 2H), 8.43 (d,  $J$  = 8.2 Hz, 2H), 8.14 (d,  $J$  = 8.2 Hz, 2H), 4.75 (d,  $J$  = 5.6 Hz, 4H), 4.32 (t,  $J$  = 6.8 Hz, 4H), 1.92–1.98 (m, 4H), 1.77–1.85 (m, 4H), 1.53–1.64 (m, 49H), 1.27–1.35 (m, 48H), 0.86–0.89 (m, 6H);  $^{13}\text{C}$  NMR (75 MHz,  $\text{CDCl}_3$ )  $\delta$  = 143.32, 135.11, 128.43, 127.71, 127.26, 123.16, 119.23, 73.75, 62.42, 34.56, 31.89, 30.62, 29.73, 29.69, 29.62, 29.55, 29.39, 26.35, 22.70, 14.13; MS (APCI, positive mode,  $\text{CH}_2\text{Cl}_2$ ):  $m/z$  (%) 869; HRMS (ESI-(+),  $\text{CH}_2\text{Cl}_2$ ): calcd for  $\text{C}_{50}\text{H}_{76}\text{O}_2\text{Br}_2$  868.9422, found 868.9418.

## Bibliography

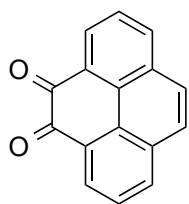
- (1) Figueira-Duarte, T. M.; Müllen, K. *Chem. Rev.* **2011**, *111*, 7260–7314.
- (2) Venkataramana, G.; Dongare, P.; Dawe, L. N.; Thompson, D. W.; Zhao, Y.; Bodwell, G. J. *Org. Lett.* **2011**, *13*, 2240–2243.
- (3) Gleiter, R.; Hopf, H. *Modern Cyclophane Chemistry*; Gleiter, R.; Hopf, H., Eds.; Wiley-VCH: We8hye8j, 2004; p. 1.
- (4) Schirch, P. F. T.; Boekelheide, V. *J. Am. Chem. Soc.* **1979**, *101*, 3125–3126.
- (5) El-Tamany, S.; Hopf, H. *Chem. Ber.* **1983**, *116*, 1682–1685.
- (6) McGlinchey, M. J.; Milosevic, S. *Isr. J. Chem.* **2012**, *52*, 30–40.
- (7) Barnes, J. C.; Jur, M.; Vermeulen, N. A.; Dale, E. J.; Stoddart, J. F. *J. Org. Chem.* **2013**, *78*, 11962–11969.
- (8) Brown, C. J.; Farthing, A. C. *Nature* **1949**, *164*, 915–916.
- (9) Pelligrin, M. *Recl. des Trav. Chim. des Pays-Bas la Belgique* **1899**, *18*, 458.
- (10) Cram, D. J.; Steinberg, H. *J. Am. Chem. Soc.* **1951**, *73*, 5691–5704.
- (11) Bodwell, G. J.; Bridson, J. N.; Houghton, T. J.; Kennedy, J. W. J.; Mannion, M. R. *Angew. Chem. Int. Ed. Engl.* **1996**, *35*, 1320–1321.
- (12) Merner, B. L.; Unikela, K. S.; Dawe, L. N.; Thompson, D. W.; Bodwell, G. J. *Chem. Commun.* **2013**, *49*, 5930–5932.
- (13) Zhang, B.; Manning, G. P.; Dobrowolski, M. A.; Cyran, M. K.; Bodwell, G. J. *Org. Lett.* **2008**, *10*, 273–276.
- (14) Bodwell, G. J.; Venkataramana, G.; Unikela, K. S. In *Fragments of Fullerenes and Carbon Nanotubes: Designed Synthesis, Unusual Reactions and Co-ordination Chemistry*; Petrukhina, M. A.; Scott, L. T., Eds.; John Wiley & Sons, Inc: Hoboken, NJ, USA, 2011; p. 440.
- (15) Yang, Y.; Mannion, M. R.; Dawe, L. N.; Kraml, C. M.; Pascal, R. A. J.; Bodwell, G. J. *J. Org. Chem.* **2012**, *77*, 57–67.

- (16) Haley, M. M.; Tykwinski, R. R. *Carbon-Rich Compounds*; 2006; p. 662.
- (17) Medinger, T.; Wilkinson, F. *Trans. Faraday Soc.* **1966**, *62*, 1785.
- (18) Casas-Solvas, J. M.; Howgego, J. D.; Davis, A. P. *Org. Biomol. Chem.* **2014**, *12*, 212–232.
- (19) Dewar, M. J. S.; Dennington, R. D. *J. Am. Chem. Soc.* **1989**, *111*, 3804–3808.
- (20) Vollmann, H.; Becker, H.; Corell, M.; Streeck, H. *Justus Liebigs Ann. Chem.* **1937**, *531*, 1–159.
- (21) Grimshaw, J.; Trocha-Grimshaw, J. *J. Chem. Soc. Perkin Trans. 1* **1965**, 1622–1623.
- (22) Ogino, K.; Iwashima, S.; Inokuchi, H.; Harada, Y. *Bull. Chem. Soc. Jpn.* **1965**, *38*, 473–477.
- (23) Yamato, T.; Miyazawa, A.; Tashiro, M. *J. Chem. Soc. Perkin Trans. 1* **1993**, 3127–3137.
- (24) Coventry, D. N.; Batsanov, A. S.; Goeta, A. E.; Howard, J. a K.; Marder, T. B.; Perutz, R. N. *Chem. Commun. (Camb)*. **2005**, 2172–2174.
- (25) Hu, J.; Zhang, D.; Harris, F. W. *J. Org. Chem.* **2005**, *70*, 707–708.
- (26) Mochida, K.; Kawasumi, K.; Segawa, Y.; Itami, K. *J. Am. Chem. Soc.* **2011**, *133*, 10716–10719.
- (27) Dixon, J. A. *J. Org. Chem.* **1959**, *24*, 1226–1229.
- (28) Griffith, W. P. *Ruthenium Oxidation Complexes: Their Uses as Homogeneous Organic Catalysis*; 15th ed.; Springer Science & Business Media, 2010; p. 273.
- (29) Pappo, R.; Allen Jr, D. S.; Lemieux, R. U.; Johnson, W. S. *J. Org. Chem.* **1956**, *21*, 478–479.
- (30) Yang, D.; Zhang, C. *J. Org. Chem.* **2001**, *66*, 4814–4818.
- (31) Yu, W.; Mei, Y.; Kang, Y.; Hua, Z.; Jin, Z. *Org. Lett.* **2004**, *6*, 3217–3219.
- (32) Trost, B. M.; Dong, G. *J. Am. Chem. Soc.* **2010**, *132*, 16403–16416.

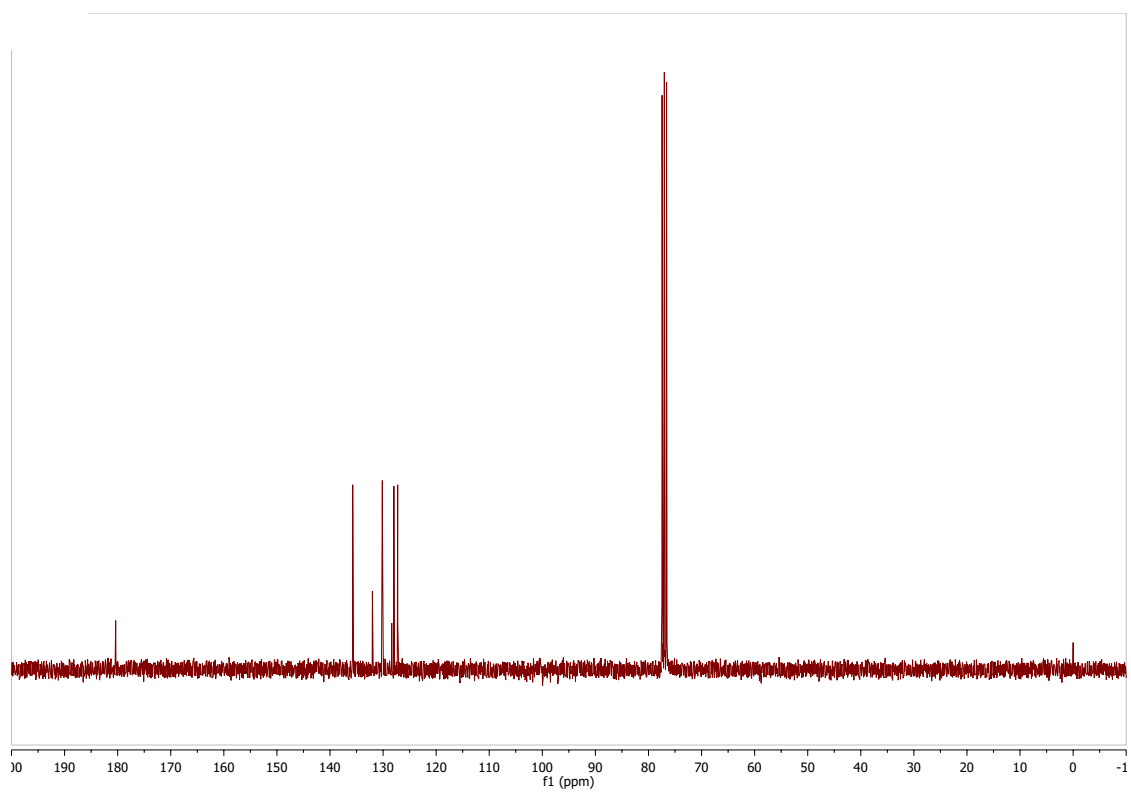
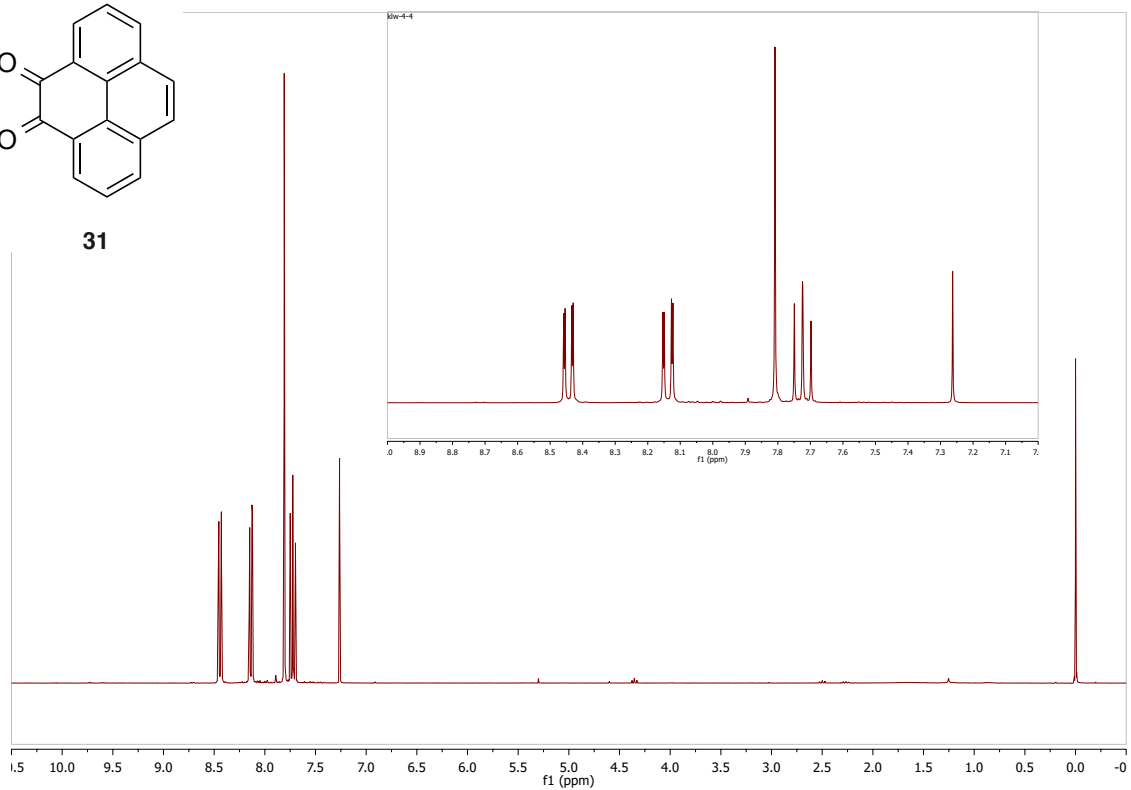
- (33) Rudolph, J.; Reddy, K. L.; Chiang, J. P.; Sharpless, K. B.; Road, N. T. P.; Jolla, L.; February, R. V. *J. Am. Chem. Soc.* **1997**, *7863*, 6189–6190.
- (34) Ferreira, P.; Xue, W. M.; Bencze, E.; Herdtweck, E.; Kühn, F. E. *Inorg. Chem.* **2001**, *40*, 5834–5841.
- (35) Kühn, F. E.; Santos, A. M.; Herrmann, W. A. *J. Chem. Soc. Dalton Trans.* **2005**, 2483–2491.
- (36) Herrmann, W. A.; Fischer, R. W.; Marz, D. W. *Angew. Chem. Int. Ed. Engl.* **1991**, *30*, 1638–1641.
- (37) Shatnawi, M. Y.; Al-Ajlouni, A. M. *Jordan J. Chem.* **2009**, *4*, 119–130.
- (38) Allen, D. W.; Tebby, J. C. *Organophosphorus Chemistry*; 33rd ed.; The Royal Society of Chemistry: Cambridge, U.K., 2003; p. 368.
- (39) Paruch, K.; Katz, T.; Incarvito, C.; Lam, K.; Rhatigan, B.; Rheingold, A. *J. Org. Chem.* **2000**, *65*, 7602–7608.
- (40) Chinchilla, R.; Najera, C. *Chem. Rev.* **2007**, *107*, 874–922.
- (41) Takeda, T.; Fix, A. G.; Haley, M. M. *Org. Lett.* **2010**, *12*, 3824–3827.
- (42) Venkataramana, G.; Bodwell, G. J. *Unpubl. results*.
- (43) Suresh, S.; Srivastava, V. C.; Mishra, I. M. *Int. J. Energy Environ. Eng.* **2012**, *3*, 32.
- (44) Wang, Z. Y. *Near-Infrared Organic Materials and Emerging Applications*; CRC Press, 2013; p. 186.
- (45) Qian, G.; Wang, Z. Y. *Chem. Asian J.* **2010**, *5*, 1006–1029.
- (46) Bergkamp, J. J.; Decurtins, S.; Liu, S. *Chem. Soc. Rev.* **2015**.
- (47) Kamtekar, K. T.; Monkman, A. P.; Bryce, M. R. *Adv. Mater.* **2010**, *22*, 572–582.
- (48) Bendikov, M.; Wudl, F.; Perepichka, D. F. *Chem. Rev.* **2004**, *104*, 4891–4946.
- (49) Chen, G.; Zhao, Y. *Org. Lett.* **2014**, *16*, 668–671.
- (50) Georghiou, P. E.; Valluru, G.; Schneider, C.; Liang, S.; Woolridge, K.; Mulla, K.; Adronov, A.; Zhao, Y. *RSC Adv.* **2014**, *4*, 31614.

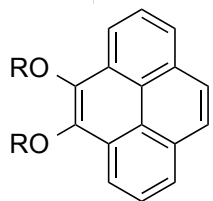
- (51) Liang, S.; Zhao, Y.; Adronov, A. *J. Am. Chem. Soc.* **2014**, *136*, 970–977.
- (52) Liu, Y.; Yu, Z.-L.; Zhang, Y.-M.; Guo, D.-S.; Liu, Y.-P. *J. Am. Chem. Soc.* **2008**, *130*, 10431–10439.
- (53) Ogoshi, T.; Takashima, Y.; Yamaguchi, H.; Harada, A. *J. Am. Chem. Soc.* **2007**, *129*, 4878–4879.
- (54) Liang, S.; Chen, G.; Zhao, Y. *J. Mater. Chem. C* **2013**, *1*, 5477.
- (55) Etika, K. C.; Jochum, F. D.; Cox, M. a.; Schattling, P.; Theato, P.; Grunlan, J. C. *Macromolecules* **2010**, *43*, 9447–9453.
- (56) Prencipe, G.; Tabakman, S. M.; Welsher, K.; Liu, Z.; Goodwin, A. P.; Zhang, L.; Henry, J.; Dai, H. *J. Am. Chem. Soc.* **2009**, *131*, 4783–4787.
- (57) Guldi, D. M.; Rahman, G. M. A.; Jux, N.; Balbinot, D.; Hartnagel, U.; Tagmatarchis, N.; Prato, M. *J. Am. Chem. Soc.* **2005**, *127*, 9830–9838.
- (58) Wang, D.; Ji, W.-X.; Li, Z.-C.; Chen, L. *J. Am. Chem. Soc.* **2006**, *128*, 6556–6557.
- (59) Ehli, C.; Rahman, G. M. A.; Jux, N.; Balbinot, D.; Guldi, D. M.; Paolucci, F.; Marcaccio, M.; Paolucci, D.; Melle-Franco, M.; Zerbetto, F.; Campidelli, S.; Prato, M. *J. Am. Chem. Soc.* **2006**, *128*, 11222–11231.
- (60) Etika, K. C.; Jochum, F. D.; Theato, P.; Grunlan, J. C. *J. Am. Chem. Soc.* **2009**, *131*, 13598–13599.
- (61) Etika, K. C.; Jochum, F. D.; Cox, M. a.; Schattling, P.; Theato, P.; Grunlan, J. C. *Macromolecules* **2010**, *43*, 9447–9453.
- (62) Li, M.; Xu, P.; Yang, J.; Ying, H.; Haubner, K.; Dunsch, L.; Yang, S. *J. Physcial Chem. C* **2011**, *115*, 4584–4593.

## Appendix

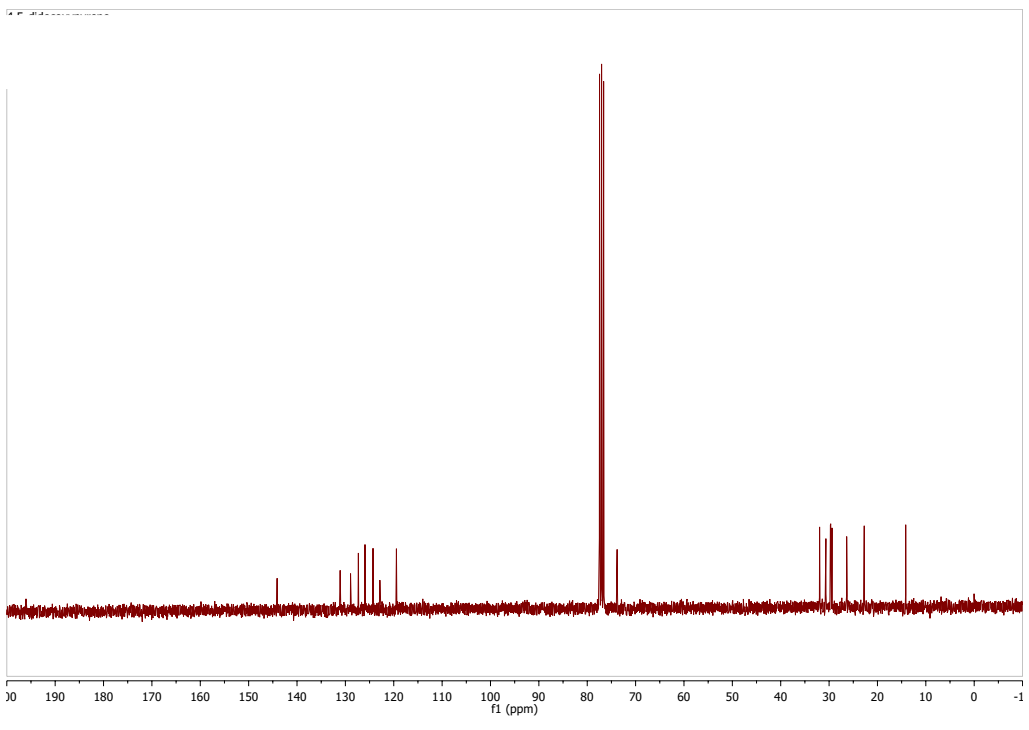
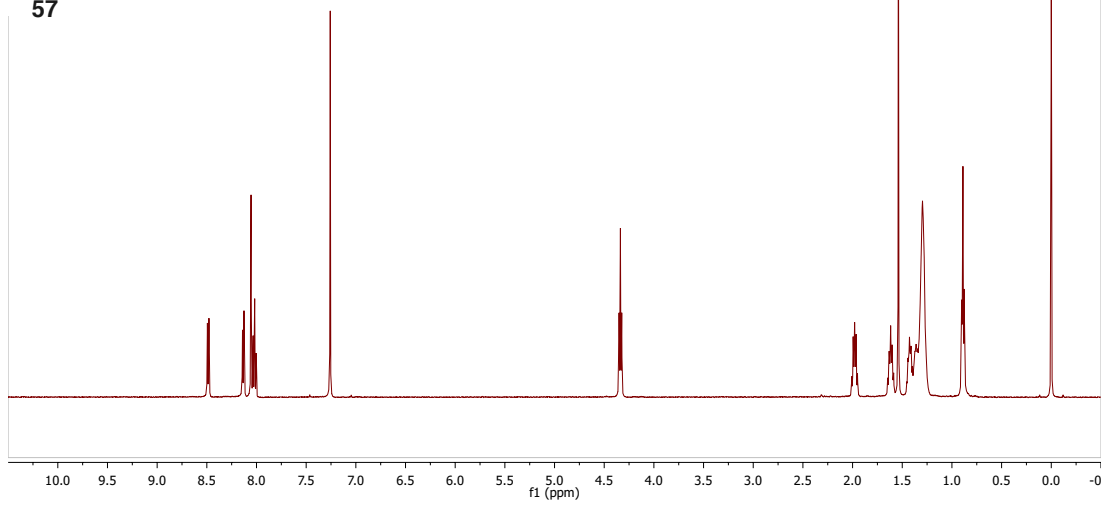
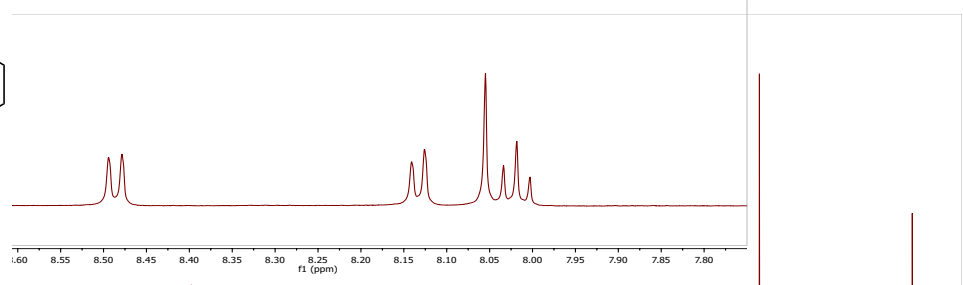


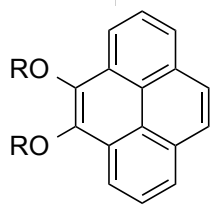
31



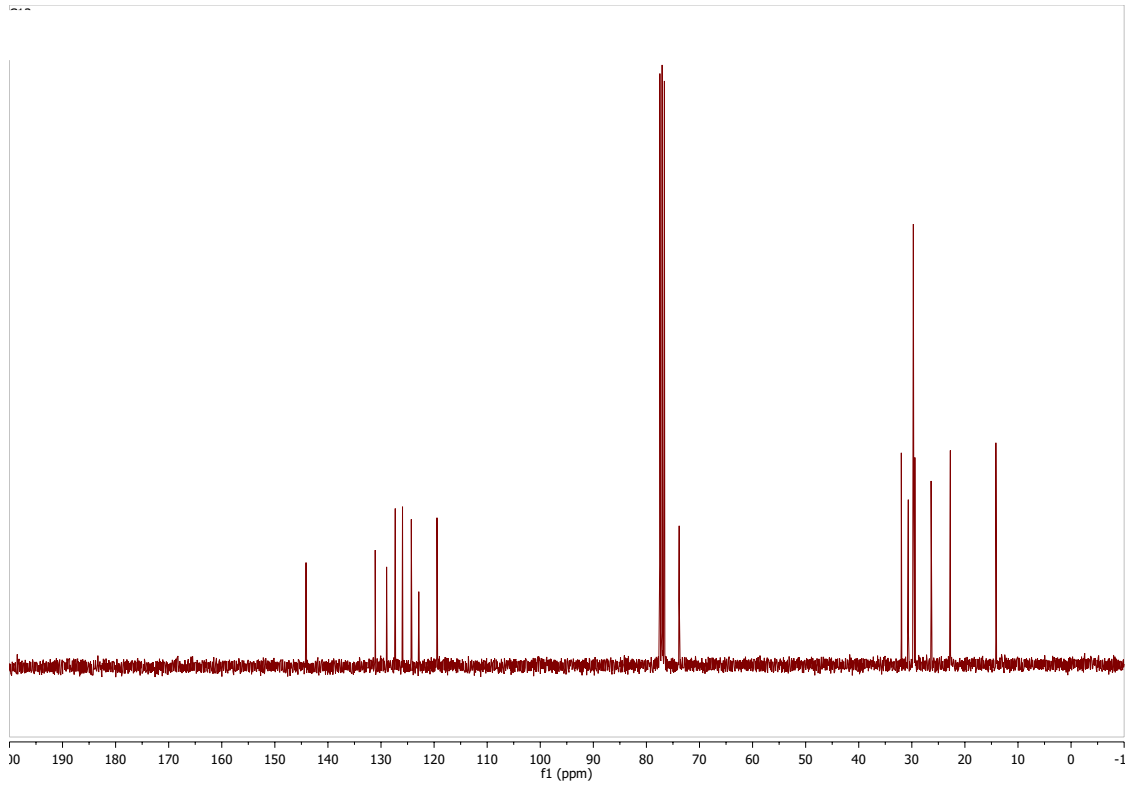
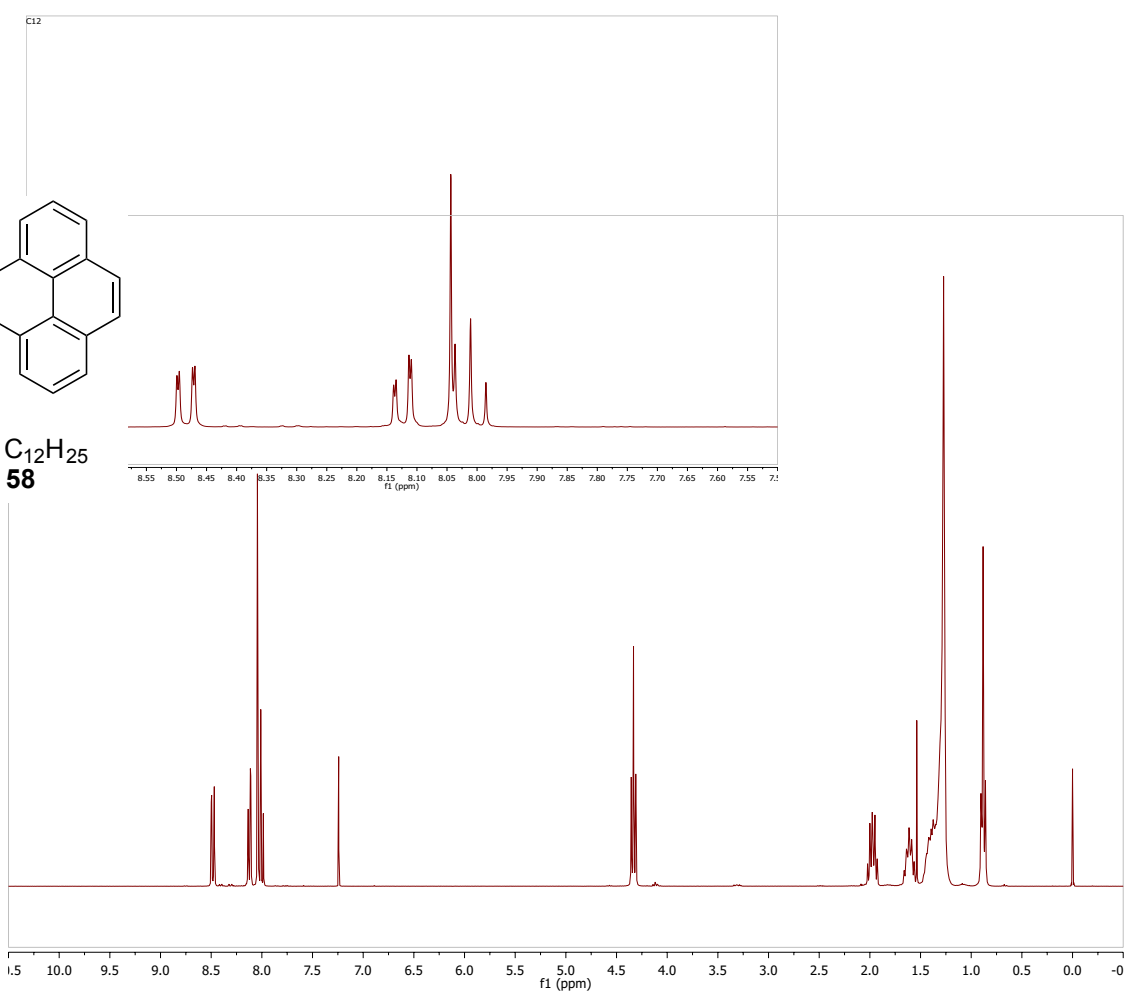


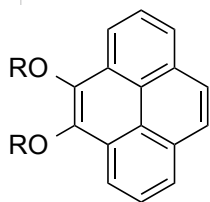
R = C<sub>10</sub>H<sub>21</sub>  
57



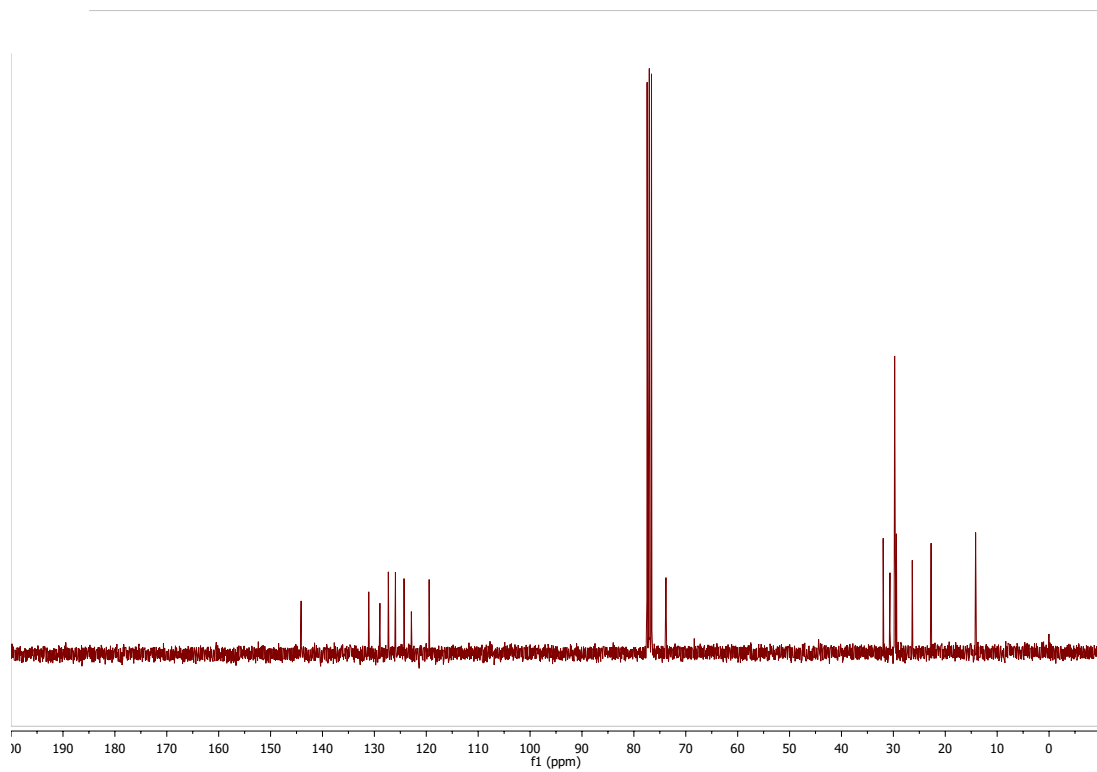
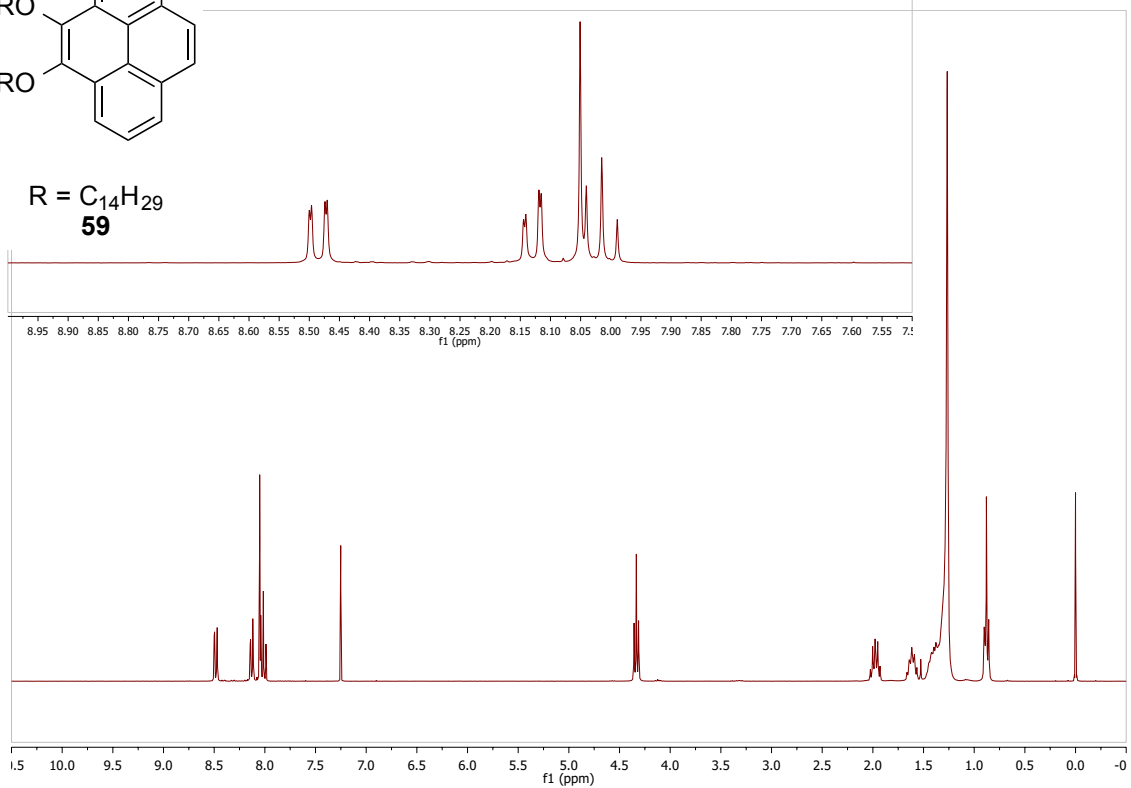


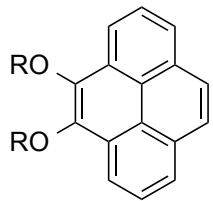
R = C<sub>12</sub>H<sub>25</sub>  
**58**



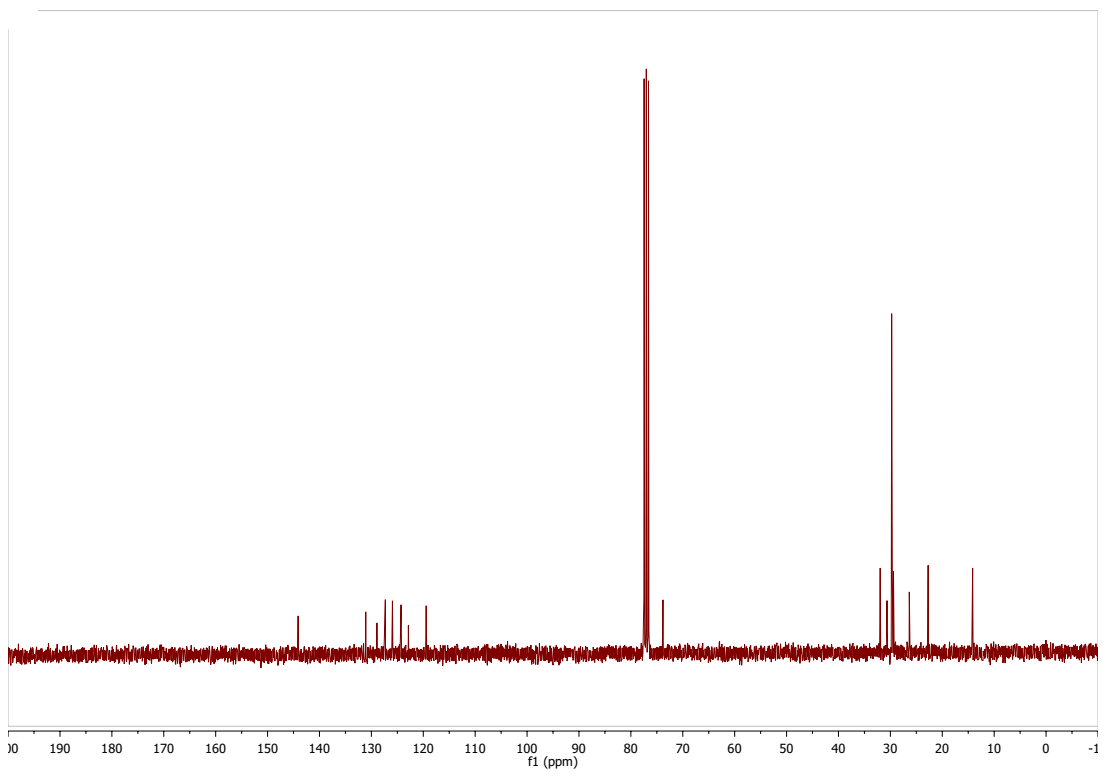
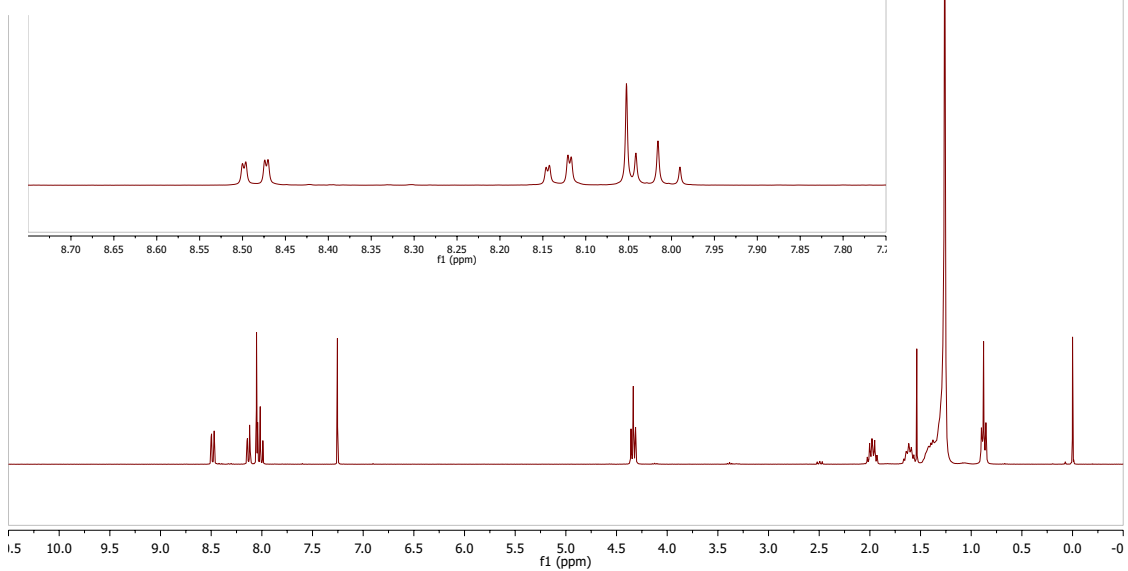


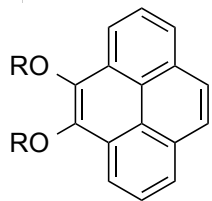
R = C<sub>14</sub>H<sub>29</sub>  
**59**



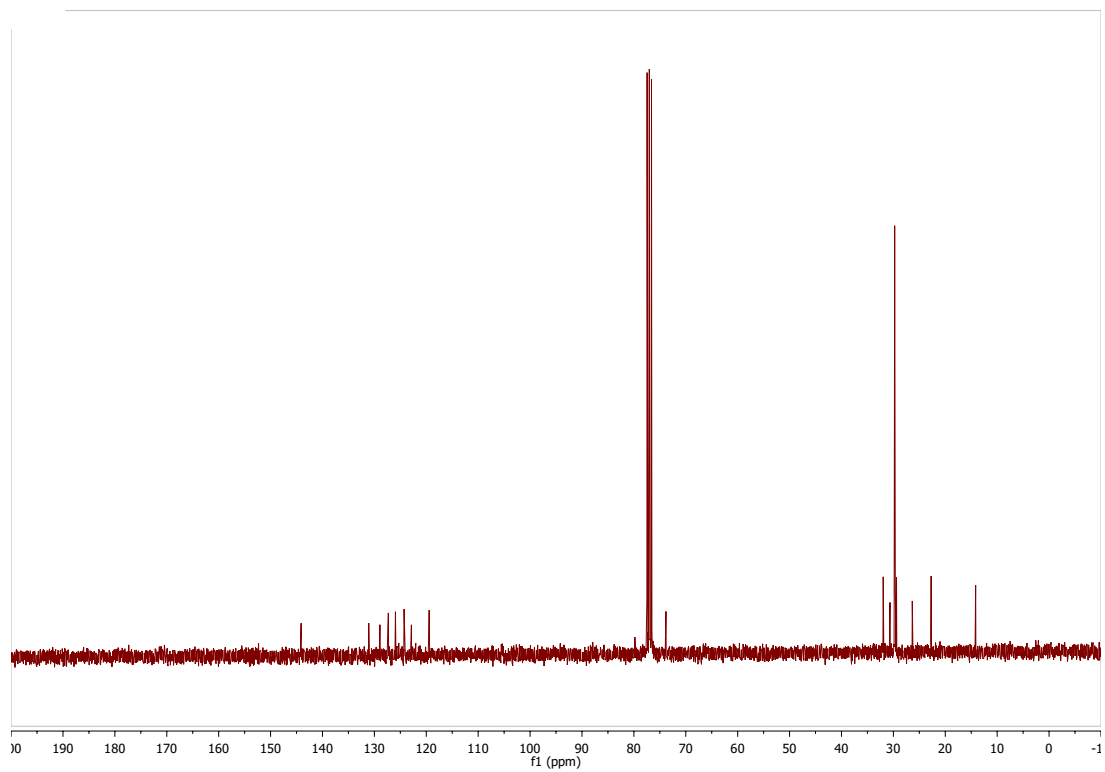
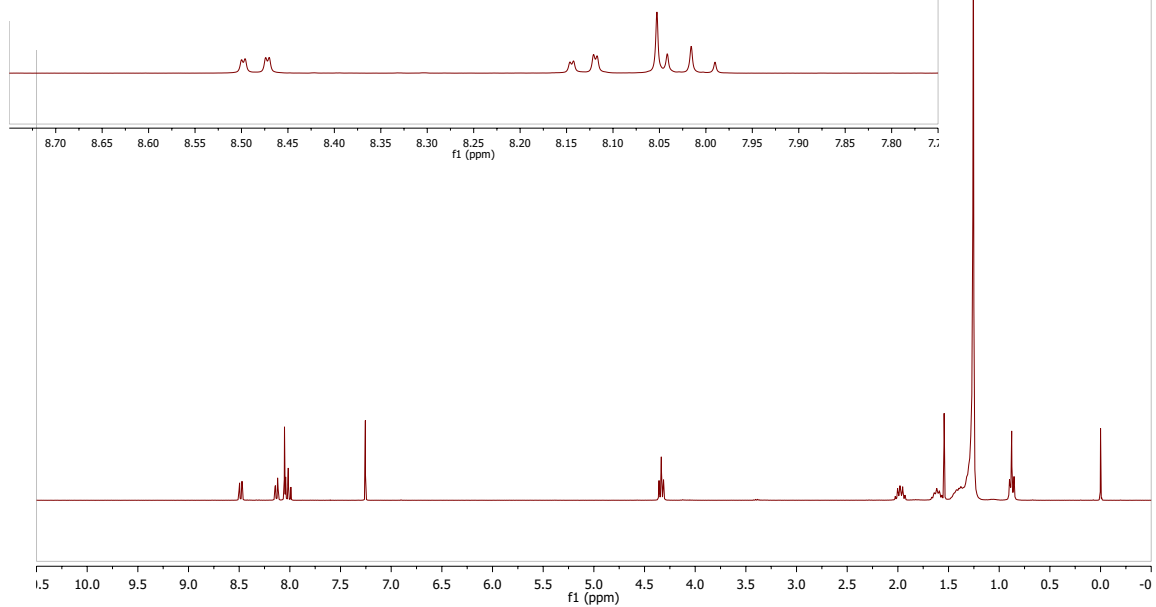


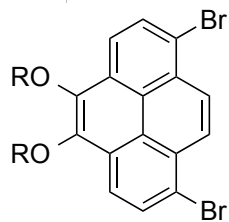
R=C<sub>16</sub>H<sub>33</sub>  
60



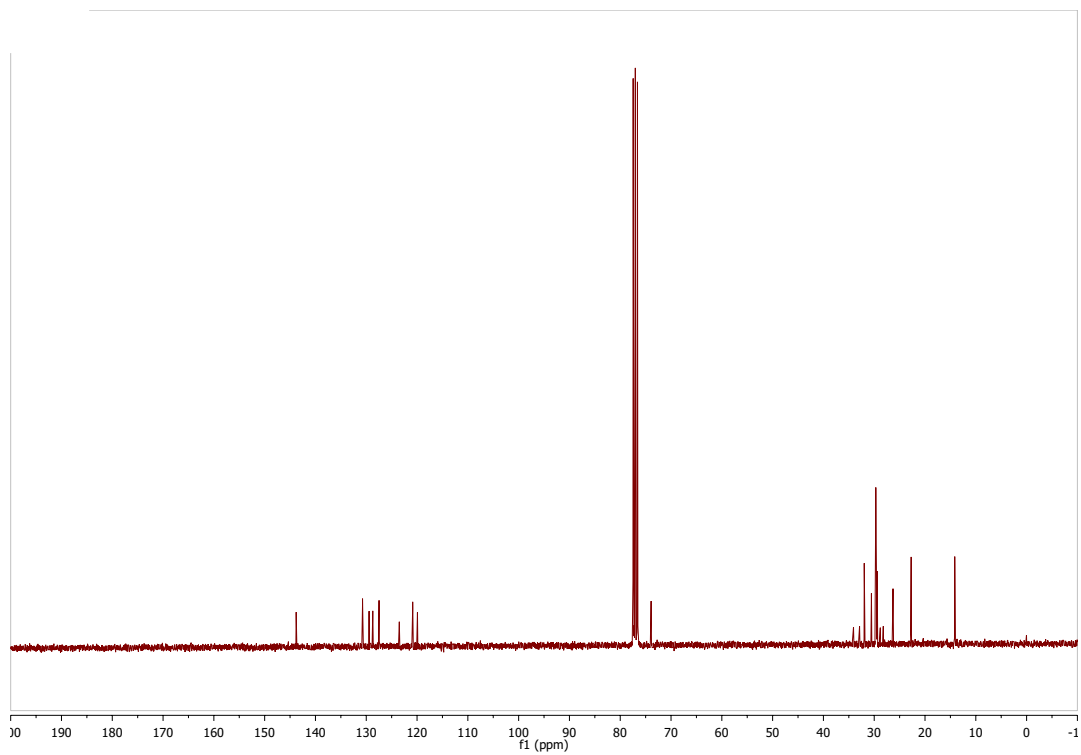
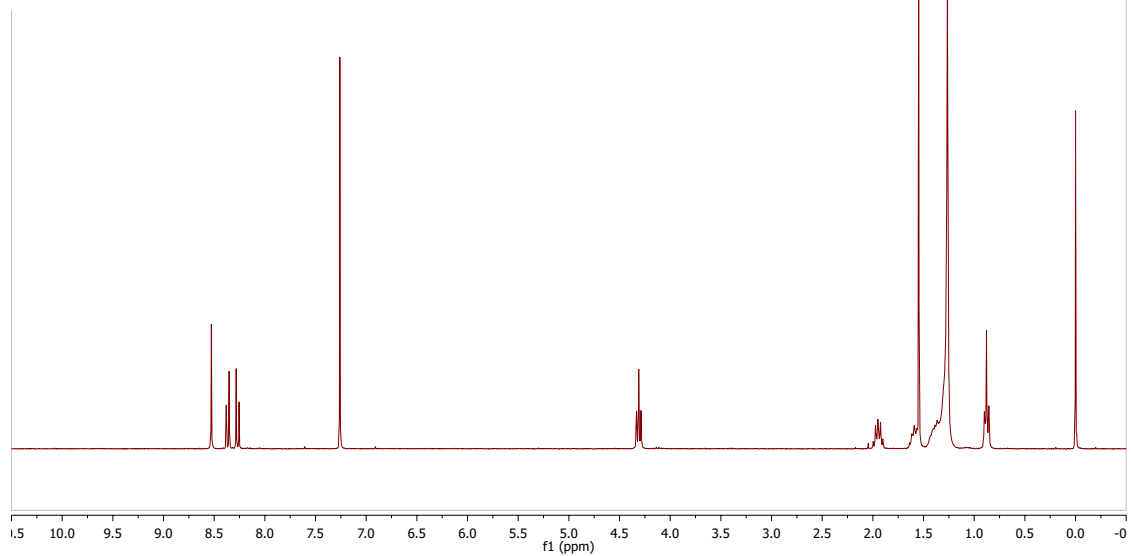
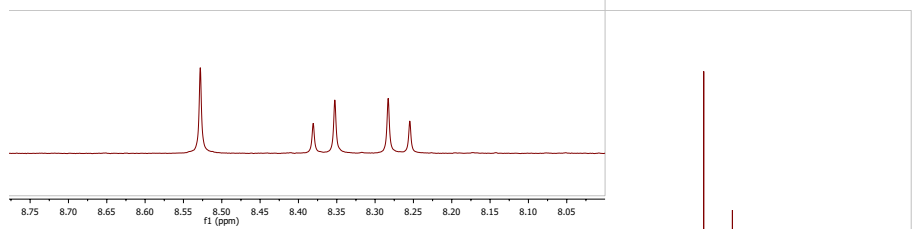


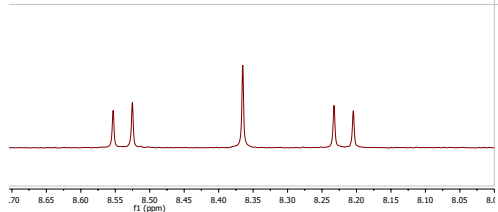
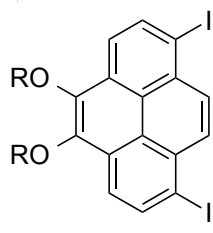
R=C<sub>20</sub>H<sub>41</sub>  
**61**



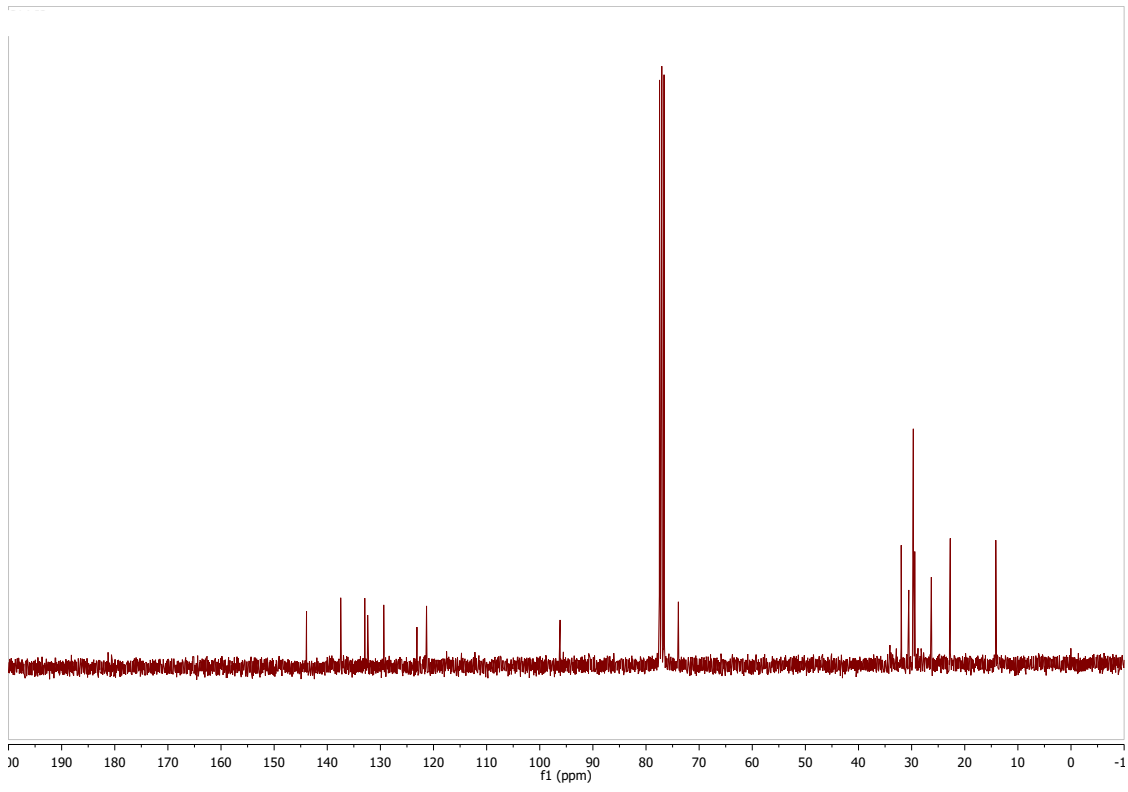
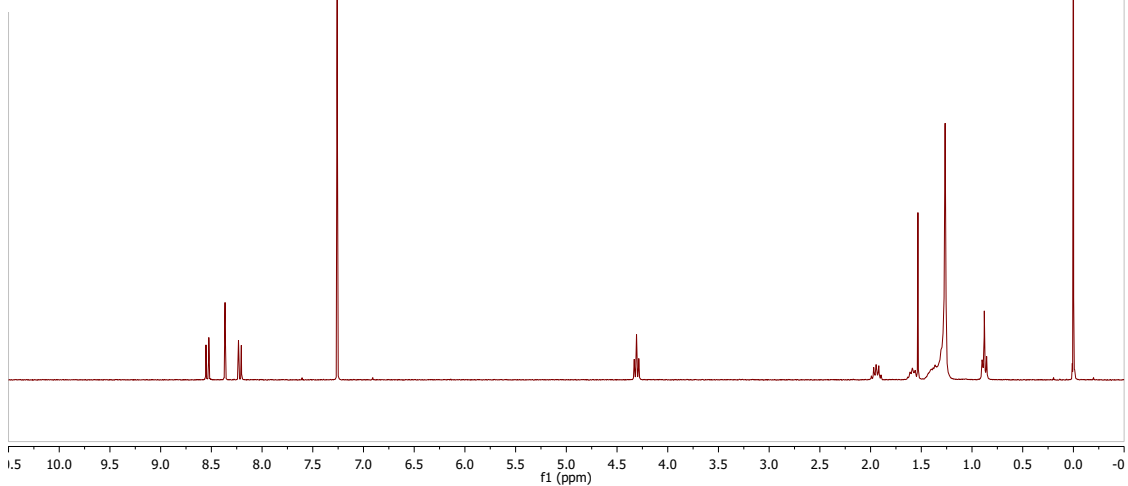


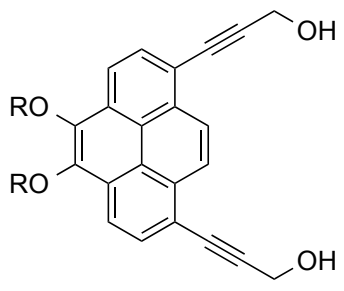
R=C<sub>14</sub>H<sub>29</sub>  
**62**



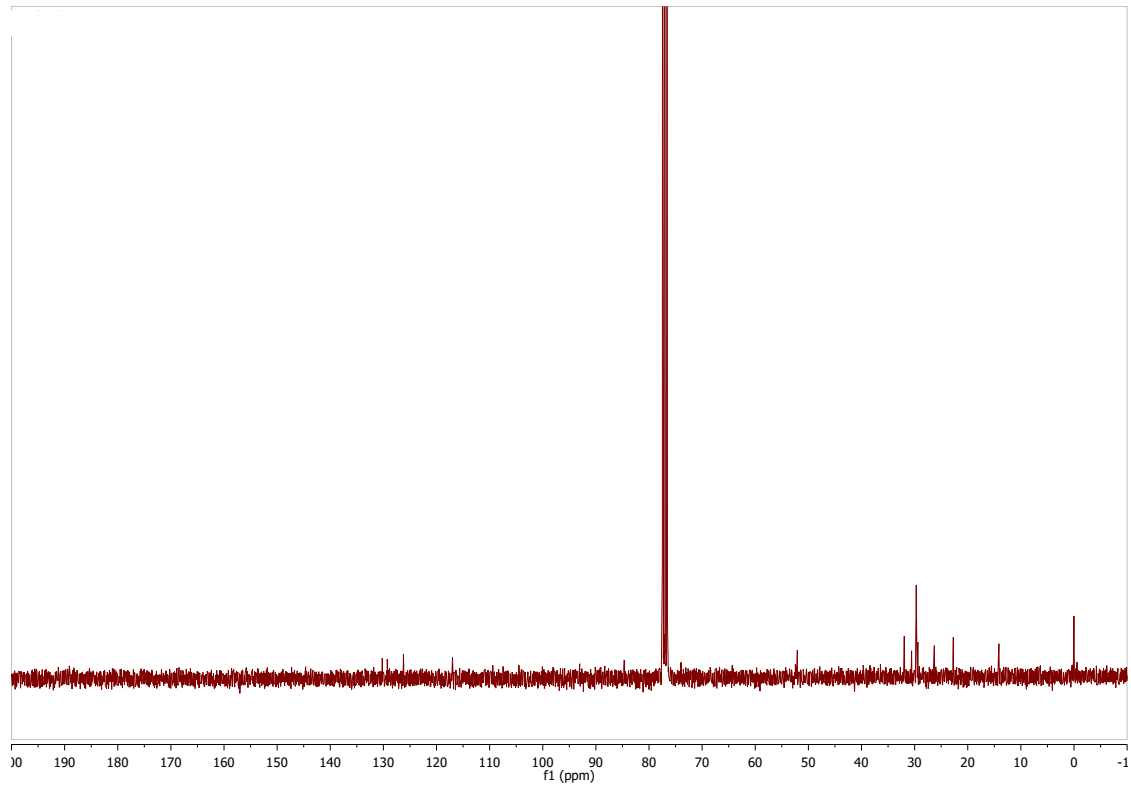
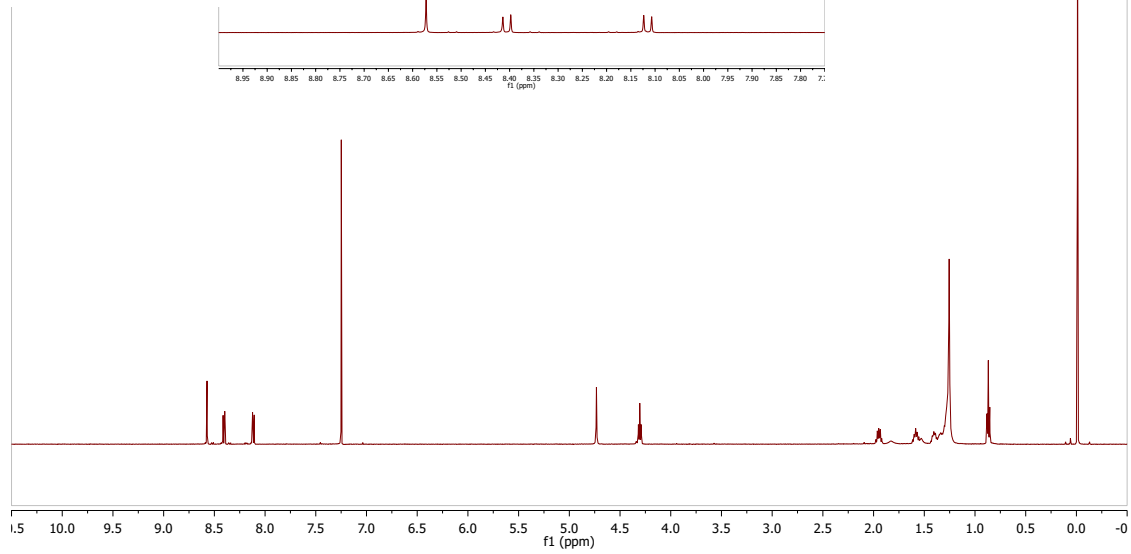


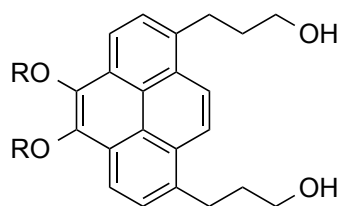
R = C<sub>14</sub>H<sub>29</sub>  
**70**





R = C<sub>14</sub>H<sub>29</sub>  
**67**





R = C<sub>14</sub>H<sub>29</sub>  
71

